

# Topological Phases of Matter: Exactly Solvable Models and Classification

Thesis by  
Zitao Wang

In Partial Fulfillment of the Requirements for the  
Degree of  
Doctor of Philosophy

The logo for the California Institute of Technology (Caltech), featuring the word "Caltech" in a bold, orange, sans-serif font.

CALIFORNIA INSTITUTE OF TECHNOLOGY  
Pasadena, California

2019  
Defended April 5, 2019

© 2019

Zitao Wang

ORCID: 0000-0002-2326-2674

All rights reserved

## ACKNOWLEDGEMENTS

This thesis would not have been possible without the help of many people. First and foremost, I would like to thank my adviser Xie Chen, for her guidance and support over the past 5 years, and for her patience and encouragement when I felt lost or stuck. Our discussions and conversations were the most memorable part of my PhD life. I learned a tremendous amount from Xie, especially the importance of being solid in my research, understanding the physics behind the mathematics thoroughly, and explaining things in a simple manner. I thank Anton Kapustin for his guidance during my first year at Caltech, and for leading me into the field of topological phases of matter. I am always amazed by how knowledgeable Anton is, and his ability to combine physical intuition with complicated mathematics. I thank Jason Alicea, for his wonderful condensed matter theory class at Caltech. I very much enjoyed and benefited a lot from his lectures. I thank the members of my thesis committee, Xie Chen, Anton Kapustin, Jason Alicea, and Manuel Endres, for offering their invaluable insight and expertise.

I thank my collaborators, Ning Bao, Chunjun Cao, Shang-Qiang Ning, Ryan Thorngren, Alex Turzillo, and Michael Walter, from whom I learned a lot. I thank my friends Feng Bi, Yu-An Chen, Yichen Huang, Shenghan Jiang, Burak Şahinoğlu, Zhan Su, Ke Ye, Kexin Yi, Yong-Liang Zhang, and especially Chunjun Cao and Haoqing Wang, for making my PhD life warm and enjoyable.

My appreciation to all the Caltech staff who helped me along the way, Laura Flower Kim, Sofie Leon, Kate McNulty, and members of the Caltech security. I thank the nurse practitioners at the Archibald Young Health Center, Divina Bautista and Alice Sogomonian, for taking care of me during my years at Caltech. I owe my deepest gratitude to my Hudson neighbor Latrell, for offering me the help when I desperately needed it.

Last but not least, I would like to thank my family and my beloved wife, Zhonghui Wu, for their constant love and support, and for always believing in me. I dedicate the thesis to them.

## ABSTRACT

In this thesis, we study gapped topological phases of matter in systems with strong inter-particle interaction. They are challenging to analyze theoretically, because interaction not only gives rise to a plethora of phases that are otherwise absent, but also renders methods used to analyze non-interacting systems inadequate. By now, people have had a relatively systematic understanding of topological orders in two spatial dimensions. However, less is known about the higher dimensional cases. In Chapter 2, we will explore three dimensional long-range entangled topological orders in the framework of Walker-Wang models, which are a class of exactly solvable models for three-dimensional topological phases that are not known previously to be able to capture these phases. We find that they can represent a class of twisted discrete gauge theories, which were discovered using a different formalism. Meanwhile, a systematic theory of bosonic symmetry protected topological (SPT) phases in all spatial dimensions have been developed based on group cohomology. A generalization of the theory to group supercohomology has been proposed to classify and characterize fermionic SPT phases in all dimensions. However, it can only handle cases where the symmetry group of the system is a product of discrete unitary symmetries. Furthermore, the classification is known to be incomplete for certain symmetries. In Chapter 3, we will construct an exactly solvable model for the two-dimensional time-reversal-invariant topological superconductors, which could be valuable as a first attempt to a systematic understanding of strongly interacting fermionic SPT phases with anti-unitary symmetries in terms of exactly solvable models. In Chapter 4, we will propose an alternative classification of fermionic SPT phases using the spin cobordism theory, which hopefully can capture all the phases missing in the supercohomology classification. We test this proposal in the case of fermionic SPT phases with  $\mathbb{Z}_2$  symmetry, where  $\mathbb{Z}_2$  is either time-reversal or an internal symmetry. We find that cobordism classification correctly describes all known fermionic SPT phases in space dimensions less than or equal to 3.

## PUBLISHED CONTENT AND CONTRIBUTIONS

Zitao Wang and Xie Chen. “Twisted gauge theories in three-dimensional Walker-Wang models”. *Phys. Rev. B* **95**, 115142 (2017). DOI: [10.1103/PhysRevB.95.115142](https://doi.org/10.1103/PhysRevB.95.115142).

Z.W. participated in the conception of the project, performed analytical and numerical calculations, and participated in the writing of the manuscript.

Zitao Wang, Shang-Qiang Ning, and Xie Chen. “Exactly solvable model for two-dimensional topological superconductors”. *Phys. Rev. B* **98**, 094502 (2018). DOI: [10.1103/PhysRevB.98.094502](https://doi.org/10.1103/PhysRevB.98.094502).

Z.W. participated in the conception of the project, performed analytical calculations, and participated in the writing of the manuscript.

Anton Kapustin, Ryan Thorngren, Alex Turzillo, and Zitao Wang. “Fermionic symmetry protected topological phases and cobordisms”. *J. High Energ. Phys.* (2015) 2015:1. DOI: [10.1007/JHEP12\(2015\)052](https://doi.org/10.1007/JHEP12(2015)052).

Z.W. participated in the conception of the project, performed analytical calculations, and participated in the writing of the manuscript.

# TABLE OF CONTENTS

Acknowledgements . . . . .	iii
Abstract . . . . .	iv
Published Content and Contributions . . . . .	v
Table of Contents . . . . .	vi
List of Illustrations . . . . .	viii
List of Tables . . . . .	xi
Chapter I: Introduction . . . . .	1
Chapter II: Twisted gauge theories in three-dimensional Walker-Wang models . . . . .	7
2.1 Introduction . . . . .	7
2.2 Review of Walker-Wang models . . . . .	9
2.3 $\mathbb{Z}_2 \times \mathbb{Z}_2$ gauge theories in the Walker-Wang models . . . . .	14
2.4 Detecting the topological order in the Walker-Wang models . . . . .	20
2.5 Summary and Discussion . . . . .	28
Chapter III: Exactly solvable model for two-dimensional topological superconductors . . . . .	31
3.1 Introduction . . . . .	31
3.2 Wave function . . . . .	33
3.3 Hamiltonian . . . . .	36
3.4 Time Reversal Invariance of the Hamiltonian and the Wave Function . . . . .	39
3.5 Why $T^2 = 1$ fermion does not work . . . . .	40
Chapter IV: Fermionic symmetry protected topological phases and cobordisms . . . . .	43
4.1 Introduction . . . . .	43
4.2 Spin and Pin structures . . . . .	44
4.3 Working assumptions . . . . .	46
4.4 Fermionic SPT phases without any symmetry . . . . .	47
4.5 Fermionic SPT phases with time-reversal symmetry . . . . .	50
4.6 Fermionic SPT phases with a unitary $\mathbb{Z}_2$ symmetry . . . . .	54
4.7 Fermionic SPT phases with a general symmetry . . . . .	56
4.8 Concluding remarks . . . . .	60
Appendix A: 3D modular transformations for Walker-Wang models on the minimal lattice . . . . .	61
A.1 $S$ matrix . . . . .	61
A.2 $T$ matrix . . . . .	62
Appendix B: Hamiltonian for Walker-Wang models on the minimal lattice . . . . .	64
B.1 Plaquette operator in the $xy$ -plane . . . . .	64
B.2 Plaquette operator in the $xz$ -plane . . . . .	67
B.3 Plaquette operator in the $yz$ -plane . . . . .	70
Appendix C: String operators for Walker-Wang models on the minimal lattice . . . . .	73
C.1 String operator along the $x$ -direction . . . . .	73

C.2 String operator along the $y$ -direction . . . . .	75
C.3 String operator along the $z$ -direction . . . . .	76
Appendix D: MES basis and canonical form for $S$ and $T$ matrices . . . . .	78
Appendix E: Proof that the $X_p$ terms commute with each other . . . . .	85
Appendix F: Quantization of the gravitational Chern-Simons action . . . . .	100
Bibliography . . . . .	102

## LIST OF ILLUSTRATIONS

<i>Number</i>	<i>Page</i>
2.1 A three-loop braiding process. The process involves a flux loop $\alpha$ sweeping out a torus enclosing a flux loop $\beta$ while both linked with a “base” flux loop $\gamma$ . The blue curves indicate the trajectory of two points on loop $\alpha$ . If $\alpha$ and $\beta$ are identical, we can similarly define the process where $\alpha$ and $\beta$ are exchanged while both linked with $\gamma$ . . . . .	8
2.2 An example of the ground state wave function of a Walker-Wang model. $a$ and $b$ here label the quasiparticle types. . . . .	10
2.3 Graphical definition of $F$ and $R$ symbols. . . . .	10
2.4 Planar projection of a trivalent resolution of the cubical lattice. . . . .	11
2.5 Plaquette term in the Walker-Wang Hamiltonian. . . . .	11
2.6 Sketch of surface excitations in a gauged SPT model. The bulk is below the plane. $q$ represents a gauge charge that can appear in the bulk and on the surface. $\chi$ represents an anyon that can appear only on the surface. $\alpha$ and $\beta$ represent the flux lines in the bulk that end on the surface. . . . .	17
2.7 Data for $\text{Rep}(Q_8)$ and $\text{Rep}(D_4)$ . The (simple) objects are the irreducible representations (charges) of either $Q_8$ or $D_4$ , defined in Eq. (2.7) and Eq. (2.8). They are all self-dual. Here $a, b = 0, 1, 2, 3$ , and $x, y = 1, 2, 3, x \neq y$ . $\chi$ is defined by $\chi(0, a) = \chi(a, 0) = 1$ , $\chi(x, x) = 1$ , and $\chi(x, y) = -1$ . The quantum dimension of a charge is defined to be the product of its Frobenius-Schur indicator and dimension. The $F$ symbols with $n = -1$ (respectively, $n = 1$ ) are the $6j$ symbols of $Q_8$ (respectively, $D_4$ ). The $R$ symbols are solutions to the hexagon equations (given the $F$ symbols) with the constraint that all charges are bosonic and have trivial mutual statistics. For $Q_8$ , there exists a unique solution, $n = -1, s_0 = 1, s_1 = s_2 = s_3 = -1$ . For $D_4$ , there exists 3 solutions, $n = 1, s_0 = 1, s_1 = -1, s_2 = 1, s_3 = 1$ , and also the ones resulting from the permutations $1 \leftrightarrow 2$ and $1 \leftrightarrow 3$ , respectively. . . . .	18
2.8 $S$ and $T$ transformations on a three-torus. . . . .	21
2.9 $T$ transformation as the Dehn twist of a hollow cylinder. . . . .	21

2.10	A “minimal” trivalent lattice on the three-torus, which consists of 4 vertices, 6 edges, and 3 plaquettes. . . . .	22
2.11	Decomposition of a three-loop braiding process into two separate braiding processes in the dimensionally-reduced 2D system. . . . .	24
3.1	The decorated domain wall approach. (a) Ground state is a superposition of all symmetry breaking domain configurations (blue and grey patches) with domain walls decorated with SPT states of one lower dimension (red curves). (b) The end point of the domain wall on the boundary (star) hosts nontrivial edge states of the lower dimensional SPT. . . . .	32
3.2	(a) illustrates the lattice structure and degrees of freedom in our model. Here 1 and $-1$ denote the eigenstates of $\tau_p^z$ with eigenvalues 1 and $-1$ , respectively. The blue bonds indicate the time-reversal domain wall. The solid red circles denote the Majorana modes $\gamma_v^\sigma$ ( $\sigma = \uparrow, \downarrow$ ). The arrow at each bond denotes the Kasteleyn orientation of the bond. (b) (respectively, (c)) is a detailed illustration of the coupling of Majorana modes away from (respectively, on) the domain wall. The dots and crosses on the solid red circles indicate the up ( $\uparrow$ ) and down ( $\downarrow$ ) spins of the Majorana modes, respectively. The yellow (respectively, grey) bond denotes the coupling of Majorana modes that share a long (respectively, short) bond. . . . .	35
3.3	(a) The 36 Majorana modes denoted by the 18 red dots in this figure are the Majorana modes surrounding the plaquette $p$ , denoted by $\partial'p$ . (b) Majorana modes (labeled 1 – 14) involved in the definition of $V_p^{\{\mu_{p,q}\}}$ when flipping the middle plaquette starting from this particular initial configuration. Red rectangles correspond to the pair projector terms involved in $V_p^{\{\mu_{p,q}\}}$ . Note that the spins of the involved Majorana modes are not shown in the figure. . . . .	38
3.4	Two configurations for spinless Majorana modes with opposite fermion parity. Extra minus signs are added to the coupling on the green bonds according to the modified coupling rule. . . . .	41
E.1	The three relevant spin configurations. Although there are in total $2^4 = 16$ kinds of spin configurations around the shared triangles, the proof of Eq. E.6 proceeds in a similar way for some of them. We find that the three cases shown here represent the three essentially different classes. . . . .	87

E.2	The spin configuration and the corresponding Majorana configuration for case I. . . . .	87
E.3	The spin configuration and the corresponding Majorana configuration for case II(a). . . . .	90
E.4	The spin configuration and the corresponding Majorana configuration for case II(b). . . . .	93

## LIST OF TABLES

<i>Number</i>	<i>Page</i>
2.1 Berry phases associated with the bulk three-loop braiding processes in the 3D $\mathbb{Z}_2 \times \mathbb{Z}_2$ gauge theories. For simplicity, we use CSL, APS-X, APS-Y, and APS-Z to label the $\mathbb{Z}_2 \times \mathbb{Z}_2$ gauge theories obtained by gauging the corresponding SPT models. . . . .	16
2.2 Summary of dimensional reduction results in the Walker-Wang models. We label the Walker-Wang models by their input data. The first row lists the $\mathbb{Z}_2 \times \mathbb{Z}_2$ gauge fluxes threaded through the “ $x$ -hole” after the $x$ -direction is compactified. The resulting 2D $\mathbb{Z}_2 \times \mathbb{Z}_2$ gauge theories on the $yz$ -plane are represented by the $\mathbb{Z}_2 \times \mathbb{Z}_2 \times \mathbb{Z}_2$ group elements in the entries. . . . .	24
4.1 <i>Spin</i> and <i>Pin</i> <sup>±</sup> Bordism Groups . . . . .	48
4.2 Interacting Fermionic SPT Phases . . . . .	48
4.3 Free Fermionic SPT Phases . . . . .	49
4.4 Classification of free fermionic SPT phases according to [84] and [34]. The “no symmetry” case corresponds to class D, the case $T^2 = 1$ corresponds to class BDI, the case $T^2 = (-1)^F$ corresponds to class DIII. . . . .	49

*Chapter 1*

## INTRODUCTION

Quantum phases of matter are phases of matter at zero temperature. It was believed that Landau's theory of symmetry breaking describes all quantum phases and quantum phase transitions. However, it was realized later that the fractional quantum hall states [1, 2] lie beyond the symmetry breaking description. They contain a new order called topological order, which is characterized not by local order parameters, but by topological invariants that reveal the global properties of the ground state wave function.

A key feature of these exotic phases is the existence of long-range entanglement in their ground state wave function [3]. That is, the ground state wave function cannot be connected to a product state by an adiabatic evolution that does not close the energy gap. The classification of topological phases can thus be formulated as a problem of classifying equivalence classes of entanglement patterns under gapped adiabatic evolution. The identity class in the classification, dubbed the short-range entangled phase, consists of all states that can be adiabatically evolved to a product state.

The classification of topological phases by their entanglement patterns does not include symmetry in the picture. If additional symmetries are present in the system, the phase diagram becomes richer in general [3]. For example, all phases described within the symmetry-breaking paradigm are short-range entangled. A long-range entangled phase may also be split into different phases depending on how the symmetry acts on the quasiparticle excitations in the system. A prototypical example is the aforementioned fractional quantum hall states. For example, a fractional quantum hall state with filling fraction  $\nu = 1/3$  has quasiparticle excitations that carry  $1/3$  of the electron charge. The  $U(1)$  charge conservation symmetry is acting projectively on the quasiparticle excitations, an example of what is known more generally as symmetry fractionalization [4]. Different symmetry fractionalization patterns give rise to different long-range entangled phases known as symmetry enriched topological (SET) phases [5–9].

More recently, it was realized that short-range entangled states can belong to different phases even if they do not break any symmetry spontaneously [10]. These phases are

known as symmetry protected topological (SPT) phases. They have the interesting property that the bulk of the material is trivial with no exotic excitations with fractional statistics, but the boundary is nontrivial as long as the symmetry is not broken. More precisely, the boundary state must realize the symmetry in an anomalous way, meaning that it cannot be realized consistently on its own, without the bulk material [11–23].

Over the past decade or so, there has been huge progress in the study of topological phases, particularly for non-interacting systems. Without inter-particle interactions, bosons simply form Bose-Einstein condensate, hence there is no nontrivial bosonic topological phases in this regime. On the other hand, free electrons form band structures. The band structures can have nontrivial topology, leading to nontrivial topological phases of free fermions. Examples include the famous topological insulators and topological superconductors in two and three spatial dimensions [24–32]. Topological insulators have a gapped bulk, and gapless boundary states of Dirac fermions. They have the interesting property that the nontrivial gapless boundary states are preserved as long as the charge conservation and time-reversal symmetries are preserved. In other words, the topological insulators are protected by these two symmetries. If either symmetry is broken – either spontaneously or explicitly – the boundary states will be gapped, and the topological insulators become ordinary band insulators. This makes them perfect examples of SPT phases. Analogously, topological superconductors can also be understood as SPT phases, with their nontrivial gapless boundary states of Majorana fermions protected by time-reversal symmetry. Building on these examples, people gradually gained more understanding of the free fermionic phases, which ultimately led to an exhaustive classification of topological phases of free fermions in all spatial dimensions, known as the ten-fold way [33, 34].

Strongly correlated topological phases, where particles interact strongly with each other, pose much greater challenges to theoretical analysis. To begin with, strong inter-particle interactions lead to a zoo of bosonic topological phases that are otherwise absent. In addition, strongly correlated fermion systems cannot be understood in terms of single particle states and the associated band structure. This renders our analysis for the free fermion systems invalid in this regime. Thus, a complete understanding of strongly correlated topological phases is still lacking, but people have had a relatively systematic understanding of a subset of them. This includes topological orders in two spatial dimensions and bosonic SPT phases in any spatial

dimensions.

The low-energy effective theory of 2D topological orders are (2+1)D topological quantum field theories (TQFT) [35–38], which are described mathematically by modular tensor categories (MTC) [38]. Therefore, the proper mathematical tools to describe 2D topological orders are the MTCs. Efforts have been made in classifying the MTCs, and a classification of those with ranks smaller than 5 is now in place [39]. Hamiltonian formulation which realizes the topological order in MTCs with zero central charge was proposed by Levin and Wen [40]. This is known as the string-net model, which we will introduce in more detail subsequently. If in addition, a 2D topological order is equipped with some symmetry, the resulting SET is properly described by the so-called  $G$ -crossed MTCs [8]. On the contrary, topological orders in higher dimensions and the mathematical framework to describe them are much less understood. In Chapter 2 of this thesis, we will make a modest exploration of a family 3D topological phases – gauge theories with a discrete gauge group – and hopefully provide a new perspective on these phases.

Meanwhile, a systematic theory of the bosonic SPT phases in all spatial dimensions have been developed in terms of fixed-point ground state wave functions and parent Hamiltonians constructed based on group cohomology [41]. A generalization of the theory based on group supercohomology has been proposed to classify and characterize fermionic SPT phases in all dimensions [42]. However, it can only handle cases where the symmetry group of the system is a product of discrete unitary symmetries. Furthermore, the classification is known to be incomplete for certain symmetries. In Chapters 3 and 4 of this thesis, we will study strongly correlated fermionic SPT phases using exactly solvable models and the cobordism formalism.

Generic strongly interacting Hamiltonians are difficult to solve, and it is almost impossible to decide what phases they belong to. Luckily, in certain cases, there exists exactly solvable models which describe the fixed points in the phase diagram under renormalization group flow. The Hamiltonians of these models consist of sums of local commuting projectors, and their ground state wave functions have zero correlation length. Besides providing explicit realization of the phases, the very existence of an exactly solvable model has nontrivial implications about the phase. First, the ground states of commuting projector Hamiltonians have efficient tensor network representation [43], allowing them to be treated numerically. Secondly, exactly solvable models can be useful in answering questions regarding many-body

localization in the corresponding phases, because an SPT phase can be realized in highly excited states of a many-body localized system if and only if it can be realized by a commuting projector Hamiltonian [44].

Examples of exactly solvable models that are relevant to this thesis include the string-net model [40], its three-dimensional analog the Walker-Wang model [45], and the decorated domain wall construction of SPT phases [46].

The string-net model describes a large class of two-dimensional topological orders that support a gapped edge [40]. String-net condensation provides a physical mechanism for the emergence of topological phases in real condensed matter systems. Local energetic constraints can cause the microscopic degrees of freedom to organize into effective extended objects, dubbed string nets. If the kinetic energy of these string nets is large, they can condense and give rise to a topological phase. The specific phase it gives rise to is determined by the structure of the string nets, and the form of the string-net condensation.

The Walker-Wang model generalizes the string-net model to describe 3D topological phases [45]. It has proven to be a useful tool in constructing exactly solvable models for 3D topological phases with a confined bulk, and an anomalous surface topological order [9, 14, 17, 47]. Like the string-net model, it models the ground state wave function of these phases as a condensate of loops. More specifically, Given a 2D topological order, the model is constructed such that the ground state wave function is a superposition of “3D string-nets” labeled by the quasiparticle content of the topological order, which describe the 2+1D space time trajectories of the quasiparticles. The coefficient in front of each configuration in the superposition is equal to the topological amplitude of the corresponding physical process.

The decorated domain wall construction provides a general approach to construct exactly solvable models for SPT phases [46]. In this approach, the ground state wave function is written as a superposition of all possible symmetry breaking configurations with the symmetry breaking domain walls decorated with SPT states of one lower dimension. The superposition restores the symmetry of the wave function. Moreover, when symmetry is broken into opposite domains, the domain wall carries the lower dimensional SPT state. When the domain wall ends on the boundary of the system, the end point hosts the edge state of the lower dimensional SPT state, reflecting the nontrivial nature of the original SPT order.

We make use of these models to address various issues regarding strongly correlated

topological phases in the following chapters.

In Chapter 2, we address the following question: Can the Walker-Wang model be adapted to realize the topological orders in 3D twisted gauge theories, which is a family of 3D topological phases with deconfined bulk excitations with fractional statistics? We give an affirmative answer to this question by studying the examples with gauge group  $\mathbb{Z}_2 \times \mathbb{Z}_2$ . We find that the Walker-Wang model can describe all the  $\mathbb{Z}_2 \times \mathbb{Z}_2$  gauge theories if the input data are taken to be the  $\mathbb{Z}_2 \times \mathbb{Z}_2$  symmetry charges and the quasiparticle content on the surface of some three-dimensional  $\mathbb{Z}_2 \times \mathbb{Z}_2$  SPT phases. More specifically, when the surface theory is non-anomalous (respectively, anomalous), the 3D  $\mathbb{Z}_2 \times \mathbb{Z}_2$  gauge theory is untwisted (respectively, twisted). We also propose a general scheme to perform modular transformations on the Walker-Wang model, which helps us identify the topological order in the models. Our construction provides a new perspective on twisted gauge theories, where the ground state wave function is a condensate of loops. It is in some sense, dual to the known Dijkgraaf-Witten description, where the ground state wave function is a condensate of membranes. By relating the Walker-Wang construction to the Dijkgraaf-Witten construction, our result opens up a way to study twisted gauge theories with fermionic charges, and correspondingly strongly interacting fermionic SPT phases and their surface states, through exactly solvable models.

In Chapter 3, we address the following question: Does a free fermion model of the two-dimensional time-reversal-invariant topological superconductor fit into the description of commuting projector models, which necessarily involves strong interactions between electrons? We will give a constructive proof of the existence of such a model. Our construction is based on the idea of decorated domain walls and makes use of the Kasteleyn orientation on a two dimensional lattice, which were used for the construction of the fermionic SPT phase with  $\mathbb{Z}_2$  symmetry by Tarantino and Fidkowski [48], and Ware et al. [49] By decorating the time-reversal domain walls with spinful Majorana chains, we are able to construct a commuting projector Hamiltonian with zero correlation length ground state wave function that realizes a strongly interacting version of the two dimensional topological superconductor. From our construction, it can be seen that the  $T^2 = -1$  transformation rule for the fermions is crucial for the existence of such a nontrivial phase; with  $T^2 = 1$ , our construction does not work. Our model could be valuable as a first attempt to a systematic understanding of strongly interacting fermionic SPT phases with anti-unitary symmetries in terms of exactly solvable models. Moreover, the method that

we used to incorporate time reversal symmetry can be generalized to cases when the total symmetry of the system is not of the direct product type, but a semidirect product of groups [50], or more generally a group extension of one by another.

In Chapter 4, we address the issue that the supercohomology classification of fermionic SPT phases [42] is incomplete and propose an alternative classification using the spin cobordism theory. We test this proposal in the case of fermionic SPT phases with  $\mathbb{Z}_2$  symmetry, where  $\mathbb{Z}_2$  is either time-reversal or an internal symmetry. We find that cobordism classification correctly describes all known fermionic SPT phases in space dimension  $D \leq 3$  and also predicts that all such phases can be realized by free fermions. In higher dimensions we predict the existence of intrinsically interacting fermionic SPT phases.

## TWISTED GAUGE THEORIES IN THREE-DIMENSIONAL WALKER-WANG MODELS

### 2.1 Introduction

It is an important problem in condensed matter physics to understand gapped quantum phases of matter. Two gapped systems are said to be equivalent if their Hamiltonians can be deformed into each other without closing the energy gap, or equivalently, if their ground states are related by a local unitary (LU) evolution [3]. We define a topological phase as an equivalence class of gapped systems under such deformation of the Hamiltonian or evolution of the ground state. Note that all systems whose ground state can be transformed into a product state through an LU evolution lie in the same phase called the short-range entangled (SRE) phase. Systems that are not in the SRE phase are said to be in the long-range entangled (LRE) phase.

Substantial progress has been made in the study of 2D topological phases. Topological phases in 2D are characterized by, for example, robust ground state degeneracy on spaces with nontrivial topology [51–53], gapless edge excitations [54, 55], quasiparticle excitations with anyonic statistics [56–58], and nonabelian Berry phases induced by modular transformations in the degenerate ground space on a torus (the  $S$  and  $T$  matrices) [59–61], which are directly related to the quasiparticle statistics. It was conjectured that the  $S$  and  $T$  matrices give complete description of a topological phase [60], and therefore serve as “non-local order parameters” of the phase [62]. Another approach to study topological phases in 2D is from an effective field theory point of view. Assuming that the macroscopic properties of the system are described by a topological quantum field theory (TQFT) [35–38], which in two spatial dimensions is described by the mathematical construction of a modular tensor category (MTC) [38], one can have an algebraic description of anyons in the system in terms of MTC. A subclass of the systems — those with vanishing thermal Hall conductivity (vanishing MTC central charge) and gapped boundary, admits a simple, exactly solvable Hamiltonian description in terms of the string-net models proposed by Levin and Wen [40].

What about 3D topological phases? A systematic understanding of topological phases in 3D systems is still lacking. An interesting family of 3D topological phases

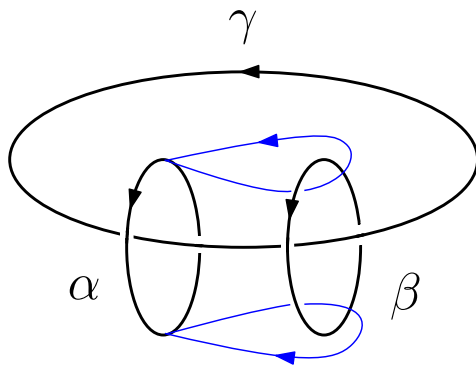


Figure 2.1: A three-loop braiding process. The process involves a flux loop  $\alpha$  sweeping out a torus enclosing a flux loop  $\beta$  while both linked with a “base” flux loop  $\gamma$ . The blue curves indicate the trajectory of two points on loop  $\alpha$ . If  $\alpha$  and  $\beta$  are identical, we can similarly define the process where  $\alpha$  and  $\beta$  are exchanged while both linked with  $\gamma$ .

is discrete gauge theories and their twisted versions, which can be described by Dijkgraaf-Witten models [63, 64]. The theory contains both point excitations and loop excitations, which are the gauge charges and flux loops, respectively. It was proposed in Ref. [65] that for twisted gauge theories with abelian gauge groups, 3D modular transformations applied to the degenerate ground states of the system on a three-torus is related to certain three-loop braiding processes illustrated in Fig. 2.1 (such braiding process has also been discussed in Ref. [66]), and can be used to distinguish different 3D twisted gauge theories. Thus, the three-loop braiding statistics (or the 3D  $S$  and  $T$  matrices) can serve as “non-local order parameters” of 3D twisted gauge theories. Dijkgraaf-Witten models provide a systematic way to study 3D twisted gauge theories. However, they fail to describe theories with (at least one) fermionic gauge charges, so it would be nice to have some other exactly solvable models, which not only give us new perspectives on 3D twisted gauge theories, but also have the potential to describe theories involving fermionic gauge charges.

Walker-Wang models [45, 47] are viable candidates to describe 3D twisted gauge theories. Given the input of a set of anyons, they provide a way to write down exactly solvable models with 3D topological order. There are two types of Walker-Wang models: Those with a trivial (short-range entangled) bulk and those with a nontrivial (long-range entangled) bulk. Quasiparticle excitations in these models are well understood. First, there are anyons that appear only on the surface of both types of models. Secondly, there are deconfined quasiparticle excitations in the

bulk of the second type of models, which can only be bosons or fermions. Besides quasiparticle excitations, Walker-Wang models also support loop excitations, but they are much less well understood. In this chapter, we address this issue by asking the question: Can Walker-Wang models describe 3D twisted gauge theories with nontrivial three-loop braiding statistics? We will give an affirmative answer to this question by solving the following two problems:

1. How do we choose the input data of the Walker-Wang models?
2. How do we determine the topological order of the output theory?

In particular, we study the examples of 3D  $\mathbb{Z}_2 \times \mathbb{Z}_2$  gauge theories. There are 4 inequivalent such theories: one untwisted gauge theory and three twisted gauge theories. We find that if we choose the input data of a Walker-Wang model to be the  $\mathbb{Z}_2 \times \mathbb{Z}_2$  symmetry charges and the anyons in the non-anomalous (respectively, anomalous) projective semion states studied in Ref. [22], the output theory is a 3D untwisted (respectively, twisted)  $\mathbb{Z}_2 \times \mathbb{Z}_2$  gauge theory. As we will see, there are 1 non-anomalous and 3 anomalous projective semion states, corresponding precisely to the 1 untwisted and 3 twisted  $\mathbb{Z}_2 \times \mathbb{Z}_2$  gauge theories, respectively.

To determine the topological order in our Walker-Wang models, we perform 3D modular transformations to their ground space on a three-torus and calculate the resulting nonabelian Berry phases. By a dimensional reduction argument, we are able to obtain the three-loop braiding statistics, which distinguish the 3D  $\mathbb{Z}_2 \times \mathbb{Z}_2$  gauge theories.

The remainder of the chapter is organized as follows: In Section 2.2, we review the Walker-Wang construction. In Section 2.3, we present the input data of the Walker-Wang models that describe the 3D  $\mathbb{Z}_2 \times \mathbb{Z}_2$  gauge theories. We also explain the physical intuition of why such input data is chosen. In Section 2.4, we introduce the methods we use to deduce the topological order in our Walker-Wang models. In Section 2.5, we summarize the results and discuss future directions. We also discuss some subtleties involved in doing 3D modular transformations on the Walker-Wang wave function. Some technical details involved in the arguments and calculations can be found in the appendices.

## 2.2 Review of Walker-Wang models

The Walker-Wang models are a class of exactly solvable models for 3D topological orders. The basic intuition behind the Walker-Wang construction is simple. Given a

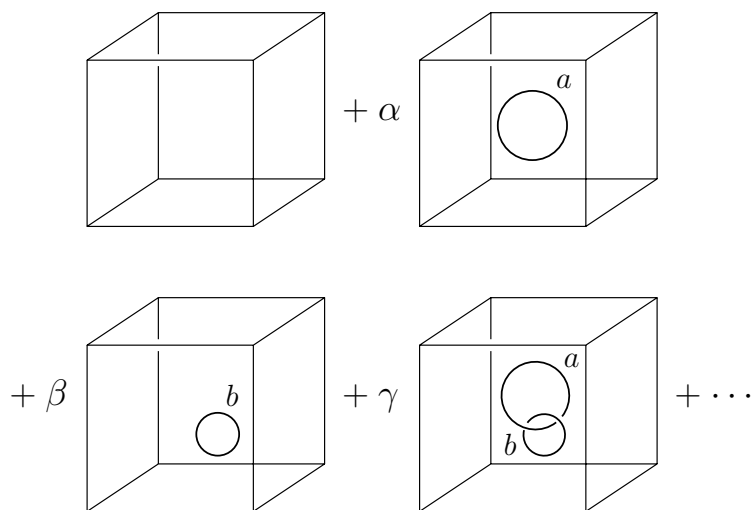


Figure 2.2: An example of the ground state wave function of a Walker-Wang model.  $a$  and  $b$  here label the quasiparticle types.

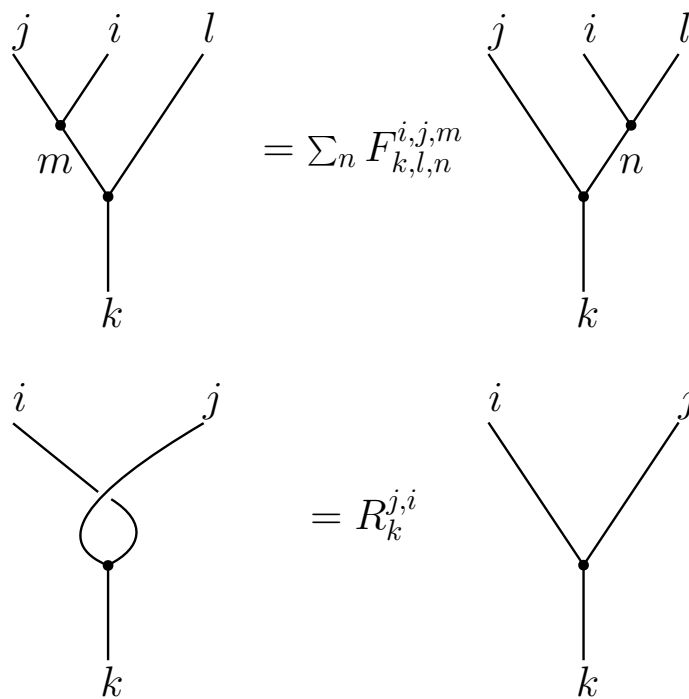


Figure 2.3: Graphical definition of  $F$  and  $R$  symbols.

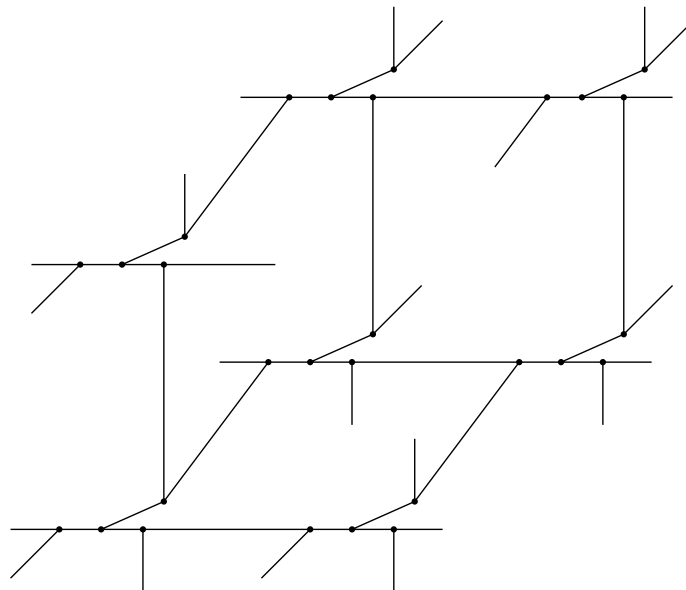


Figure 2.4: Planar projection of a trivalent resolution of the cubic lattice.

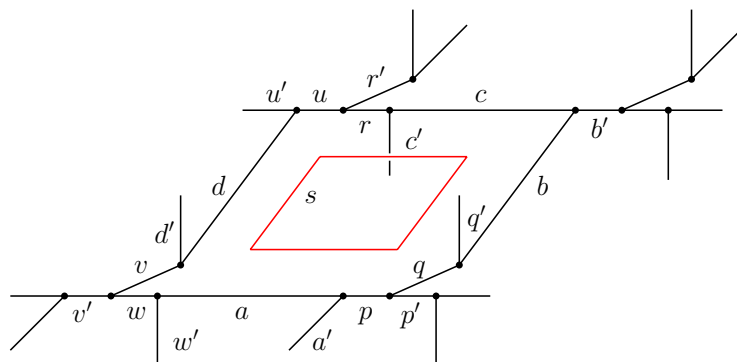


Figure 2.5: Plaquette term in the Walker-Wang Hamiltonian.

2D anyon theory, the model is constructed such that the ground state wave function is a superposition of “3D string-nets” labeled by the anyon types, which describe the 2+1D space time trajectories of the anyons (Fig. 2.2). The coefficient in front of each configuration is equal to the topological amplitude of the corresponding anyon process. It can be evaluated by using the graphical rules depicting the algebraic data of the anyon theory, captured essentially by the  $F$  and  $R$  symbols defined in Fig. 2.3, which specify the fusion and braiding rules of the anyons, respectively. The bulk-boundary correspondence described above is similar in spirit to the correspondence between quantum Hall wave functions and the edge conformal field theories. There the systems are in one dimension lower, and the bulk wave function is expressed as a correlator in the boundary CFT.

Mathematically, the input anyon theory of a Walker-Wang model is described by a braided fusion category  $\mathcal{A}$ . If  $\mathcal{A}$  is modular, which means that the only quasiparticle that braids trivially with itself and all other quasiparticles in  $\mathcal{A}$  is the vacuum, the output theory would have a trivial bulk and a surface with topological order described by  $\mathcal{A}$ , and the model belongs to the first type of Walker-Wang models we introduced in the previous section. On the other hand, if  $\mathcal{A}$  is non-modular, the output theory would have a nontrivial bulk, and the model belongs to the second type of Walker-Wang models. The surface theory in this case is more complicated because it contains not only the quasiparticles in  $\mathcal{A}$ , but also the endpoints of bulk loop excitations that are cut open by the system boundary.

To be more concrete, let us illustrate with two examples. First, we consider the simplest nontrivial input  $\mathcal{A}$  possible, which consists of only the vacuum  $I$  and a boson  $e$ .  $\mathcal{A}$  is non-modular because  $e$  is distinct from the vacuum but braids trivially with everything in  $\mathcal{A}$ . A Walker-Wang model with such input describes the 3D  $\mathbb{Z}_2$  gauge theory with  $e$  being the  $\mathbb{Z}_2$  gauge charge, which is deconfined in the bulk and on the boundary [47]. Next, we modify  $\mathcal{A}$  a bit by replacing the boson  $e$  with a semion  $s$ .  $\mathcal{A}$  becomes modular in this case, because  $s$  braids nontrivially with itself. A Walker-Wang model with the modified input has a trivial bulk and a deconfined semion excitation  $s$  on the boundary [47].

In general, deconfined bulk quasiparticle excitations of a Walker-Wang model correspond to quasiparticles in the symmetric center  $\mathcal{Z}(\mathcal{A})$  of the input braided fusion category  $\mathcal{A}$ . A quasiparticle belongs to  $\mathcal{Z}(\mathcal{A})$  if it has trivial braiding with itself and all other quasiparticles in  $\mathcal{A}$ . If  $\mathcal{A}$  is modular,  $\mathcal{Z}(\mathcal{A})$  is trivial, which is consistent with the fact that a Walker-Wang model with modular input has a trivial bulk. If  $\mathcal{A}$  is non-modular, it is known that there are two possibilities for  $\mathcal{Z}(\mathcal{A})$  [67]: (1)  $\mathcal{Z}(\mathcal{A})$  contains only bosons. In this case, it can be identified with the set of irreducible representations of some finite group  $G$ ; (2)  $\mathcal{Z}(\mathcal{A})$  contains at least one fermion. In this case, it can also be identified with the set of irreducible representations of some finite group  $G$ , but each representation comes with a parity, and the set is split into even and odd sectors, corresponding to the bosons and fermions in  $\mathcal{Z}(\mathcal{A})$ , respectively. Thus, the deconfined bulk quasiparticle excitations of a Walker-Wang model with non-modular input correspond to the irreducible representations of some finite group, and it is plausible that the bulk topological order of the model is a gauge theory of the corresponding group.

Before delving into the exploration of the above possibility, let us review some details

of Walker-Wang models. We closely follow Ref. [45] and refer the reader there for further details. Walker-Wang models are defined on a fixed planar projection of a trivalent resolution of the cubic lattice as shown in Fig. 2.4. The Hilbert space of a model defined on the lattice is spanned by all labelings of the edges by the input anyon types. The Hamiltonian is of the form

$$H = - \sum_v A_v - \sum_p B_p, \quad (2.1)$$

where  $A_v$  is a vertex term which enforces the fusion rules at  $v$  by giving an energy penalty to string configurations that violate the fusion rules at  $v$ , and  $B_p$  is a plaquette term of the form  $B_p = \sum_s d_s B_p^s$ , where the summation is over all the input anyon types  $s$ , weighted by the quantum dimension of  $s$ . Each  $B_p^s$  acts on the anyon labels of the edges around plaquette  $p$ , in a way determined by the anyon labels of the edges adjoining  $p$ . More explicitly, the matrix element of  $B_p^s$  sandwiched between states with plaquette edges  $(a'', b'', c'', d'', p'', q'', r'', u'', v'', w'')$  and  $(a, b, c, d, p, q, r, u, v, w)$  is given by

$$\begin{aligned} (B_p^s)_{(a,b,c,d,p,q,r,u,v,w)}^{(a'',b'',c'',d'',p'',q'',r'',u'',v'',w'')} &= R_q^{bq'} (R_c^{rc'})^* (R_{q''}^{b''q'})^* \times \\ &R_{c''}^{r''c'} F_{a'pa}^{sa''p''} F_{p'qp}^{sp''q''} F_{q'bq}^{sq''b''} F_{b'cb}^{sb''c''} F_{c'rc}^{sc''r''} F_{r''us}^{sr''u''} F_{u'du}^{su''d''} \times \\ &F_{d''vd}^{sd''v''} F_{v'wv}^{sv''w''} F_{w'aw}^{sw''a''}, \end{aligned} \quad (2.2)$$

The above expression looks rather complicated, but there is a simple graphical way of understanding the action of  $B_p^s$ . Namely,  $B_p^s$  temporarily displaces certain links ( $c'$  and  $q'$  in Fig. 2.5) and fuses a loop with anyon label  $s$  to the skeleton of  $p$ . One can check that all terms in the Hamiltonian commute, and the model is exactly solvable.

To be able to discuss point and loop excitations in Walker-Wang models, we also need to define string operators and membrane operators in these models. The string operators have a graphical definition analogous to that of the plaquette operators. Namely, to create a pair of quasiparticle excitations  $\alpha \in \mathcal{A}$  at two points, we just need to lay an  $\alpha$ -string connecting the two points, and then fuse it to the edges of the lattice. Furthermore, one can show that the string operator commutes (respectively, fails to commute) with the plaquette operators threaded by the string if  $\alpha \in \mathcal{Z}(\mathcal{A})$  (respectively,  $\alpha \notin \mathcal{Z}(\mathcal{A})$ ), and the corresponding quasiparticles are deconfined (respectively, confined) in the bulk. On the other hand, all quasiparticles in  $\mathcal{A}$  are deconfined on the boundary, because string operators restricted to the boundary do not thread any plaquettes and hence there is no energy penalty associated with

them. Unlike the string operators, in general, we do not know how to implement membrane operators in Walker-Wang models, but as we will show below, we can deduce the statistics of the loop excitations without explicitly writing down the membrane operators.

### 2.3 $\mathbb{Z}_2 \times \mathbb{Z}_2$ gauge theories in the Walker-Wang models

In this section, we discuss how the 3D  $\mathbb{Z}_2 \times \mathbb{Z}_2$  gauge theories can be described by Walker-Wang models. In particular, we ask the question: How do we find the input data of the Walker-Wang models that will generate the twisted gauge theories? Our insight into solving this problem comes from the study of 3D  $\mathbb{Z}_2 \times \mathbb{Z}_2$  symmetry protected topological (SPT) phases, which are a class of gapped short-range entangled phases of matter protected by a global symmetry. A nontrivial SPT phase has the interesting property that its surface state is anomalous [19–22], meaning that it cannot exist on its own and must be realized as the boundary of some system in one dimension higher. This implies that a gapped symmetric surface of a nontrivial SPT phase must have nontrivial topological order, and that the symmetry must fractionalize on the anyons in an anomalous way. Specifically to the  $\mathbb{Z}_2 \times \mathbb{Z}_2$  SPTs, we will first review a particular kind of gapped symmetric surface states of these SPTs, called the projected semion states. We will introduce its anyon content, and the symmetry fractionalization pattern of  $\mathbb{Z}_2 \times \mathbb{Z}_2$  on the anyons. Next, we couple the systems to a  $\mathbb{Z}_2 \times \mathbb{Z}_2$  gauge field, and study the surface theories of the gauged systems. Finally, it is known that upon gauging, a trivial (respectively, nontrivial) SPT becomes an untwisted (respectively, twisted) gauge theory [68], which leads us to propose a Walker-Wang model description of the  $\mathbb{Z}_2 \times \mathbb{Z}_2$  gauge theories based on the surface anyon content of the gauged  $\mathbb{Z}_2 \times \mathbb{Z}_2$  SPTs.

#### Projective semion states and 3D $\mathbb{Z}_2 \times \mathbb{Z}_2$ SPTs

The projective semion states are 2D symmetry fractionalization patterns with a semion and a  $\mathbb{Z}_2 \times \mathbb{Z}_2$  symmetry, first introduced and analyzed in Ref. [22] and Ref. [20]. They may be considered as variants of the Kalmeyer-Laughlin chiral spin liquid (CSL) [69].

We first give a brief review of the Kalmeyer-Laughlin CSL. The topological order of the theory is the same as that of the  $\nu = 1/2$  bosonic fractional quantum Hall state. The only nontrivial quasiparticle is a semion, which has topological spin  $i$  and fuses into the vacuum with another semion. Moreover, the semion carries a spin-1/2, transforming projectively under the  $SO(3)$  symmetry. The CSL can thus

be understood as a symmetry fractionalization pattern of  $SO(3)$  on a semion. The theory is non-anomalous, because it can be realized in a purely 2D system with the explicit construction in Ref. [69].

To describe the projective semion states, we reduce the  $SO(3)$  symmetry to a  $\mathbb{Z}_2 \times \mathbb{Z}_2$  subgroup, consisting of rotations along the  $x$ ,  $y$ , and  $z$  axes by 180 degrees, which we denote by  $g_x$ ,  $g_y$ , and  $g_z$ , respectively. By restricting the spin-1/2 representation of  $SO(3)$  to this reduced symmetry group, we obtain a projective representation of  $\mathbb{Z}_2 \times \mathbb{Z}_2$ :

$$\text{CSL: } g_x = i\sigma_x, \quad g_y = i\sigma_y, \quad g_z = i\sigma_z. \quad (2.3)$$

The CSL is therefore a symmetry fractionalization pattern of  $\mathbb{Z}_2 \times \mathbb{Z}_2$  on a semion where the semion carries a half charge under all nontrivial group elements, because acting a nontrivial group element twice on a spin-1/2 is equivalent to rotating the spin-1/2 by 360 degrees along the corresponding axis, which results in a phase factor of  $-1$ .

However, the CSL is not the only possible symmetry fractionalization pattern of  $\mathbb{Z}_2 \times \mathbb{Z}_2$  on a semion. The semion can also transform under other projective representations of  $\mathbb{Z}_2 \times \mathbb{Z}_2$ . More specifically, the semion can carry either integral or half-integral charges under the nontrivial elements of  $\mathbb{Z}_2 \times \mathbb{Z}_2$ , and we have 3 variants of the CSL, called the ‘‘anomalous projective semion’’ (APS) states, where the symmetry action on the semion can be represented as

$$\begin{aligned} \text{APS-X: } & g_x = i\sigma_x, \quad g_y = \sigma_y, \quad g_z = \sigma_z, \\ \text{APS-Y: } & g_x = \sigma_x, \quad g_y = i\sigma_y, \quad g_z = \sigma_z, \\ \text{APS-Z: } & g_x = \sigma_x, \quad g_y = \sigma_y, \quad g_z = i\sigma_z. \end{aligned} \quad (2.4)$$

If we take  $g_x$  and  $g_y$  to be the two generators of  $\mathbb{Z}_2 \times \mathbb{Z}_2$ , the APS-X, APS-Y, and APS-Z theories correspond to the cases where the semion carries a half charge under either the first, second, or both generators, respectively. It was argued in Ref. [22] and Ref. [20] that the addition of such half charges to the CSL, though compatible with the fusion rules of the semion, leads to anomalies in the theory. This can be seen via the violation of the pentagon equations for the symmetry defects [22] or the failure in promoting the global symmetry to a gauge symmetry [20] in the effective field theory (dubbed the ’t Hooft anomaly [70]). The anomalous projective semion theories are therefore not realizable in purely 2D systems. Nevertheless, they can

Table 2.1: Berry phases associated with the bulk three-loop braiding processes in the 3D  $\mathbb{Z}_2 \times \mathbb{Z}_2$  gauge theories. For simplicity, we use CSL, APS-X, APS-Y, and APS-Z to label the  $\mathbb{Z}_2 \times \mathbb{Z}_2$  gauge theories obtained by gauging the corresponding SPT models.

	$\theta_{x,y}$	$\theta_{y,x}$
CSL	0	0
APS-X	0	$\pi/2$
APS-Y	$\pi/2$	0
APS-Z	$\pi/2$	$\pi/2$

be realized on the boundary of some nontrivial 3D  $\mathbb{Z}_2 \times \mathbb{Z}_2$  SPT phases. Exactly solvable models for such 3D SPT phases based on the “decorated” Walker-Wang models were constructed in Ref. [22]. More specifically, the semion Walker-Wang model studied in Ref. [47] is decorated with unitary linear representations of  $\mathbb{Z}_2 \times \mathbb{Z}_2$ , such that the ground state wave function is a loop gas of semion lines dressed with  $\mathbb{Z}_2 \times \mathbb{Z}_2$  Haldane chains. The endpoints of open semion lines, which are deconfined semion excitations on the boundary, carry projective representations of  $\mathbb{Z}_2 \times \mathbb{Z}_2$  as in Eq. (2.4). Therefore, the boundary of the 3D SPT phases are precisely the anomalous projective semion states. Similarly, one can construct a trivial 3D SPT phase which realizes the non-anomalous projective semion state on its boundary. With a slight modification of the  $\mathbb{Z}_2 \times \mathbb{Z}_2$  Haldane chains, the boundary semion excitations can be made to transform under  $\mathbb{Z}_2 \times \mathbb{Z}_2$  as in Eq. (2.3), as desired for a CSL. We will not delve into the details of the construction. The interested reader may refer to Ref. [22] for more information.

### Gauging the $\mathbb{Z}_2 \times \mathbb{Z}_2$ symmetry

Now, suppose we couple the models discussed above to a  $\mathbb{Z}_2 \times \mathbb{Z}_2$  gauge field. We obtain a 3D untwisted (respectively, twisted)  $\mathbb{Z}_2 \times \mathbb{Z}_2$  gauge theory if the system is in a trivial (respectively, nontrivial) SPT phase. These  $\mathbb{Z}_2 \times \mathbb{Z}_2$  gauge theories can be distinguished by the following three-loop braiding processes in the bulk: (1) Two  $g_x$ -flux loops exchanged while both linked with a  $g_y$ -flux loop; (2) Two  $g_y$ -flux loops exchanged while both linked with a  $g_x$ -flux loop. We denote the associated Berry phases by  $\theta_{x,y}$  and  $\theta_{y,x}$ , respectively. The numerical values of  $\theta_{x,y}$  and  $\theta_{y,x}$  for the various 3D  $\mathbb{Z}_2 \times \mathbb{Z}_2$  gauge theories are listed in Table 2.1.

It is shown in Ref. [71] that the gauged systems host three types of excitations on or near the surface (Fig. 2.6): (1) gauge charges that can appear in the bulk and on the

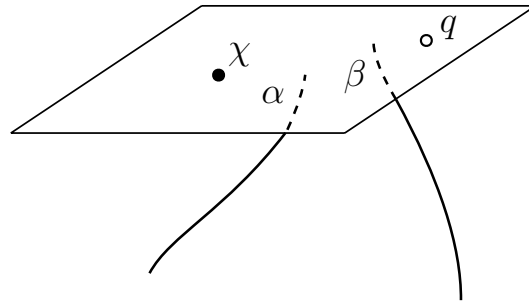


Figure 2.6: Sketch of surface excitations in a gauged SPT model. The bulk is below the plane.  $q$  represents a gauge charge that can appear in the bulk and on the surface.  $\chi$  represents an anyon that can appear only on the surface.  $\alpha$  and  $\beta$  represent the flux lines in the bulk that end on the surface.

boundary; (2) flux loops in the bulk that become open flux lines when ending on the boundary; (3) anyons that are pinned to the boundary. It is further argued in the same reference that each surface anyon  $\tilde{\chi}$  in the gauged model is naturally associated with a surface anyon  $\chi$  in the ungauged model.  $\chi$  is referred to as the “anyonic flux” carried by  $\tilde{\chi}$ . In our case, the only nontrivial surface anyon in the ungauged model is a semion  $s$ . Correspondingly, there is one and only one nontrivial surface anyon in the gauged model, which is  $\tilde{s}$ . The set of excitations in the gauged model therefore consists of  $\tilde{s}$  and the gauge charges and flux loops of  $\mathbb{Z}_2 \times \mathbb{Z}_2$ .

Having understood the excitations in the 3D  $\mathbb{Z}_2 \times \mathbb{Z}_2$  gauge theories, let us try to incorporate them into the Walker-Wang construction of the 3D  $\mathbb{Z}_2 \times \mathbb{Z}_2$  gauge theories. Since the deconfined quasiparticle excitations on the surface include the  $\mathbb{Z}_2 \times \mathbb{Z}_2$  gauge charges and the anyon with anyonic flux  $s$ , based on the physical picture that the bulk wave function of a Walker-Wang model is the space time trajectories of the quasiparticles on the surface, we expect that if we use the  $\mathbb{Z}_2 \times \mathbb{Z}_2$  gauge charges and the surface anyon  $\tilde{s}$  to write a Walker-Wang model, we should get a 3D  $\mathbb{Z}_2 \times \mathbb{Z}_2$  gauge theory. In the next subsection, we will make this idea more concrete by explicitly constructing the input data for the Walker-Wang models that describe the  $\mathbb{Z}_2 \times \mathbb{Z}_2$  gauge theories.

### Input data of the Walker-Wang models

We start by introducing some notations. We denote by  $\rho_I$ ,  $\rho_x$ ,  $\rho_y$ , and  $\rho_z$  the 1-dimensional representations of  $\mathbb{Z}_2 \times \mathbb{Z}_2$ , defined by

$$\begin{aligned} \rho_I(g_x) &= 1, & \rho_I(g_y) &= 1, \\ \rho_x(g_x) &= -1, & \rho_x(g_y) &= 1, \end{aligned}$$

Fusion rules:	Quantum dimensions and topological spins:
$1 \times 1 = 0, 2 \times 2 = 0, 3 \times 3 = 0$	$d_0 = d_1 = d_2 = d_3 = 1, d_m = 2n$
$1 \times 2 = 3, 2 \times 3 = 1, 3 \times 1 = 2$	$\theta_0 = \theta_1 = \theta_2 = \theta_3 = \theta_m = 1$
$1 \times m = m, 2 \times m = m, 3 \times m = m$	
$m \times m = 0 + 1 + 2 + 3$	
R symbols:	F symbols:
$R_a^{0,a} = R_a^{a,0} = R_0^{a,a} = 1$	$F_{abc,c,ab}^{b,a,ab} = F_{m,m,m}^{b,a,ab} = F_{m,b,ab}^{a,m,m} = F_{ab,m,b}^{m,a,m} = F_{ab,a,m}^{m,m,b} = 1$
$R_{xy}^{x,y} = -1$	$F_{m,b,m}^{m,a,m} = F_{b,m,m}^{a,m,m} = \chi(a,b)$
$R_m^{a,m} = R_m^{m,a} = s_a$	$F_{m,m,b}^{m,m,a} = n\chi(a,b)/2$
$R_a^{m,m} = ns_a$	

Figure 2.7: Data for  $\text{Rep}(Q_8)$  and  $\text{Rep}(D_4)$ . The (simple) objects are the irreducible representations (charges) of either  $Q_8$  or  $D_4$ , defined in Eq. (2.7) and Eq. (2.8). They are all self-dual. Here  $a, b = 0, 1, 2, 3$ , and  $x, y = 1, 2, 3, x \neq y$ .  $\chi$  is defined by  $\chi(0, a) = \chi(a, 0) = 1$ ,  $\chi(x, x) = 1$ , and  $\chi(x, y) = -1$ . The quantum dimension of a charge is defined to be the product of its Frobenius-Schur indicator and dimension. The  $F$  symbols with  $n = -1$  (respectively,  $n = 1$ ) are the  $6j$  symbols of  $Q_8$  (respectively,  $D_4$ ). The  $R$  symbols are solutions to the hexagon equations (given the  $F$  symbols) with the constraint that all charges are bosonic and have trivial mutual statistics. For  $Q_8$ , there exists a unique solution,  $n = -1, s_0 = 1, s_1 = s_2 = s_3 = -1$ . For  $D_4$ , there exists 3 solutions,  $n = 1, s_0 = 1, s_1 = -1, s_2 = 1, s_3 = 1$ , and also the ones resulting from the permutations  $1 \leftrightarrow 2$  and  $1 \leftrightarrow 3$ , respectively.

$$\begin{aligned} \rho_y(g_x) &= 1, & \rho_y(g_y) &= -1, \\ \rho_z(g_x) &= -1, & \rho_z(g_y) &= -1, \end{aligned} \tag{2.5}$$

We start by introducing some notations. We denote by  $Q_8$  the quaternion group, and  $D_4$  the dihedral group of order 8, defined by the presentations

$$\begin{aligned} Q_8 &= \langle x, y | x^2 = y^2 = (xy)^2, x^4 = 1 \rangle, \\ D_4 &= \langle x, y | x^4 = y^2 = (xy)^2 = 1 \rangle. \end{aligned} \tag{2.6}$$

We denote by  $G$  either  $Q_8$  or  $D_4$ . The irreducible representations (charges) of  $G$  consist of four 1-dimensional charges, given by

$$\begin{aligned} \rho_0(x) &= 1, & \rho_0(y) &= 1, \\ \rho_1(x) &= 1, & \rho_1(y) &= -1, \end{aligned}$$

$$\begin{aligned}\rho_2(x) &= -1, & \rho_2(y) &= 1, \\ \rho_3(x) &= -1, & \rho_3(y) &= -1,\end{aligned}\tag{2.7}$$

and one 2-dimensional charge, given by

$$\begin{aligned}m(x) &= i\sigma_z, & m(y) &= i\sigma_y, & \text{for } G &= Q_8, \\ m(x) &= i\sigma_z, & m(y) &= \sigma_x, & \text{for } G &= D_4.\end{aligned}\tag{2.8}$$

For simplicity, we denote the 1-dimensional charges  $\rho_a$  of  $G$  by  $a$  ( $a = 0, 1, 2, 3$ ), which form a  $\mathbb{Z}_2 \times \mathbb{Z}_2$  group under the tensor product of representations. The charges of  $G$  form a braided fusion category  $\text{Rep}(G)$  with the fusion and braiding data presented in Fig. 2.7. It is known that a Walker-Wang model with input data  $\text{Rep}(G)$  describes a 3D untwisted  $G$ -gauge theory [40].

Next, we construct the input data for the Walker-Wang models that describe the  $\mathbb{Z}_2 \times \mathbb{Z}_2$  gauge theories. It is useful to first study the fusion rules satisfied by the quasiparticles on the surface. From representation theory, we know that the tensor product of the projective representation of  $\mathbb{Z}_2 \times \mathbb{Z}_2$  carried by the semion  $s$  (Eq. (2.3) or Eq. (2.4)) with itself gives a reducible linear representation of  $\mathbb{Z}_2 \times \mathbb{Z}_2$ , which can be further decomposed into a direct sum of the four 1-dimensional representations of  $\mathbb{Z}_2 \times \mathbb{Z}_2$ . After the gauging procedure, the symmetry charges are promoted to gauge charges, which are deconfined quasiparticle excitations, and the fusion rule of representations becomes the fusion rule of quasiparticles:

$$\tilde{s} \times \tilde{s} = 0 + 1 + 2 + 3,\tag{2.9}$$

where we have identified the charges of  $\mathbb{Z}_2 \times \mathbb{Z}_2$  with the 1-dimensional charges of  $G$  on the right hand side. Eq. (2.9) is identical to the fusion between two 2-dimensional charges  $m$  of  $G$  in Fig. 2.7, provided that we further identify  $\tilde{s}$  with  $m$ . However, the topological spin of  $\tilde{s}$  (respectively,  $m$ ) is  $i$  (respectively, 1), so  $m$  needs to be “twisted” by a semion before we can make the identification. The precise meaning of this is that we multiply all the  $F$  symbols  $F_{mmb}^{mma}$  ( $a, b = 0, 1, 2, 3$ ) in Fig. 2.7 by  $-1$ , and all the  $R$  symbols  $R_a^{mm}$  ( $a = 0, 1, 2, 3$ ) in Fig. 2.7 by  $i$ . One can check that  $\text{Rep}(G)$  remains a consistent braided fusion category after the modifications, i.e., the pentagon equations and hexagon equations are satisfied. For convenience, we will denote the modified category by  $\text{Rep}_s(G)$ .<sup>1</sup> Furthermore,

<sup>1</sup>Fusion categories with fusion rules that of  $\text{Rep}(G)$  and  $\text{Rep}_s(G)$  are actually examples of the Tambara-Yamagami categories [72] based on the group  $\mathbb{Z}_2 \times \mathbb{Z}_2$ . Not all Tambara-Yamagami categories admit consistent braiding as  $\text{Rep}(G)$  and  $\text{Rep}_s(G)$  do.

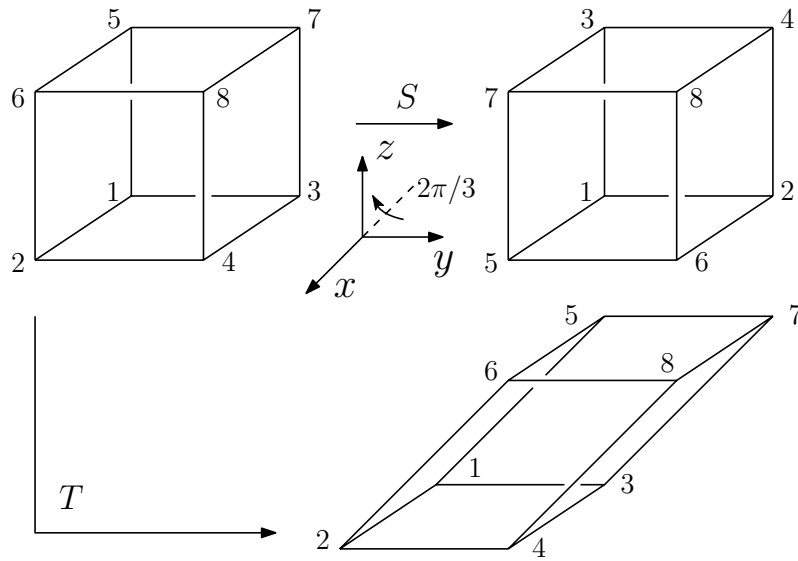
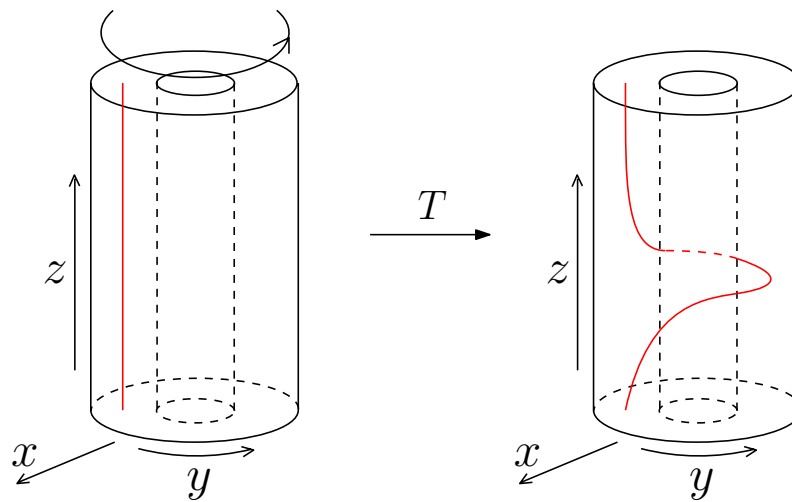
comparison between Eq. (2.8) and Eq. (2.3) (respectively, Eq. (2.4)) shows that we should take  $G$  to be  $Q_8$  (respectively,  $D_4$ ) if  $s$  carries the projective representation in Eq. (2.3) (respectively, Eq. (2.4)).<sup>2</sup> Therefore, after the identification above, the fusion and braiding information of the quasiparticles on the surface of a 3D untwisted (respectively, twisted)  $\mathbb{Z}_2 \times \mathbb{Z}_2$  gauge theory are neatly captured by the braided fusion category  $\text{Rep}_s(Q_8)$  (respectively,  $\text{Rep}_s(D_4)$ ), which leads us to the proposal that a Walker-Wang model with input  $\text{Rep}_s(Q_8)$  (respectively,  $\text{Rep}_s(D_4)$ ) describes a 3D untwisted (respectively, twisted)  $\mathbb{Z}_2 \times \mathbb{Z}_2$  gauge theory.

Physically, the semion-twisted 2-dimensional charge of  $G$  is an anyon, which is confined in the bulk and deconfined on the boundary because it braids nontrivially with itself. The 1-dimensional charges of  $G$  remain deconfined in the bulk and on the boundary. The set of quasiparticle excitations in the Walker-Wang models therefore agrees with that in the  $\mathbb{Z}_2 \times \mathbb{Z}_2$  gauge theories described in Section 2.3, provided that our identification between the twisted 2-dimensional charge of  $G$  and the surface anyon  $\tilde{s}$  is correct. The identification between the 1-dimensional charges of  $G$  and the  $\mathbb{Z}_2 \times \mathbb{Z}_2$  gauge charges are natural because their fusion and braiding data are identical. In the next section, we will give a more direct verification that the Walker-Wang models we proposed indeed describe the  $\mathbb{Z}_2 \times \mathbb{Z}_2$  gauge theories. More specifically, we will compute the three-loop braiding statistics in our models and check that they agree with those listed in Table 2.1.

## 2.4 Detecting the topological order in the Walker-Wang models

In this section, we verify that the Walker-Wang models we proposed in the previous section describe the 3D  $\mathbb{Z}_2 \times \mathbb{Z}_2$  gauge theories. Our approach is to do 3D modular transformations to the ground space of our Walker-Wang models on a three-torus and calculate the resulting nonabelian Berry phases. Similar methods have been used to determine the topological order in chiral spin liquid [73], 2D topological orders represented by tensor networks [74, 75], 2D string-net models [76], and untwisted or twisted quantum double models in 2D [77] and 3D [65, 78, 79]. Furthermore, by making a dimensional reduction argument, we are able to deduce the three-loop braiding statistics of our models. We can compare them with the data listed in Table 2.1 to determine which  $\mathbb{Z}_2 \times \mathbb{Z}_2$  gauge theory a particular model is describing.

<sup>2</sup>It is a mathematical fact that given a projective representation of a group  $G$ , one can lift it to a linear representation of a different group  $C$ , which is a central extension of  $G$ . In our cases, one can actually show that the projective representation in Eq. (2.3) (respectively, Eq. (2.4)) can be lifted to a linear representation of  $Q_8$  (respectively,  $D_4$ ), which is a central extension of  $\mathbb{Z}_2 \times \mathbb{Z}_2$  by  $\mathbb{Z}_2$ .

Figure 2.8:  $S$  and  $T$  transformations on a three-torus.Figure 2.9:  $T$  transformation as the Dehn twist of a hollow cylinder.

### $S$ and $T$ matrices from 3D modular transformations

The 3D modular transformations are elements of the mapping class group of the three-torus  $\text{MCG}(\mathbb{T}^3) = \text{SL}(3, \mathbb{Z})$ . The group has two generators,  $S$  and  $T$ , which are of the form

$$S = \begin{pmatrix} 0 & 0 & 1 \\ 1 & 0 & 0 \\ 0 & 1 & 0 \end{pmatrix}, \quad \text{and} \quad T = \begin{pmatrix} 1 & 0 & 0 \\ 0 & 1 & 1 \\ 0 & 0 & 1 \end{pmatrix}. \quad (2.10)$$

If we represent the three-torus as a cube with opposite faces identified, and if we draw the cube in a right-handed coordinate frame as in Fig. 2.8, then  $S$  is a clockwise

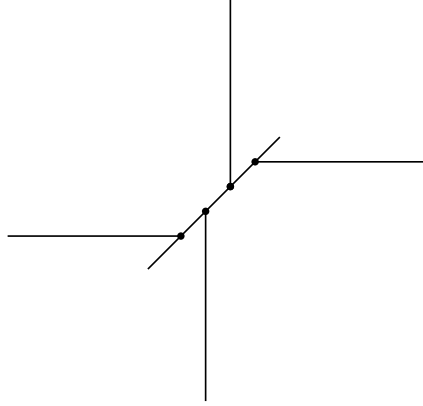


Figure 2.10: A “minimal” trivalent lattice on the three-torus, which consists of 4 vertices, 6 edges, and 3 plaquettes.

rotation of the cube by  $120^\circ$  along a diagonal, and  $T$  is a shear transformation in the  $yz$ -plane. There is another way to visualize the  $T$  transformation. By closing the periodic direction of the cube along the  $z$  axis, we can equivalently think of the three-torus as a hollow cylinder with the top and bottom faces identified, and inner and outer faces identified (Fig. 2.9). The  $T$  transformation then becomes the Dehn twist of the hollow cylinder along the  $yz$ -plane.

Note that the 2D modular transformations in the  $yz$ -plane, generated by

$$S_{yz} = \begin{pmatrix} 1 & 0 & 0 \\ 0 & 0 & -1 \\ 0 & 1 & 0 \end{pmatrix}, \quad \text{and} \quad T_{yz} = \begin{pmatrix} 1 & 0 & 0 \\ 0 & 1 & 1 \\ 0 & 0 & 1 \end{pmatrix}, \quad (2.11)$$

form an  $SL(2, \mathbb{Z})$  subgroup of  $SL(3, \mathbb{Z})$ , so they can be written as a combination of  $S$ ,  $T$ , and their inverses. In particular,

$$S_{yz} = (T^{-1}S)^3(ST)^2ST^{-1}, \quad \text{and} \quad T_{yz} = T. \quad (2.12)$$

A presentation of  $SL(3, \mathbb{Z})$  is obtained by specifying the relations among the generators [? ]:

$$\begin{aligned} S^3 &= S_{yz}^4 = (S_{yz}S)^2 = (T^{-1}SS_{yz}^2S^{-1})^2 = I, \\ S^{-1}TSTS^{-1}T^{-1}ST^{-1} &= S_{yz}S^{-1}TSS_{yz}^{-1}, \\ (T^{-1}S_{yz}^{-1})^3 &= (S_{yz})^2, \quad [S_{yz}TS_{yz}^{-1}, STS^{-1}] = I, \\ [S_{yz}TS_{yz}^{-1}, S^{-1}TS] &= I, \end{aligned} \quad (2.13)$$

where  $[A, B] = ABA^{-1}B^{-1}$  denotes the commutator of matrices  $A$  and  $B$ .

Since Walker-Wang models are fixed-point models and are scale-invariant, we can apply the  $S$  and  $T$  transformations to a model defined on a “minimal” trivalent lattice on the three-torus (Fig. 2.10). The Hilbert space of a model defined on the lattice is spanned by all labelings of the edges by the input anyon types that are consistent with the fusion rules. Each such labeling can be denoted by a sextuple  $(i, j, k, l, m, n)$ , where each entry corresponds to a particular input anyon type. For the modified  $Q_8$  and  $D_4$  input data discussed in Section 2.3, the Hilbert spaces on the lattice are all of dimension 176. The matrix elements of the  $S$  and  $T$  matrices are derived in Appendix A, and are given by

$$\begin{aligned} S_{(i,j,k,l,m,n)}^{(k,i,j,\tilde{n},\tilde{m},\tilde{l})} &= F_{km\tilde{l}}^{jil} F_{j\tilde{i}\tilde{n}}^{kmn} F_{j\tilde{n}\tilde{m}}^{j\tilde{l}m}, \\ T_{(i,j,k,l,m,n)}^{(i,\tilde{l},k,m,\tilde{n},\tilde{j})} &= F_{km\tilde{n}}^{k\tilde{j}n} F_{in\tilde{j}}^{k\tilde{l}j} (R_{\tilde{l}}^{kj})^* F_{j\tilde{l}}^{mkl} R_m^{kl}. \end{aligned} \quad (2.14)$$

Note that there is an additional complication due to the non-abelian fusion rules of the input anyons. By computing the Hamiltonian of our Walker-Wang models on the minimal lattice (see Appendix B), we find that the ground space of the Hamiltonian is only a 64 dimensional subspace of the 176 dimensional Hilbert space on the lattice, so the ground state degeneracy of our models matches that of the 3D  $\mathbb{Z}_2 \times \mathbb{Z}_2$  gauge theories. To restrict the modular transformations to be within the ground space, we need to diagonalize the Hamiltonian, and project the  $S$  and  $T$  matrices to the ground space of the Hamiltonian, as explained in the appendix. The 64 by 64  $S$  and  $T$  matrices thus obtained satisfy the relations in Eq. (2.13), so that they form a representation of the  $SL(3, \mathbb{Z})$  group. They encode all the braiding statistics of our 3D topological orders, but it takes a bit more work to read them out, which is done in the next subsection.

### Dimensional reduction and three-loop braiding statistics from the $S$ and $T$ matrices.

We first review the dimensional reduction phenomenon in 3D discrete gauge theories and its connection to the three-loop braiding processes. For our purposes, it suffices to consider theories with an abelian gauge group  $G$  and abelian statistics. It was observed in Ref. [78] and Ref. [79] that the 2D modular matrices  $S_{yz}$  and  $T_{yz}$  of a 3D  $G$ -gauge theory  $C^{3D}$  admit the following direct sum decomposition:

$$S_{yz} = \bigoplus_g S_{yz,g}, \quad T_{yz} = \bigoplus_g T_{yz,g}, \quad (2.15)$$

where  $g$  runs over all gauge fluxes (group elements) of  $G$ , and each pair  $(S_{yz,g}, T_{yz,g})$  describes some particular 2D  $G$ -gauge theory  $C_g^{2D}$ . Furthermore, the basis in

Table 2.2: Summary of dimensional reduction results in the Walker-Wang models. We label the Walker-Wang models by their input data. The first row lists the  $\mathbb{Z}_2 \times \mathbb{Z}_2$  gauge fluxes threaded through the “ $x$ -hole” after the  $x$ -direction is compactified. The resulting 2D  $\mathbb{Z}_2 \times \mathbb{Z}_2$  gauge theories on the  $yz$ -plane are represented by the  $\mathbb{Z}_2 \times \mathbb{Z}_2 \times \mathbb{Z}_2$  group elements in the entries.

	Trivial	$g_x$	$g_y$	$g_z$
$\text{Rep}_s(Q_8)$	1	1	1	1
$\text{Rep}_s(D_4)$	1	$\omega_2$	$\omega_{12}$	$\omega_2\omega_{12}$
$\text{Rep}_s(D_4)$ with $1 \leftrightarrow 2$	1	$\omega_{12}$	$\omega_1$	$\omega_1\omega_{12}$
$\text{Rep}_s(D_4)$ with $1 \leftrightarrow 3$	1	$\omega_2\omega_{12}$	$\omega_1\omega_{12}$	$\omega_1\omega_2$

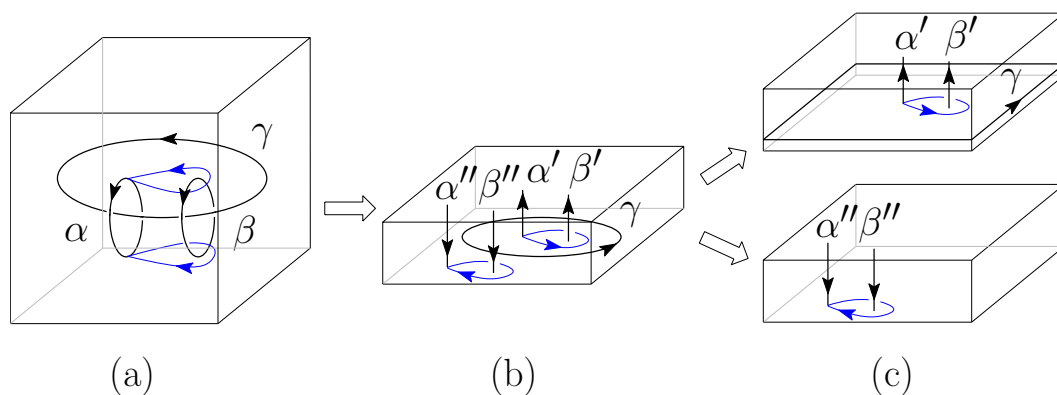


Figure 2.11: Decomposition of a three-loop braiding process into two separate braiding processes in the dimensionally-reduced 2D system.

which  $S_{yz}$  and  $T_{yz}$  take the above block diagonal form consists of the simultaneous eigenstates of the charge Wilson loop operators along the  $x$ -axis.

The above observations can be understood in terms of the dimensional reduction of the 3D  $G$ -gauge theory  $C^{3D}$ . Physically, it implies that if we put the 3D  $G$ -gauge theory  $C^{3D}$  on a three-torus and make one spatial dimension (say the  $x$ -direction) of the three-torus very small, then  $C^{3D}$  can be viewed as a direct sum of 2D  $G$ -gauge theories  $C_g^{2D}$  with degenerate ground state energy:

$$C^{3D} = \bigoplus_g C_g^{2D}. \quad (2.16)$$

The degeneracy is accidental and can be lifted by fixing a  $G$ -gauge flux  $g$  through the hole bound by the  $x$ -axis (dubbed the “ $x$ -hole” following Ref. [66]). This reduces the 3D  $G$ -gauge theory  $C^{3D}$  to the 2D  $G$ -gauge theory  $C_g^{2D}$ . The gauge flux  $g$  can be detected by winding the  $G$ -gauge charges around the “ $x$ -hole” and studying the associated Aharonov-Bohm phases. Therefore, the ground space of each sector  $C_g^{2D}$

is actually the eigenspace of the charge Wilson loop operators along the  $x$ -axis with a particular set of eigenvalues, which agrees with the observations in the previous paragraph.

To deduce the three-loop braiding statistics in  $C^{3D}$ , we adopt the approach from Ref. [66] to decompose a three-loop braiding process in a 3D system into two separate processes in the dimensionally-reduced 2D systems. More specifically, let us consider the three-loop braiding process depicted in Fig. 2.1, where a flux loop  $\alpha$  sweeps out a torus which contains another flux loop  $\beta$  while both linked with a “base” flux loop  $\gamma$ . We denote the Berry phase associated with the above braiding process by  $\theta_{\alpha\beta,\gamma}$ . Without loss of generality, we suppose that  $\gamma$  lies in the  $yz$ -plane, and  $\alpha$  and  $\beta$  lie in the  $xy$ -plane. After we compactify the  $x$ -direction into a small circle,  $\alpha$  extends across the  $x$ -direction, fuses with itself, and splits into two noncontractible loops  $\alpha'$  and  $\alpha''$  (Fig. 2.11(b)). Similarly,  $\beta$  fuses with itself and splits into  $\beta'$  and  $\beta''$ . The three-loop braiding process can then be decomposed into two separate processes in which  $\alpha'$  is braided around  $\beta'$  inside the base loop  $\gamma$  and  $\alpha''$  is braided around  $\beta''$  outside the base loop  $\gamma$  (Fig. 2.11(b)). For the first process, we can stretch  $\gamma$  so that it subtends the  $yz$ -plane (Fig. 2.11(c)). This leaves a flux line  $\gamma$  threaded through the “ $x$ -hole”, which reduces the 3D  $G$ -gauge theory  $C^{3D}$  to the 2D  $G$ -gauge theory  $C_{\phi_\gamma}^{2D}$ , where  $\phi_\gamma$  denotes the gauge flux carried by the loop  $\gamma$ . Similarly, for the second process, we can shrink  $\gamma$  till it fuses and annihilates with itself (Fig. 2.11(c)). This leaves no gauge flux through the “ $x$ -hole”, and  $C^{3D}$  is reduced to  $C_0^{2D}$ , where we denote the group identity of  $G$  by 0. In the 2D limit, noncontractible flux loops along the  $x$ -direction become point-like gauge fluxes in the 2D  $G$ -gauge theories, because the extent of the  $x$ -direction is negligible compared with that of the  $y$  and  $z$ -directions. Therefore, the three-loop braiding process in  $C^{3D}$  that we started with is reduced to two separate braiding processes between gauge fluxes in  $C_{\phi_\gamma}^{2D}$  and  $C_0^{2D}$ . This implies the following relation between the associated Berry phases:

$$\theta_{\alpha\beta,\gamma} = \theta_{\alpha'\beta'}^{2D}(\gamma) - \theta_{\alpha''\beta''}^{2D}(0), \quad (2.17)$$

where the first and second terms on the right hand side are the Berry phases resulting from braiding  $\alpha'$  around  $\beta'$  in  $C_{\phi_\gamma}^{2D}$  and  $\alpha''$  around  $\beta''$  in  $C_0^{2D}$ , respectively. The relative minus sign takes into account the fact that the two pairs of gauge fluxes are braided in opposite directions.

Now, we carry out the above procedure to analyze the dimensional reduction phenomenon and compute the three-loop braiding statistics in our Walker-Wang models.

First, we apply the relations in Eq. (2.12) to obtain the 2D modular matrices  $S_{yz}$  and  $T_{yz}$  from the 3D modular matrices  $S$  and  $T$ . Then we compute the charge string operators along the non-contractible loops along the  $x$ ,  $y$ , and  $z$  axes (see Appendix C), which we denote by  $W_x^s$ ,  $W_y^s$ , and  $W_z^s$ , respectively. Here  $s = 0, 1, 2, 3$  labels the  $\mathbb{Z}_2 \times \mathbb{Z}_2$  charges. Without loss of generality, we identify 1 with  $g_x$ , and 2 with  $g_y$ . Next, we do a basis transformation, and rewrite  $S_{yz}$  and  $T_{yz}$  in the simultaneous eigenstates of  $W_x^s$ ,  $W_y^s$ , and  $W_z^s$ . We find that if we organize the basis states according to the eigenvalues of  $W_x^s$  (equivalently the eigenvalues of the pair  $(W_x^1, W_x^2)$ ),  $S_{yz}$  and  $T_{yz}$  are block diagonal with each block of size 16 by 16. For simplicity, we denote by  $S_{a,b}$  and  $T_{a,b}$  ( $a, b = \pm 1$ ) the block corresponding to  $(W_x^1, W_x^2) = (a, b)$ . Since  $W_x^1$  (respectively,  $W_x^2$ ) detects the  $g_x$  (respectively,  $g_y$ ) flux through the “ $x$ -hole”,  $(S_{a,b}, T_{a,b})$  describes the 2D topological order obtained by making the  $x$ -direction of the three-torus into a small circle, and threading some particular  $\mathbb{Z}_2 \times \mathbb{Z}_2$  flux  $\nu(a, b)$  through the “ $x$ -hole”, where  $\nu(a, b) = 0, g_x, g_y$ , or  $g_z$  for  $(a, b) = (1, 1), (-1, 1), (1, -1)$ , or  $(-1, -1)$ , respectively.

Note that  $S_{a,b}$  and  $T_{a,b}$  are written in the simultaneous eigenstates of  $W_y^s$  and  $W_z^s$ , and are not yet presented in their canonical form, where the entries of the  $S$  and  $T$  matrices are the braiding statistics and topological spins of quasiparticles, respectively. It is shown in Ref. [73] that by choosing the basis states in the ground space to be the minimum entropy states (MESs), one can put  $S$  and  $T$  into the canonical form. The MESs are the simultaneous eigenstates of the charge string operators and flux string operators that encircle the two-torus. Without loss of generality, we define our MESs to be the simultaneous eigenstates of  $W_y^s$  and  $V_y^s$ , where we denote the flux string operators along the  $y$ -axis by  $V_y^s$ . The flux string operators are the flux membrane operators in the  $xy$ -plane before we dimensionally reduce our system to the  $yz$ -plane. In general, we do not know how to implement the membrane operators in Walker-Wang models, so it is hard to write down  $V_y^s$  explicitly. However, we do know that  $V_y^s$  and  $W_z^s$  satisfy the following commutation and anticommutation relations:

$$\begin{aligned}
\{W_z^1, V_y^1\} &= 0, & [W_z^1, V_y^2] &= 0, & \{W_z^1, V_y^3\} &= 0, \\
\{W_z^2, V_y^1\} &= 0, & \{W_z^2, V_y^2\} &= 0, & \{W_z^2, V_y^3\} &= 0, \\
\{W_z^3, V_y^1\} &= 0, & \{W_z^3, V_y^2\} &= 0, & [W_z^3, V_y^3] &= 0.
\end{aligned} \tag{2.18}$$

This follows from the Aharonov-Bohm interaction between gauge charges and flux loops in a 3D gauge theory. We are able to deduce from this the basis transformation from the simultaneous eigenstates of  $W_y^s$  and  $W_z^s$  to the MESs. For details about the basis transformation, we refer the reader to Appendix D.

After rewriting  $S_{a,b}$  and  $T_{a,b}$  in the MES basis, we find that they are identical to the 2D modular matrices of the 2D  $\mathbb{Z}_2 \times \mathbb{Z}_2$  gauge theories. There are 8 inequivalent such theories: 1 untwisted gauge theory and 7 twisted gauge theories. They can be distinguished by a triple  $(\theta_x, \theta_y, \theta_{xy})$ , where the first, second and third entries are the Berry phases associated with the exchange of two  $g_x$  fluxes, the exchange of two  $g_y$  fluxes, and the braiding of a  $g_x$  flux around a  $g_y$  flux, respectively.  $\theta_x$  and  $\theta_y$  can take value either 0 or  $\pi/2$ , and  $\theta_{xy}$  can take value either 0 or  $-\pi/2$ , and the 8 combinations correspond to the 8 different 2D  $\mathbb{Z}_2 \times \mathbb{Z}_2$  gauge theories. The 8 theories are classified by the cohomology group  $H^3(\mathbb{Z}_2 \times \mathbb{Z}_2, U(1)) = \mathbb{Z}_2 \times \mathbb{Z}_2 \times \mathbb{Z}_2$ . The trivial element of the group corresponds to the untwisted gauge theory, and the 7 nontrivial elements correspond to the twisted gauge theories. The three generators of the group (written multiplicatively), which we denote by  $\omega_1$ ,  $\omega_2$ , and  $\omega_{12}$ , can be taken to be the 2D twisted  $\mathbb{Z}_2 \times \mathbb{Z}_2$  gauge theories with  $(\theta_x, \theta_y, \theta_{xy}) = (\pi/2, 0, 0)$ ,  $(0, \pi/2, 0)$ , and  $(0, 0, -\pi/2)$ , respectively. Each dimensionally-reduced 2D  $\mathbb{Z}_2 \times \mathbb{Z}_2$  gauge theory can then be represented by a combination of the three generators. The results are summarized in Table 2.2.

To compute the three-loop braiding statistics in our Walker-Wang models, we follow our earlier discussion to decompose a three-loop braiding process into two separate braiding processes in the dimensionally-reduced 2D systems and find the relation between their associated Berry phases. In particular, the three-loop braiding process considered in Section 2.3, where two  $g_x$ -flux loops are exchanged while both linked with a  $g_x$ -flux loop, can be decomposed into the following two braiding processes in 2D: (1) Two  $g_y$  fluxes exchanged inside a  $g_y$ -flux loop; (2) Two  $g_x$  fluxes exchanged outside the  $g_y$ -flux loop. Therefore, we have the following relation between the associated Berry phases:

$$\theta_{x,y} = \theta_x^{2D}(y) - \theta_x^{2D}(0), \quad (2.19)$$

where the first and second terms on the right hand side are the Berry phases resulting from exchanging two  $g_x$  fluxes either inside or outside a  $g_y$ -flux loop, respectively. Similar analysis applies to the case where the roles of  $g_x$  and  $g_y$  are switched and we have the following expression:

$$\theta_{y,x} = \theta_y^{2D}(x) - \theta_y^{2D}(0). \quad (2.20)$$

Let us now apply Eq. (2.19) and Eq. (2.20) to two examples. First, we consider a Walker-Wang model with input  $\text{Rep}_s(Q_8)$ . From Table 2.2, we know that after dimensional reduction, we get the 2D untwisted  $\mathbb{Z}_2 \times \mathbb{Z}_2$  gauge theory both inside

and outside each  $\mathbb{Z}_2 \times \mathbb{Z}_2$  flux loop, which implies that

$$\begin{aligned}\theta_x^{2D}(0) &= \theta_y^{2D}(0) = 0, \\ \theta_x^{2D}(y) &= \theta_y^{2D}(x) = 0.\end{aligned}\tag{2.21}$$

Hence

$$\theta_{x,y} = 0, \quad \theta_{y,x} = 0,\tag{2.22}$$

and the Walker-Wang model describes the 3D untwisted  $\mathbb{Z}_2 \times \mathbb{Z}_2$  gauge theory.

Next, we consider a Walker-Wang model with input  $\text{Rep}_s(D_4)$ . As in the previous example, we get 2D  $\mathbb{Z}_2 \times \mathbb{Z}_2$  gauge theories both inside and outside each  $\mathbb{Z}_2 \times \mathbb{Z}_2$  flux loop after dimensional reduction. The only difference is that the  $\mathbb{Z}_2 \times \mathbb{Z}_2$  gauge theory is twisted inside a nontrivial flux loop. More specifically, we get the 2D twisted  $\mathbb{Z}_2 \times \mathbb{Z}_2$  gauge theory represented by the  $\mathbb{Z}_2 \times \mathbb{Z}_2 \times \mathbb{Z}_2$  group element  $\omega_2$  (respectively,  $\omega_{12}$ ) inside a  $g_x$ -flux (respectively,  $g_y$ -flux) loop. We can deduce from this that

$$\theta_x^{2D}(y) = 0, \quad \theta_y^{2D}(x) = \frac{\pi}{2}.\tag{2.23}$$

Together with

$$\theta_x^{2D}(0) = \theta_y^{2D}(0) = 0,\tag{2.24}$$

they imply that

$$\theta_{x,y} = 0, \quad \theta_{y,x} = \frac{\pi}{2},\tag{2.25}$$

and the Walker-Wang model describes a 3D twisted  $\mathbb{Z}_2 \times \mathbb{Z}_2$  gauge theory (the APS-X theory).

We can carry out similar computations for Walker-Wang models with the other two sets of input data in Table 2.2. We find that when we permute the labels 1 and 2 (respectively, 1 and 3) in  $\text{Rep}_s(D_4)$ , the resulting Walker-Wang model describes the APS-Y (respectively, APS-Z) theory.

## 2.5 Summary and Discussion

In this chapter, we studied in detail the realization of the 3D  $\mathbb{Z}_2 \times \mathbb{Z}_2$  gauge theories, both twisted and untwisted, in terms of Walker-Wang models. Our proposal is based on the study of the surface topological order of  $\mathbb{Z}_2 \times \mathbb{Z}_2$  gauge theories [20, 22]. We propose that if we take the input data of a Walker-Wang model to be the  $\mathbb{Z}_2 \times \mathbb{Z}_2$  symmetry charges and the surface anyon content of a trivial (respectively, nontrivial) 3D  $\mathbb{Z}_2 \times \mathbb{Z}_2$  SPT (or rather their corresponding excitations in the gauged models), the output theory is a 3D untwisted (respectively, twisted)  $\mathbb{Z}_2 \times \mathbb{Z}_2$  gauge theory.

To check the validity of our proposal, we perform 3D modular transformations to the ground space of our Walker-Wang models on the three-torus and extract the resulting  $S$  and  $T$  matrices. By making a dimensional reduction argument, we are able to deduce the three-loop braiding statistics from the  $S$  and  $T$  matrices, which determine the topological order in our models.

Note that there is a subtlety involved in doing modular transformations in Walker-Wang models. In Walker-Wang models, we work with a fixed planar projection of the 3D trivalent lattice. The strings living on the lattice are actually ribbons with the blackboard framing. Therefore, it is important that we choose to calculate Berry phases associated with the modular transformations that preserve the projection of the 3D lattice (equivalently, the framing of the ribbon graphs). This is solely for the sake of convenience. Otherwise, we need to transform the ribbon graphs back to the original framing after the modular transformations, and this introduces extra factors into the wave function. This is precisely the reason why we did not calculate the Berry phases associated with the 2D modular transformation  $S_{yz}$  directly in Section 2.4.  $S_{yz}$  changes the framing of the ribbon graphs, whereas  $S$  and  $T$  do not. Thus, it is easier to first calculate  $S$  and  $T$ , and deduce  $S_{yz}$  from the relation Eq. (2.12).

So far we have only considered the Walker-Wang construction of 3D  $\mathbb{Z}_2 \times \mathbb{Z}_2$  gauge theories. It would be interesting to generalize the construction to other 3D discrete gauge theories. It would also be interesting to find the connection between the Walker-Wang description and the Dijkgraaf-Witten description of these discrete gauge theories. Note that the ground state wave function in the former (respectively, latter) description is a condensate of loops (respectively, membranes), so the two descriptions should be dual to each other in some sense. It would be nice to make this duality more concrete and study how general it is. Another interesting direction is to generalize the Walker-Wang construction to discrete gauge theories with (at least one) fermionic gauge charges. The simplest example of this kind is a 3D  $\mathbb{Z}_2$  gauge theory with fermionic  $\mathbb{Z}_2$  gauge charges. This theory can be described by a Walker-Wang model [40]. One can simply take a Walker-Wang model describing the 3D  $\mathbb{Z}_2$  gauge theory, and “twisting” the  $R$  symbols of the input data by a fermion. More precisely,  $R_0^{11}$  takes the value  $-1$  in the fermionic case and  $1$  in the bosonic case, where  $1$  labels the  $\mathbb{Z}_2$  gauge charge, and  $0$  labels the vacuum. This example is interesting because Dijkgraaf-Witten models fail to describe discrete gauge theories with fermionic gauge charges. It would be nice to have a Walker-Wang description

for more of such fermionic discrete gauge theories, especially ones that are twisted. A detailed study of such cases is beyond the scope of this thesis.

## EXACTLY SOLVABLE MODEL FOR TWO-DIMENSIONAL TOPOLOGICAL SUPERCONDUCTORS

### 3.1 Introduction

The discovery of topological insulators and superconductors [24–27, 30, 31] demonstrates that a fermionic system can exhibit nontrivial topological properties if the fermions occupy a band structure with nontrivial topology. The topological nature of the systems is manifested physically in the existence of gapless edge modes around a gapped bulk, which cannot be removed unless certain symmetry is explicitly or spontaneously broken. It is also manifested at symmetry defects on the boundary of the system. For example, in a 2D topological superconductor, a time-reversal domain wall on the 1D boundary hosts a Majorana zero mode and in a 3D topological superconductor, a time-reversal domain wall on the 2D boundary hosts a chiral Majorana mode. A complete classification of topological insulators and superconductors in free fermion systems was given in Refs. [34, 80]. Such “Symmetry Protected Topological (SPT)” order was found in interacting boson systems as well. A whole class of exactly solvable models with commuting projector Hamiltonian and zero correlation length ground state wave function were constructed to realize such bosonic SPT order [41, 81].

Can topological insulators and superconductors discovered in the free fermion setup be realized with exactly solvable models as well? This question is interesting not only out of pure theoretical curiosity; it is also crucial for formulating a general framework for both fermionic and bosonic SPT phases which may lead to the discovery of new phases and a complete classification. Moreover, it can be useful in answering questions regarding many-body localization in such phases when strong disorder is present[44]. In this paper, we focus on the case of 2D topological superconductor.

If an exactly solvable model is possible, it necessarily involves interactions as the free fermion ground states always have a nonzero correlation length due to the nontrivial topology of the band structure [44]. Refs. [82, 83] gave the exactly solvable model realization of a large class of fermionic SPT phases which are protected by symmetries of the form  $G_b \times \mathbb{Z}_2^f$ , where  $G_b$  denotes symmetry transformation on

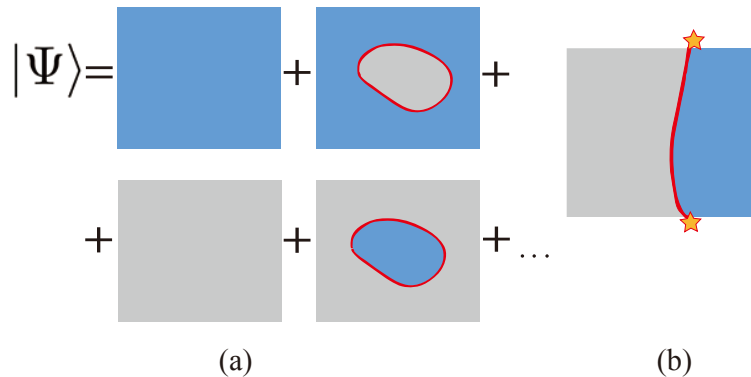


Figure 3.1: The decorated domain wall approach. (a) Ground state is a superposition of all symmetry breaking domain configurations (blue and grey patches) with domain walls decorated with SPT states of one lower dimension (red curves). (b) The end point of the domain wall on the boundary (star) hosts nontrivial edge states of the lower dimensional SPT.

some bosonic degrees of freedom in the system and  $\mathbb{Z}_2^f$  is the fermion parity part of the symmetry. The symmetry protecting the topological superconductor falls out of this class. In the topological superconductor, time-reversal symmetry acts as  $T^2 = P_f$ , where  $P_f$  is the fermion parity operator generating the  $\mathbb{Z}_2^f$  symmetry group. Therefore, the total symmetry group is  $Z_4$ , with the odd group elements being anti-unitary.

The decorated domain wall construction provides a different approach for constructing exactly solvable models for SPT phases [46]. In this approach, the ground state wave function is written as a superposition of all possible symmetry breaking configurations with the symmetry breaking domain walls decorated with SPT states of one lower dimension, as shown in Fig. 3.1(a). The superposition guarantees that the total wave function is symmetric. Moreover, when symmetry is broken into opposite domains, the domain wall carries the lower dimensional SPT state. When the domain wall ends on the boundary of the system, the end point hence hosts the edge state of the lower dimensional SPT state, reflecting the nontrivial nature of the original SPT order, as shown in Fig. 3.1(b).

In a topological superconductor with helical Majorana edge mode, a mass term can gap out the edge mode while breaking time-reversal symmetry. On the symmetry domain wall, there is an isolated Majorana mode. Therefore, if the topological superconductor can be written in the decorated domain wall way, we should decorate the time-reversal domain walls with Majorana chains.

Decorating symmetry domain walls with Majorana chains has proven to be more difficult than with bosonic chains. A breakthrough was made recently in Refs. [48, 49] where a fermionic SPT phase with  $\mathbb{Z}_2 \times \mathbb{Z}_2^f$  symmetry was realized by decorating the  $\mathbb{Z}_2$  domain walls with 1D Majorana chains. Although the protecting symmetry is still of the form  $G_b \times \mathbb{Z}_2^f$ , this particular phase cannot be realized using the method of Ref. [82]. It was realized that the incorporation of a Kasteleyn orientation on the two dimensional lattice, which corresponds to a discrete version of spin structure in 2D, is crucial for a consistent decoration.

Using the Kasteleyn orientation, we present a decorated domain wall construction of the 2D topological superconductor in this paper. Our construction is different from that of the  $\mathbb{Z}_2 \times \mathbb{Z}_2^f$  SPT phase in an important way. In the case of  $\mathbb{Z}_2 \times \mathbb{Z}_2^f$ , the Majorana chain used for decoration does not transform under the  $\mathbb{Z}_2$  part of the symmetry, which acts only on the symmetry domains. In the case of topological superconductor, time reversal acts both on the symmetry domains and on the Majorana chains decorated onto the symmetry domain walls. In fact, the way the Majorana chains transform under time reversal is crucial for the construction as we know that topological superconductivity only exists for  $T^2 = -1$  fermions but not the  $T^2 = +1$  ones. Indeed, after we present carefully how a zero correlation length wave function and a commuting projector Hamiltonian can be constructed for  $T^2 = -1$  fermions, we will be able to see why a similar construction fails for the  $T^2 = +1$  ones. Our discussion below focuses on the Honeycomb lattice, but the construction works for any trivalent lattice using the same convention as defined below.

### 3.2 Wave function

Consider the planar trivalent lattice in Fig. 3.2 together with a Kasteleyn orientation, i.e., orientation of the bonds of the lattice for which any plaquette has an odd number of clockwise-oriented bonds. There are two types of faces in the lattice: the 12-sided faces, which we will refer to as plaquettes, and the triangular faces, which we will refer to as triangles. Let  $t(v)$  and  $t(w)$  be the triangles that contain the vertices  $v$  and  $w$ , respectively. The bonds of the lattice also come in two types: the ‘short’ bonds which connect different triangles ( $t(v) \neq t(w)$ ), and the ‘long’ bonds that are in the same triangle ( $t(v) = t(w)$ ).

The Hilbert space of our model consists of a bosonic spin-1/2 located on each plaquette  $p$ , acted on by the Pauli operators  $\tau_p^x$ ,  $\tau_p^y$ ,  $\tau_p^z$ , and a pair of complex fermions located on each short bond  $l$ , created and annihilated by operators  $c_l^{\sigma\dagger}$  and

$c_l^\sigma$  ( $\sigma = \uparrow, \downarrow$ ), respectively. Let  $l = \langle \overrightarrow{vv'} \rangle$  be oriented from vertex  $v$  to vertex  $v'$ . Each complex fermion on  $l$  can be represented by a pair of Majorana modes

$$\begin{aligned}\gamma_v^\sigma &= c_l^{\sigma\dagger} + c_l^\sigma, \\ \gamma_{v'}^\sigma &= i(c_l^{\sigma\dagger} - c_l^\sigma),\end{aligned}\tag{3.1}$$

located at  $v$  and  $v'$ , respectively. We can also define a fictitious spin-1/2 degree of freedom  $\tau_t$  on each triangle following the majority rule: The value of  $\tau_t$  is set to 1 if the majority of the three plaquettes bordering  $t$  have  $\tau_p^z = 1$ , and is set to  $-1$  otherwise.

Our system has a time-reversal symmetry  $T$ , which acts on both the plaquette spins and the complex fermions. In the eigenbasis of  $\tau_p^z$ ,  $T$  maps between the two eigenstates of  $\tau_p^z$ :

$$T : |1\rangle \rightarrow |-1\rangle, \quad |-1\rangle \rightarrow |1\rangle,\tag{3.2}$$

together with the complex conjugation operation in this basis. The fictitious spins on the triangles will also be flipped due to the majority rule. Since any fixed plaquette spin configuration in the  $\tau^z$  basis breaks time-reversal symmetry, we will refer to a domain of plaquette spins in the same  $\tau^z$  basis state as a time-reversal domain. Furthermore,  $c_l^\sigma$  transforms as a Kramers doublet under  $T$ :  $c_l^\uparrow \rightarrow c_l^\downarrow$ ,  $c_l^\downarrow \rightarrow -c_l^\uparrow$ . Written in terms of the Majorana modes, we have:

$$T : \begin{cases} \gamma_v^\uparrow \rightarrow \gamma_v^\downarrow \\ \gamma_v^\downarrow \rightarrow -\gamma_v^\uparrow \end{cases}, \quad \begin{cases} \gamma_{v'}^\uparrow \rightarrow -\gamma_{v'}^\downarrow \\ \gamma_{v'}^\downarrow \rightarrow \gamma_{v'}^\uparrow \end{cases}.\tag{3.3}$$

where the Kasteleyn orientation points from  $v$  to  $v'$ .

Now we describe in detail how we decorate the time-reversal domain walls with Majorana chains. Away from the domain wall, we pair up Majorana modes that share a short bond  $\langle \overrightarrow{vv'} \rangle$  as  $i\gamma_v^\uparrow\gamma_{v'}^\uparrow + i\gamma_v^\downarrow\gamma_{v'}^\downarrow$ . On a domain wall, we pick out one Majorana mode  $\gamma_v^{\sigma_v}$  from each vertex  $v$  and pair them along the long bonds  $\langle \overrightarrow{vw} \rangle$  as  $i\gamma_v^{\sigma_v}\gamma_w^{\sigma_w}$  so that they form a Majorana chain. The spin label  $\sigma_v$  is determined as follows: If the left hand side of the short bond is a  $|1\rangle$  domain,  $\sigma_v = \uparrow$ ; otherwise,  $\sigma_v = \downarrow$ . After the Majorana modes of the  $\sigma_v$  species pair into Majorana chains, we are left with exactly one unpaired Majorana mode on each vertex on the domain wall. The two unpaired Majorana modes that share a short bond  $\langle \overrightarrow{vv'} \rangle$  will have the same spin  $\bar{\sigma}_v$  which can be paired as  $i\gamma_v^{\bar{\sigma}_v}\gamma_{v'}^{\bar{\sigma}_{v'}}$ . This is the same kind of coupling

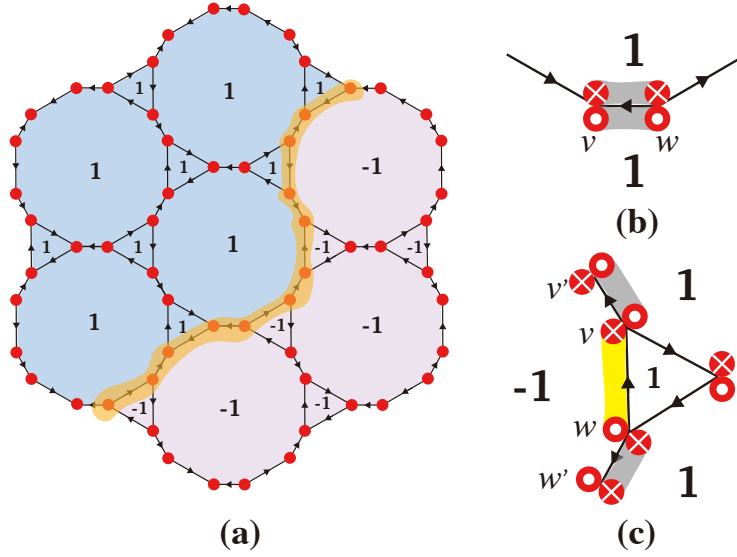


Figure 3.2: (a) illustrates the lattice structure and degrees of freedom in our model. Here 1 and  $-1$  denote the eigenstates of  $\tau_p^z$  with eigenvalues 1 and  $-1$ , respectively. The blue bonds indicate the time-reversal domain wall. The solid red circles denote the Majorana modes  $\gamma_v^\sigma$  ( $\sigma = \uparrow, \downarrow$ ). The arrow at each bond denotes the Kasteleyn orientation of the bond. (b) (respectively, (c)) is a detailed illustration of the coupling of Majorana modes away from (respectively, on) the domain wall. The dots and crosses on the solid red circles indicate the up ( $\uparrow$ ) and down ( $\downarrow$ ) spins of the Majorana modes, respectively. The yellow (respectively, grey) bond denotes the coupling of Majorana modes that share a long (respectively, short) bond.

as that away from the domain wall, but with only one species of Majorana modes. Fig. 3.2 (b) and (c) give a pictorial illustration of these coupling rules.

The ground state wave function of a topological superconductor is then given by the superposition of all possible time-reversal domain configurations with domain walls decorated with Majorana chains. It satisfies the following properties: It's time-reversal invariant, and every configuration in the superposition has the same fermion parity. The latter fact is ensured by the Kasteleyn orientation. The reason for this is very similar to that presented in Ref. [48, 49] although here we have two species of fermion modes.

To see the time-reversal invariance, we note that time reversal acts by flipping the plaquette spins, and transforms the Majorana modes in a way that conforms to the decoration rules introduced above. In particular, for Majorana modes not on a domain wall, they pair as  $i\gamma_v^\uparrow\gamma_{v'}^\uparrow + i\gamma_v^\downarrow\gamma_{v'}^\downarrow$  on a short bond which is invariant under time reversal. For Majorana modes on a domain wall, the decoration rule

says that the modes that form (do not form) Majorana chains flip their spin when the plaquette spins are flipped, which is consistent with the time-reversal transformation action. Moreover, the pairing terms along the domain wall, whose signs are fixed by the Kasteleyn orientation, exactly map into each other under time reversal without any sign ambiguity. To see this, first notice that for the modes which do not form Majorana chains, the pairing maps from  $i\gamma_v^{\sigma_v}\gamma_{v'}^{\sigma_{v'}}$  to  $i\gamma_v^{\bar{\sigma}_v}\gamma_{v'}^{\bar{\sigma}_{v'}}$ , which are both consistent with the Kasteleyn orientation. Secondly, for the modes that are involved in forming Majorana chains, one can check that the pairing term  $i\gamma_v^{\sigma_v}\gamma_w^{\sigma_w}$  is mapped into  $i\gamma_v^{\bar{\sigma}_v}\gamma_w^{\bar{\sigma}_w}$  which are both consistent with the Kasteleyn orientation.<sup>1</sup> Therefore, we can conclude that time reversal maps from one to another the decorated domain wall configurations in the superposition. The whole superposition is then time-reversal invariant if the weight of the time-reversal partner configurations are complex conjugate of each other. This will be demonstrated in detail in Section 3.4.

### 3.3 Hamiltonian

The Hamiltonian of our model can be written as

$$H = H_{\text{decorate}} + H_{\text{tunnel}}, \quad (3.4)$$

where  $H_{\text{decorate}}$  will be defined to realize the domain wall decoration described in the above section for each plaquette spin configuration, and  $H_{\text{tunnel}}$  will be defined to tunnel between the different plaquette spin configurations.

More explicitly, let  $D_{\langle \overline{vw} \rangle} = \frac{1}{2} \left( 1 - \tau_{f_{\overline{vw}}}^z \tau_{f'_{\overline{vw}}}^z \right)$  be the operator which detects if the bond (either short or long)  $\langle \overline{vw} \rangle$  is on a domain wall.  $f_{\overline{vw}}$  denotes the left-hand-side face of the bond  $\langle \overline{vw} \rangle$ ;  $f'_{\overline{vw}}$  denotes the right-hand-side one. If  $\langle \overline{vw} \rangle$  is a long bond, we denote by  $\langle \overline{vv'} \rangle$  ( $\langle \overline{ww'} \rangle$ ) the short bond that includes vertex  $v(w)$ .<sup>2</sup> We can define two operators  $W_{vw}^{\pm} = \frac{1}{4} \left( 1 \pm \tau_{f_{\overline{vw}}}^z \right) \left( 1 \mp \tau_{f'_{\overline{vw}}}^z \right)$  to determine which  $\gamma_{v,w}^s$  ( $s = \uparrow, \downarrow$ ) to pair in the Majorana chain on the domain wall. If  $W_{vw}^+ = 1$ ,  $W_{vw}^- = 0$ , the pairing over the long bond  $\langle \overline{vw} \rangle$  is  $i\gamma_v^{\uparrow}\gamma_w^{\downarrow}$ ; if  $W_{vw}^- = 1$ ,  $W_{vw}^+ = 0$ , it is  $i\gamma_v^{\downarrow}\gamma_w^{\uparrow}$ . If both are zero,  $\langle \overline{vw} \rangle$  is not on a domain wall.

<sup>1</sup>The way  $\gamma_v^{\sigma_v}$  transforms into  $\gamma_v^{\bar{\sigma}_v}$  depends on the orientation of the short bond  $\langle vv' \rangle$  and similarly for  $w$ . One can check that with all four orientation possibilities, this conclusion is always true.

<sup>2</sup>The overline on top of  $\overline{vv'}$  means that if  $v$  is oriented to  $v'$ ,  $\overline{vv'} = \overline{vv'}$ , otherwise  $\overline{vv'} = \overline{v'v}$ .

Now we write the decoration part of the Hamiltonian as

$$\begin{aligned}
H_{\text{decorate}} = & - \sum_{\substack{\langle \vec{vw} \rangle \\ t(v)=t(w)}} [iD_{\langle \vec{vw} \rangle} W_{vw}^+ \gamma_v^\uparrow \gamma_w^\downarrow + iD_{\langle \vec{vw} \rangle} W_{vw}^- \gamma_v^\downarrow \gamma_w^\uparrow] \\
& - \sum_{\substack{\langle \vec{vw} \rangle \\ t(v) \neq t(w)}} [iD_{\langle \vec{vw} \rangle} \left( \frac{1 + \tau_f^z}{2} \right) \gamma_v^\downarrow \gamma_w^\downarrow + iD_{\langle \vec{vw} \rangle} \left( \frac{1 - \tau_f^z}{2} \right) \gamma_v^\uparrow \gamma_w^\uparrow \\
& \quad + i \left( \frac{1 - D_{\langle \vec{vw} \rangle}}{2} \right) (\gamma_v^\uparrow \gamma_w^\uparrow + \gamma_v^\downarrow \gamma_w^\downarrow)], \tag{3.5}
\end{aligned}$$

where  $t(v)$  (respectively,  $t(w)$ ) denotes the triangular face that includes the vertex  $v$  (respectively,  $w$ ).  $H_{\text{tunnel}}$  can be defined by

$$H_{\text{tunnel}} = \sum_p \tau_p^x X_p, \tag{3.6}$$

where the sum over  $p$  only involves the plaquettes, not the triangles. The plaquette term  $X_p$  rearranges the Majorana chains to comply with the domain wall decoration rules defined above after  $\tau_p^x$  is applied. Specifically,

$$X_p = \sum_{\substack{\mu_p = \pm 1 \\ \{\mu_q = \pm 1\}}} V_p^{\{\mu_{p,q}\}} \Pi_p P_p^{\{\mu_{p,q}\}}, \tag{3.7}$$

where the sum over  $\{\mu_q = \pm 1\}$  denotes the summation over all the adjacent plaquette spin configurations around  $p$ .<sup>3</sup> The operators  $P_p^{\{\mu_{p,q}\}}$  and  $\Pi_p$  are projectors:  $P_p^{\{\mu_{p,q}\}}$  projects onto bosonic spin states with precisely  $\tau_p^z = \mu_p$  and  $\tau_q^z = \mu_q$ , and  $\Pi_p$  projects onto states in the fermionic Hilbert space that conform to those spin configurations:

$$P_p^{\{\mu_{p,q}\}} = \left( \frac{1 + \tau_p^z \mu_p}{2} \right) \prod_{\{q\}} \left( \frac{1 + \tau_q^z \mu_q}{2} \right) \tag{3.8}$$

$$\begin{aligned}
\Pi_p = & \prod_{\substack{\langle \vec{vw} \rangle \in \partial' p \\ t(v)=t(w)}} D_{\langle \vec{vw} \rangle} \left[ W_{vw}^+ \left( \frac{1 + i\gamma_v^\uparrow \gamma_w^\downarrow}{2} \right) + W_{vw}^- \left( \frac{1 + i\gamma_v^\downarrow \gamma_w^\uparrow}{2} \right) \right] \\
& \prod_{\substack{\langle \vec{vw} \rangle \in \partial' p \\ t(v) \neq t(w)}} \left\{ \left( \frac{1 - D_{\langle \vec{vw} \rangle}}{2} \right) \left( \frac{1 + i\gamma_v^\uparrow \gamma_w^\uparrow}{2} \right) \left( \frac{1 + i\gamma_v^\downarrow \gamma_w^\downarrow}{2} \right) + \right.
\end{aligned}$$

<sup>3</sup>Note that by using the ‘‘majority rule’’, one can extend the spin configuration from plaquettes to triangles.

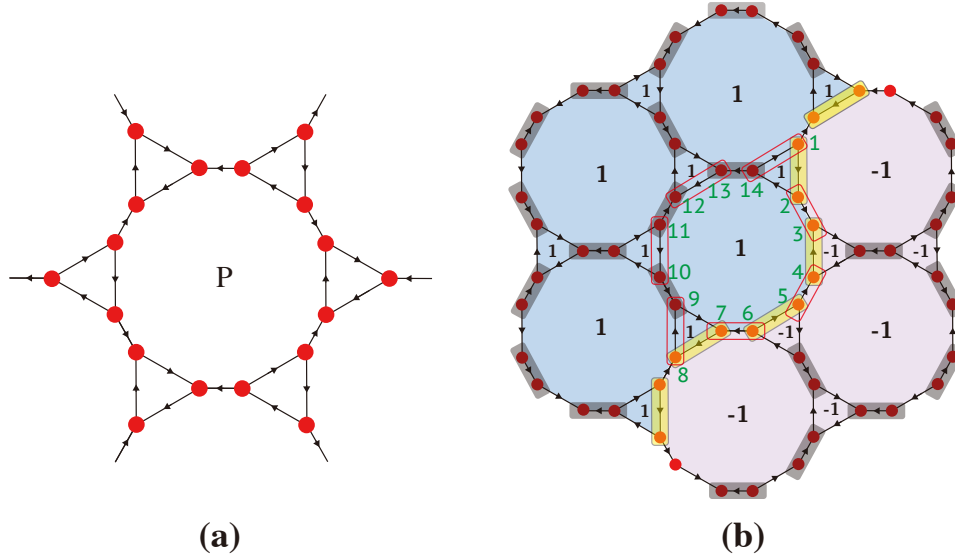


Figure 3.3: (a) The 36 Majorana modes denoted by the 18 red dots in this figure are the Majorana modes surrounding the plaquette  $p$ , denoted by  $\partial'p$ . (b) Majorana modes (labeled 1 – 14) involved in the definition of  $V_p^{\{\mu_{p,q}\}}$  when flipping the middle plaquette starting from this particular initial configuration. Red rectangles correspond to the pair projector terms involved in  $V_p^{\{\mu_{p,q}\}}$ . Note that the spins of the involved Majorana modes are not shown in the figure.

$$D_{\langle \vec{vw} \rangle} \left[ \left( \frac{1 + \tau_{f_{vw}}^z}{2} \right) \left( \frac{1 + i\gamma_v^\downarrow \gamma_w^\downarrow}{2} \right) + \left( \frac{1 - \tau_{f_{vw}}^z}{2} \right) \left( \frac{1 + i\gamma_v^\uparrow \gamma_w^\uparrow}{2} \right) \right]. \quad (3.9)$$

Here  $\partial'p$  includes the 36 Majoranas in the triangles surrounding the plaquette  $p$ , as shown in Fig. 3.3(a). The first line and third line of Eq. (3.9) enforce the pairing of Majorana modes on the domain wall, and the second line of Eq. (3.9) enforces the pairing of Majorana modes away from the domain wall.

The third part in the definition of  $X_p$  is

$$V_p^{\{\mu_{p,q}\}} = 2^{-\frac{n+1}{2}} (1 + is_{2,3}\gamma_2^{\sigma_2}\gamma_3^{\sigma_3})(1 + is_{4,5}\gamma_4^{\sigma_4}\gamma_5^{\sigma_5}) \dots (1 + is_{2n,1}\gamma_{2n}^{\sigma_{2n}}\gamma_1^{\sigma_1}), \quad (3.10)$$

which takes the initial fermion configuration  $|\Psi_i\rangle$  determined by  $\Pi_p$  corresponding to a fixed bosonic configuration determined by  $P_p^{\{\mu_{p,q}\}}$ , and maps it to  $|\Psi_f\rangle$ . The constant in the front is chosen so that  $|\Psi_f\rangle$  has the same norm as  $|\Psi_i\rangle$ . The labels  $\sigma_i$  ( $i = 1, 2, \dots, 2n$ ) can take values  $\uparrow$  and  $\downarrow$ , specifying the spins of the Majorana modes, and are determined by the bosonic spin configuration on and around the

plaquette  $p$  following the aforementioned decoration rules. The Majorana modes  $\gamma_i$  are arranged so that the initial state satisfy  $i s_{2i-1,2i} \gamma_{2i-1}^{\sigma_{2i-1}} \gamma_{2i}^{\sigma_{2i}} = 1$ . Then  $V_p^{\{\mu_p, q\}}$  maps this state into a state  $|\Psi_f\rangle$  with  $i s_{2i,2i+1} \gamma_{2i}^{\sigma_{2i}} \gamma_{2i+1}^{\sigma_{2i+1}} = 1$ . Here  $s_{i,j} = 1$  if the edge  $\langle v_i v_j \rangle$  points from  $v_i$  to  $v_j$  and  $s_{i,j} = -1$  otherwise. A pictorial illustration is given in Fig. 3.3(b).

$V_p^{\{\mu_p, q\}}$  defined above determines the relative weight and phase factor of different configurations. With repeated application of  $V_p$  and  $\tau_p^x$ , we can start from any initial configuration (including both boson and fermion degrees of freedom) satisfying  $H_{\text{decorate}}$ , and reach any other final configuration. The total ground state wave function is then a superposition of all the configurations obtained in this way. The fact that the relative weight and phase factor of different configurations can be uniquely and consistently determined is guaranteed by the commutativity of different  $V_p$  terms, which we prove in Appendix E. Moreover, as we will discuss in Section 3.4, the Hamiltonian thus defined is time-reversal invariant and ensures the time-reversal invariance of the ground state wave function.

### 3.4 Time Reversal Invariance of the Hamiltonian and the Wave Function

Recall that time reversal acts on the spins and fermions as  $T = \prod \tau_x \otimes \prod (i\sigma_y)K$ , where  $K$  is the complex conjugation operator. Under time reversal, terms in the Hamiltonian change as follows:

$$\begin{aligned}
D_{\vec{vw}} &\rightarrow D_{\vec{vw}} \\
i(\gamma_v^\uparrow \gamma_w^\uparrow + \gamma_v^\downarrow \gamma_w^\downarrow) &\rightarrow i(\gamma_v^\uparrow \gamma_w^\uparrow + \gamma_v^\downarrow \gamma_w^\downarrow) \\
W_{vw}^+ i \gamma_v^\uparrow \gamma_w^\downarrow &\leftrightarrow W_{vw}^- i \gamma_v^\downarrow \gamma_w^\uparrow \\
\left(\frac{1 + \tau_f^z}{2}\right) \gamma_v^\downarrow \gamma_w^\downarrow &\leftrightarrow \left(\frac{1 - \tau_f^z}{2}\right) \gamma_v^\uparrow \gamma_w^\uparrow
\end{aligned} \tag{3.11}$$

Therefore  $H_{\text{decorate}}$  is time reversal invariant. It is not obvious that the tunneling term is also time reversal invariant, we need to check it explicitly. First, the spin term  $\tau_p^x$  is invariant under time reversal. Similar to  $H_{\text{decorate}}$ , it is obvious that the  $\Pi_p$ 's are even under time reversal.  $P_p^{\{\mu_p, \mu_q\}}$  is mapped to its time reversal partner because  $T P_p^{\{\mu_p, \mu_q\}} T^{-1} = P_p^{\{-\mu_p, -\mu_q\}}$ . It can be explicitly checked that  $V_p^{\{\mu_p, q\}}$  is also mapped to its time reversal partner under time reversal. Therefore, we see that

$$T V_p^{\{\mu_p, q\}} \Pi_p P_p^{\{\mu_p, q\}} T^{-1} = V_p^{\{-\mu_p, -\mu_q\}} \Pi_p P_p^{\{-\mu_p, -\mu_q\}}. \tag{3.12}$$

Although  $X_p^{\{\mu_p, q\}} \Pi_p P_p^{\{\mu_p, q\}}$  alone is not time reversal invariant, the sum of all configurations of  $\{\mu_p, \mu_q\}$  is invariant under time reversal.

Finally, let us come back to prove that the ground state wave function is time-reversal invariant. It suffices to prove that the weights of two configurations related by time reversal are complex conjugate of each other. Let us consider a fermionic state  $|\Psi_f\rangle$  obtained by acting a sequence of plaquette operators on the initial fermionic state  $|\Psi_i\rangle$  associated with the plaquette spin configuration where  $\tau_p^z = 1$  for all  $p$ :  $|\Psi_f\rangle = V_{p_1} V_{p_2} \dots V_{p_n} |\Psi_i\rangle$ . The fermionic state  $|\Psi_f^T\rangle$  associated with the time-reversal partner of this configuration can be obtained by acting another sequence of plaquette operators on the initial fermionic state:  $|\Psi_f^T\rangle = V_{p'_1} V_{p'_2} \dots V_{p'_m} |\Psi_i\rangle$ , where  $p'_1 \cup p'_2 \cup \dots \cup p'_m$  form the complementary region of  $p_1 \cup p_2 \cup \dots \cup p_n$ . Note that the boundary of both regions agree. Using similar tricks as in Eq. (A11) of Ref. [48] for spinless fermions, we find that both  $V_{p_1} V_{p_2} \dots V_{p_n}$  and  $V_{p'_1} V_{p'_2} \dots V_{p'_m}$  can be reduced to the product of a sequence of projectors which act only on the Majoranas lying on the boundary of the region  $p_1 \cup p_2 \cup \dots \cup p_n$ :

$$V_{p_1} V_{p_2} \dots V_{p_n} = 2^{-\frac{n+1}{2}} (1 + i s_{2,3} \gamma_2^{\sigma_2} \gamma_3^{\sigma_3}) (1 + i s_{4,5} \gamma_4^{\sigma_4} \gamma_5^{\sigma_5}) \dots (1 + i s_{2n,1} \gamma_{2n}^{\sigma_{2n}} \gamma_1^{\sigma_1}), \quad (3.13)$$

$$V_{p'_1} V_{p'_2} \dots V_{p'_m} = 2^{-\frac{n+1}{2}} (1 + i s_{2,3} \gamma_2^{\bar{\sigma}_2} \gamma_3^{\bar{\sigma}_3}) (1 + i s_{4,5} \gamma_4^{\bar{\sigma}_4} \gamma_5^{\bar{\sigma}_5}) \dots (1 + i s_{2n,1} \gamma_{2n}^{\bar{\sigma}_{2n}} \gamma_1^{\bar{\sigma}_1}). \quad (3.14)$$

Furthermore, both  $p_1 \cup p_2 \cup \dots \cup p_n$  and  $p'_1 \cup p'_2 \cup \dots \cup p'_m$  are in the  $\tau_p^z = -1$  configuration. Therefore, by the coupling rules we introduced earlier,  $\sigma_i$  and  $\bar{\sigma}_i$  must be the opposite of each other for  $i = 1, 2, \dots, 2n$ . Hence Eq. (3.13) and Eq. (3.14) can be mapped into each other term by term under time reversal. Hence the weights associated with  $|\Psi_f\rangle$  and  $|\Psi_f^T\rangle$  are complex conjugate of each other.

### 3.5 Why $T^2 = 1$ fermion does not work

We now discuss why our decoration procedure discussed above does not work for spinless fermions with  $T^2 = 1$ . In particular, we will argue that if one decorates the time reversal domain walls with spinless Majorana chains, then the requirement of time reversal invariance for the wave function is not compatible with the requirement that any two decorated domain wall configurations in the superposition have the same fermion parity. This is consistent with the fact that there are no nontrivial fermionic short-range entangled phases with  $T^2 = 1$ .

Let the spinless complex fermion on a short bond  $l = \langle \overrightarrow{vv'} \rangle$  be created and annihilated by operators  $c_l$  and  $c_l^\dagger$ , respectively. We first represent the complex fermion by a pair of Majorana modes  $\gamma_v = c_l^\dagger + c_l$ ,  $\gamma_{v'} = i(c_l^\dagger - c_l)$  located at vertices  $v$  and  $v'$ , respectively. Under time reversal,  $T : c_l \rightarrow c_l$ . Written in terms of the Majorana

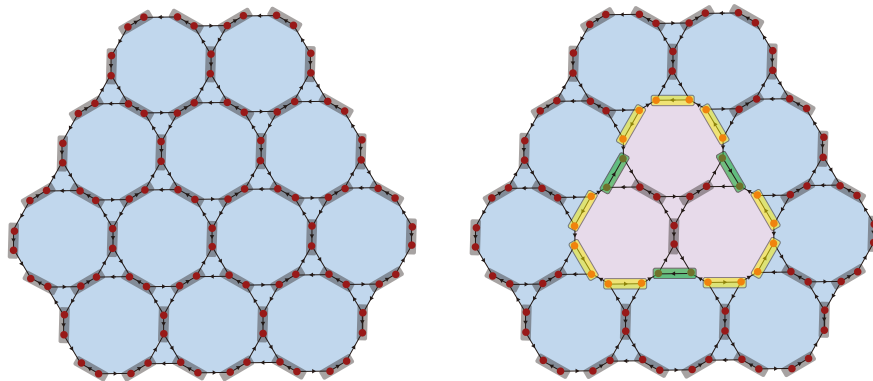


Figure 3.4: Two configurations for spinless Majorana modes with opposite fermion parity. Extra minus signs are added to the coupling on the green bonds according to the modified coupling rule.

modes, we have:

$$T : \gamma_v \rightarrow \gamma_v, \quad \gamma_{v'} \rightarrow -\gamma_{v'}. \quad (3.15)$$

We may decorate the time-reversal domain walls with Majorana chains in a way similar to the  $T^2 = -1$  case. Away from the domain wall, we pair up Majorana modes that share a short bond  $l = \langle \overrightarrow{vv'} \rangle$  as  $i\gamma_v\gamma_{v'}$ . On a domain wall, we pair up Majorana modes that share a long bond  $\tilde{l} = \langle \overrightarrow{vw} \rangle$  as  $i\gamma_v\gamma_w$ .

However, there is an issue with the above pairing rules, because it does not preserve time-reversal invariance. In particular, let us consider the pairing of Majorana modes that shares a long bond  $\tilde{l} = \langle \overrightarrow{vw} \rangle$  on a domain wall. For the specific Kasteleyn orientation we are working with, the short bonds  $\langle vv' \rangle$  and  $\langle ww' \rangle$  must have opposite Kasteleyn orientations. This implies that  $\gamma_v$  and  $\gamma_w$  transform identically under time reversal, which renders the coupling term  $i\gamma_v\gamma_w$  odd under time reversal.

One may try to resolve this issue by adding a minus sign to the coupling when the left hand side of the long bond is in the  $|1\rangle$  state. But this inevitably breaks the fermion parity invariance. Consider the two plaquette spin configurations in Fig. 3.4. Due to the Kasteleyn orientation, the two configurations will have the same fermion parity if we stick to the original coupling rule which breaks time-reversal invariance. The modified coupling rule introduces some extra minus signs into the fermion parity of the second configuration and the number of minus signs is exactly equal to the number of clockwise oriented bonds on the domain wall, which is three in this case.

Therefore, with the modified coupling rule, the two configurations have opposite fermion parity.

## FERMIONIC SYMMETRY PROTECTED TOPOLOGICAL PHASES AND COBORDISMS

### 4.1 Introduction

Classification of symmetry protected topological (SPT) phases has been a subject of intensive activity over the last few years. In the case of free fermions, a complete classification has been achieved in [34, 84] using such ideas as Anderson localization and K-theory. In the case of bosonic systems, all SPT phases are intrinsically interacting, so one has to use entirely different methods. Interactions are also known to affect fermionic SPT phases [85–88]. Recently it has been proposed that cobordism theory can provide a complete classification of both bosonic and fermionic interacting SPT phases in all dimensions. This improves on the previous proposal that group cohomology classifies interacting bosonic SPT phases [41], while group supercohomology [42] classifies interacting fermionic SPT phases. For bosonic systems with time-reversal and  $U(1)$  symmetries the cobordism proposal has been tested in [89] and [90] respectively. Cobordism theory has been found to describe all known bosonic SPT phases with such symmetries in  $D \leq 3$ . In this paper we test the proposal further by studying fermionic SPT phases with  $\mathbb{Z}_2$  symmetry.

The  $\mathbb{Z}_2$  symmetry in question can be either unitary or anti-unitary. In the former case we will assume that the symmetry is internal (does not act on space-time). In the latter case it must reverse the direction of time, so we will call it time-reversal symmetry. In either case, the generator can square either to 1 or to  $(-1)^F$  (fermion parity). Fermionic SPT phases with time-reversal symmetry are also known as topological superconductors, so in particular we describe a classification scheme for interacting topological superconductors.

Compared to the bosonic case, fermionic SPT phases present several related difficulties. First of all, one needs to decide what one means by a fermionic system. In a continuum Lorentz-invariant field theory, anti-commuting fields are also spinors with respect to the Lorentz group, but condensed matter systems are usually defined on a lattice and lack Lorentz invariance on the microscopic level. Thus the connection between spin and statistics need not hold. A related issue is that all fermionic

systems have  $\mathbb{Z}_2$  symmetry called fermionic parity, usually denoted  $(-1)^F$ . But all observables, including the Hamiltonian and the action, are bosonic, i.e. invariant under  $(-1)^F$ . In a sense, every fermionic system has a  $\mathbb{Z}_2$  gauge symmetry, which means that the partition function must depend on a choice of a background  $\mathbb{Z}_2$  gauge field. It is tempting to identify this gauge field with the spin structure. However, it is not clear how a spin structure should be defined for a lattice system, except in the case of toroidal geometry.<sup>1</sup>

Instead of dealing with all these difficult questions, in this paper we take a more “phenomenological” approach: we make a few assumptions about the long-distance behavior of SPT phases which parallel those for bosonic SPT phases, and then test these assumptions by comparing the results in space-time dimensions  $d \leq 4$  with those available in the condensed matter literature. For various reasons, we limit our selves to the cases of no symmetry, time-reversal symmetry, and unitary  $\mathbb{Z}_2$  symmetry. Having found agreement with the known results, we make a conjecture about the classification of fermionic SPT phases with any symmetry group  $G$ .

## 4.2 Spin and Pin structures

A smooth oriented  $d$ -manifold  $M$  equipped with a Riemannian metric is said to have a spin structure if the transition functions for the tangent bundle, which take values in  $SO(d)$ , can be lifted to  $Spin(d)$  while preserving the cocycle condition on triple overlaps of coordinate charts. Let us unpack this definition. On a general manifold one cannot choose a global coordinate system, so one covers  $M$  with coordinate charts  $U_i$ ,  $i \in I$ . If over every coordinate chart  $U_i$  one picks an orthonormal basis of vector fields with the correct orientation, then on double overlaps  $U_{ij} = U_i \cap U_j$  they are related by transition functions  $g_{ij}$  which take values in the group  $SO(d)$  and satisfy on  $U_{ijk} = U_i \cap U_j \cap U_k$  the cocycle condition:

$$g_{ij}g_{jk} = g_{ik}. \quad (4.1)$$

The group  $SO(d)$  has a double cover  $Spin(d)$ , i.e. one has  $SO(d) = Spin(d)/\mathbb{Z}_2$ . One can lift every smooth function  $g_{ij} : U_{ij} \rightarrow SO(d)$  to a smooth function  $h_{ij} : U_{ij} \rightarrow Spin(d)$ , with a sign ambiguity. Thus on every  $U_{ijk}$  one has

$$h_{ij}h_{jk} = \pm h_{ik}. \quad (4.2)$$

$M$  has a spin structure if and only if one can choose the functions  $h_{ij}$  so that the sign on the right-hand side is  $+1$  for all  $U_{ijk}$ . We also identify spin structures which are

<sup>1</sup>In 2d, there is a good combinatorial description of spin structures via so called Kasteleyn orientations [91]. But a generalization of this construction to higher dimensions is unknown.

related by  $Spin(d)$  gauge transformations:

$$h_{ij} \mapsto h'_{ij} = h_i h_{ij} h_j^{-1}, \quad h_i : U_i \rightarrow Spin(d).$$

A spin structure allows one to define Weyl spinors on  $M$ .

For  $d < 4$  every oriented  $d$ -manifold admits a spin structure, but it is not unique, in general. Namely, given any spin structure, one can modify it by multiplying every  $h_{ij}$  by constants  $\zeta_{ij} = \pm 1$  satisfying

$$\zeta_{ij}\zeta_{jk} = \zeta_{ik}.$$

Such constants define a Čech 1-cochain on  $M$  with values in  $\mathbb{Z}_2$ . The same data also parameterize  $\mathbb{Z}_2$  gauge fields on  $M$ , thus any two spin structures differ by a  $\mathbb{Z}_2$  gauge field. It is easy to see that gauge fields differing by  $\mathbb{Z}_2$  gauge transformations lead to equivalent transformations of spin structures, so the number of inequivalent spin structures is equal to the order of the Čech cohomology group  $H^1(M, \mathbb{Z}_2)$ , whose elements label gauge-equivalence classes of  $\mathbb{Z}_2$  gauge fields.

In dimension  $d > 3$  not every oriented manifold admits a spin structure. For example, the complex projective plane  $\mathbb{C}P^2$  does not admit a spin structure. Nevertheless, if a spin structure on  $M$  exists, the above argument still shows that the number of inequivalent spin structures is given by  $|H^1(M, \mathbb{Z}_2)|$ . The necessary and sufficient condition for the existence of a spin structure is the vanishing of the 2nd Stiefel-Whitney class  $w_2(M) \in H^2(X, \mathbb{Z}_2)$ . This condition is purely topological and thus does not depend on the choice of Riemannian metric on  $M$ .

If  $M$  is not oriented, the transition functions  $g_{ij}$  take values in  $O(d)$  rather than  $SO(d)$ . They still satisfy (4.1). An analog of  $Spin$  group in this case is called a  $Pin$  group. In the absence of orientation, fermions transform in a representation of the  $Pin$  group. In fact, for all  $d > 0$  there exist two versions of the  $Pin$  group called  $Pin^+(d)$  and  $Pin^-(d)$ . They both have the property  $Pin^\pm(d)/\mathbb{Z}_2 = O(d)$ . The difference between  $Pin^+$  and  $Pin^-$  is the way a reflection of any one of coordinate axis is realized on fermions. Let  $r \in O(d)$  be such a reflection. It satisfies  $r^2 = 1$ . If  $\tilde{r} \in Pin^\pm(d)$  is a pre-image of  $r$ , it can satisfy either  $\tilde{r}^2 = 1$  or  $\tilde{r}^2 = -1$ . The first possibility corresponds to  $Pin^+$ , while the second one corresponds to  $Pin^-$ .

If we are given an unoriented  $d$ -manifold  $M$ , we can ask whether it admits  $Pin^+$  or  $Pin^-$  structures (that is, lifts of transition functions to either  $Pin^+(d)$  or  $Pin^-(d)$  so that the condition (4.2) on triple overlaps is satisfied). The conditions for this

are again topological: in the case of  $Pin^+$  it is the vanishing of  $w_2(M)$ , while in the case of  $Pin^-$  it is the vanishing of  $w_2(M) + w_1(M)^2$ . Note that if  $M$  happens to be orientable, then  $w_1(M) = 0$ , so the two conditions coincide and reduce to the condition that  $M$  admit a  $Spin$  structure.

Note that these topological conditions are nontrivial already for  $d = 2$ . More precisely, for  $d = 2$  one has a relation between Stiefel-Whitney classes  $w_1^2 + w_2 = 0$ , so every 2d manifold admits a  $Pin^-$  structure, but not necessarily a  $Pin^+$  structure. For example the real projective plane  $\mathbb{RP}^2$  admits only  $Pin^-$  structures, while the Klein bottle admits both  $Pin^+$  and  $Pin^-$  structures. Similarly, not every 3-manifold admits a  $Pin^+$  structure, but all 3-manifolds admit a  $Pin^-$  structure.

### 4.3 Working assumptions

We assume that fermionic SPTs in  $d$  space-time dimensions without time-reversal symmetry can be defined on any oriented smooth  $d$ -manifold  $M$  equipped with a spin structure. Similarly, we assume that fermionic SPTs with time-reversal symmetry can be defined on any smooth manifold  $M$  equipped with a  $Pin^+$  or  $Pin^-$  structure (we will see below that  $Pin^+$  corresponds to  $T^2 = (-1)^F$  while  $Pin^-$  corresponds to  $T^2 = 1$ ). If there are additional symmetries beyond  $(-1)^F$  and time-reversal,  $M$  can carry a background gauge field for this symmetry.

We also assume that given such  $M$ , a long-distance effective action is defined. The action is related to the partition function by  $Z = \exp(2\pi i S_{eff})$ , thus  $S_{eff}$  is defined modulo integers. The trivial SPT phase corresponds to the trivial (zero) action. The effective action is additive under the disjoint union of manifolds. It also changes sign under orientation-reversal. In the case of SPT phases with time-reversal symmetry, this implies  $2S_{eff} \in \mathbb{Z}$ .

The effective action, in general, is not completely topological: it may depend on the Levi-Civita connection on  $M$ . Such actions are gravitational Chern-Simons terms and can exist if  $d = 4k - 1$ . Since we will be interested only in low-dimensional SPT phases, the only case of interest is  $d = 3$ . The correspond gravitational Chern-Simons term has the form

$$S_{CS} = \frac{k}{192\pi} \int \text{Tr}(\omega d\omega + \frac{2}{3}\omega^3),$$

where the trace is in the adjoint representation of  $SO(3)$ . Note that such a term makes sense only on an orientable 3-manifold and therefore can appear only if the symmetry group of the SPT phase does not involve time reversal.

In the bosonic case, one can show that  $k$  must be an integral multiple of 16. In the fermionic case,  $k$  can be an arbitrary integer. The quantization of  $k$  is explained in Appendix F.

The physical meaning of  $S_{CS}$  is that it controls the thermal Hall response of the SPT phases [92]. The thermal Hall conductivity is proportional to  $k$  [92]:

$$\kappa_{xy} = \frac{k\pi k_B^2 T}{12\hbar},$$

where  $T$  is the temperature and  $k_B$  is the Boltzmann constant. Thus for both bosonic and fermionic SPT phases the quantity  $\kappa_{xy}/T$  is quantized, but in the fermionic case the quantum is smaller than in the bosonic case by a factor 16. This is derived in Appendix F.

SPT phases with a particular symmetry form an abelian group, where the group operation amounts to forming the composite system. The effective action is additive under this operation. Taking the inverse corresponds to applying time-reversal to the SPT phase. The effective action changes sign under this operation. Thus the effective action can be regarded as a homomorphism from the set of SPT phases to  $\mathbb{R}/\mathbb{Z} \simeq U(1)$ .

The difference of two SPT phases with the same thermal Hall conductivity is an SPT phase with zero thermal Hall conductivity. Thus it is sufficient to classify SPT phases with zero thermal Hall conductivity. In such a case the action is purely topological. Our final assumption is that this topological action depends only on the bordism class of  $M$ . Equivalently, we assume that if  $M$  is a boundary of some  $d + 1$ -manifold with the same structure ( $Spin$  or  $Pin^\pm$ , as the case may be), then  $S_{eff}$  vanishes. This assumption is supposed to encode locality.

#### 4.4 Fermionic SPT phases without any symmetry

In the case when the only symmetry is  $(-1)^F$ , the manifold  $M$  can be assumed to be a compact oriented manifold with a spin structure. As explained above, without loss of generality we may assume that the action is purely topological (depends only on the spin bordism class of  $M$ ). Thus possible effective actions in space-time dimension  $d$  are classified by elements of the group  $\text{Hom}(\Omega_d^{Spin}(pt), U(1))$ , where  $\Omega_d^{Spin}(pt)$  is the group of bordism classes of spin manifold of dimension  $d$ .

The spin bordism groups  $\Omega_d^{Spin}(pt)$  have been computed by Anderson, Brown, and Peterson [93]. In low dimensions, one gets

$$\Omega_1^{Spin}(pt) = \mathbb{Z}_2, \quad \Omega_2^{Spin}(pt) = \mathbb{Z}_2, \quad \Omega_3^{Spin}(pt) = 0, \quad \Omega_4^{Spin}(pt) = \mathbb{Z},$$

Table 4.1: *Spin* and *Pin*<sup>±</sup> Bordism Groups

$d = D + 1$	$\Omega_d^{Spin}(pt)$	$\Omega_d^{Pin^-}(pt)$	$\Omega_d^{Pin^+}(pt)$	$\Omega_d^{Spin}(B\mathbb{Z}_2)$
1	$\mathbb{Z}_2$	$\mathbb{Z}_2$	0	$\mathbb{Z}_2^2$
2	$\mathbb{Z}_2$	$\mathbb{Z}_8$	$\mathbb{Z}_2$	$\mathbb{Z}_2^2$
3	0	0	$\mathbb{Z}_2$	$\mathbb{Z}_8$
4	$\mathbb{Z}$	0	$\mathbb{Z}_{16}$	$\mathbb{Z}$
5	0	0	0	0
6	0	$\mathbb{Z}_{16}$	0	0
7	0	0	0	$\mathbb{Z}_{16}$
8	$\mathbb{Z}^2$	$\mathbb{Z}_2^2$	$\mathbb{Z}_2 \times \mathbb{Z}_{32}$	$\mathbb{Z}^2$
9	$\mathbb{Z}_2^2$	$\mathbb{Z}_2^2$	0	$\mathbb{Z}_2^4$
10	$\mathbb{Z}_2^2 \times \mathbb{Z}$	$\mathbb{Z}_2 \times \mathbb{Z}_8 \times \mathbb{Z}_{128}$	$\mathbb{Z}_2^3$	$\mathbb{Z}_2^4 \times \mathbb{Z}$

Table 4.2: Interacting Fermionic SPT Phases

$d = D + 1$	no symmetry	$T^2 = 1$	$T^2 = (-1)^F$	unitary $\mathbb{Z}_2$
1	$\mathbb{Z}_2$	$\mathbb{Z}_2$	0	$\mathbb{Z}_2^2$
2	$\mathbb{Z}_2$	$\mathbb{Z}_8$	$\mathbb{Z}_2$	$\mathbb{Z}_2^2$
3	$\mathbb{Z}$	0	$\mathbb{Z}_2$	$\mathbb{Z}_8 \times \mathbb{Z}$
4	0	0	$\mathbb{Z}_{16}$	0
5	0	0	0	0
6	0	$\mathbb{Z}_{16}$	0	0
7	$\mathbb{Z}^2$	0	0	$\mathbb{Z}_{16} \times \mathbb{Z}^2$
8	0	$\mathbb{Z}_2^2$	$\mathbb{Z}_2 \times \mathbb{Z}_{32}$	0
9	$\mathbb{Z}_2^2$	$\mathbb{Z}_2^2$	0	$\mathbb{Z}_2^4$
10	$\mathbb{Z}_2^2$	$\mathbb{Z}_2 \times \mathbb{Z}_8 \times \mathbb{Z}_{128}$	$\mathbb{Z}_2^3$	$\mathbb{Z}_2^4$

If a bordism group contains a free part, its Pontryagin dual has a  $U(1)$  factor. This means that the corresponding effective action can depend on a continuous parameter. If we want to classify SPT phases up to homotopy, we can ignore such parameters. This is equivalent to only considering the torsion subgroup of  $\Omega_d^{Spin}(pt)$ . Thus we propose that SPT phases in dimension  $d$  are classified by elements of the Pontryagin dual of the torsion subgroup of  $\Omega_d^{Spin}(pt)$ . We will denote this group  $\Omega_{Spin}^{d,tors}(pt)$ .

The groups  $\Omega_d^{Spin}$  are displayed in Table 1. The classification of interacting fermionic SPT phases can be deduced from it in the manner just described and is displayed in Table 2. For comparison, the classification of free fermionic SPT phases described in [84] and [34] is shown in Table 3. We see that there are nontrivial interacting

Table 4.3: Free Fermionic SPT Phases

$d = D + 1 \bmod 8$	no symmetry	$T^2 = 1$	$T^2 = (-1)^F$
1	$\mathbb{Z}_2$	$\mathbb{Z}_2$	0
2	$\mathbb{Z}_2$	$\mathbb{Z}$	$\mathbb{Z}_2$
3	$\mathbb{Z}$	0	$\mathbb{Z}_2$
4	0	0	$\mathbb{Z}$
5	0	0	0
6	0	$\mathbb{Z}$	0
7	$\mathbb{Z}$	0	0
8	0	$\mathbb{Z}_2$	$\mathbb{Z}$

Table 4.4: Classification of free fermionic SPT phases according to [84] and [34]. The “no symmetry” case corresponds to class D, the case  $T^2 = 1$  corresponds to class BDI, the case  $T^2 = (-1)^F$  corresponds to class DIII.

fermionic SPT phases with zero thermal Hall response in  $D = 0$  and 1 but not in  $D = 2$  and 3. However, for  $D = 2$  there is a phase with a nontrivial thermal Hall response; it is also present in the table of free fermionic SPT phases. In higher dimensions the number of phases grows rapidly. For instance, the effective action can be any combination of the Stiefel-Whitney numbers modulo  $w_1$  and  $w_2$  (such effective actions correspond to fermionic phases which are independent of the spin structure on  $M$  and thus can also be regarded as bosonic phases).

Let us consider the cases  $d = 1$  and  $d = 2$  in slightly more detail. For  $d = 1$ , there is only one connected closed manifold, namely, the circle. There are two spin structures on a circle: the periodic one and the anti-periodic one. The nontrivial effective action assigns a different sign to each spin structure and is multiplicative over disjoint unions. From the point of view of quantum mechanics, such an effective action corresponds to the  $d = 1$  SPT phase whose unique ground state is fermionic.

In two space-time dimensions, the situation is more complicated. Spin structures on an oriented 2d manifold  $X$  can be thought of as  $\mathbb{Z}_2$  valued quadratic forms on  $H_1(X, \mathbb{Z}_2)$  satisfying  $q(x + y) = q(x) + x \cap y + q(y) \pmod{2}$ , where  $x \cap y$  denotes the  $\mathbb{Z}_2$  intersection pairing. The bordism invariant is the Arf invariant, which is the obstruction to finding a Lagrangian subspace for this quadratic form. The effective action for the nontrivial SPT phase in  $D = 1$  is given by the Arf invariant [94]

$$S(q) = \frac{1}{\sqrt{|H^1(X, \mathbb{Z}_2)|}} \sum_{A \in H^1(X, \mathbb{Z}_2)} \exp(2\pi i q(A)/2). \quad (4.3)$$

Another way to describe the Arf invariant is to consider zero modes for the chiral Dirac operator. Their number modulo 2 is an invariant of the spin structure and coincides with the Arf invariant [95]. In string theory, spin structures for which the Arf invariant is even (respectively, odd) are called even (respectively, odd).

The spin cobordism classification is consistent with existing results in condensed matter literature. Fidkowski and Kitaev [85] have considered the Majorana chain with just fermion parity. There are two distinct phases: one where all sites are decoupled and unoccupied in the unique ground state and one with dangling Majorana operators which can be paired into a gapless Dirac mode representing a two-fold ground state degeneracy. In the absence of any symmetry beyond  $(-1)^F$ , a four-fermion interaction can gap out the dangling modes in pairs, so these are the only two phases.

#### 4.5 Fermionic SPT phases with time-reversal symmetry

##### General considerations

In the presence of time-reversal symmetry, the manifold  $M$  can be unorientable. As discussed in section 2, there are two distinct unoriented analogs of a spin structure, called  $Pin^+$  and  $Pin^-$  structures. They should correspond to the two possibilities for the action of time-reversal:  $T^2 = 1$  and  $T^2 = (-1)^F$ .

Naively, it seems that  $T^2 = 1$  should correspond to  $Pin^+$  and  $T^2 = (-1)^F$  should correspond to  $Pin^-$ . Indeed, for  $Pin^+$  the reflection of a coordinate axis acts on a fermion by an element  $\tilde{r}$  satisfying  $\tilde{r}^2 = 1$ , while for  $Pin^-$  it acts by  $\tilde{r}$  satisfying  $\tilde{r}^2 = -1$ . However, one should take into account that the groups  $Pin^\pm$  are suitable for space-time of Euclidean signature. A reflection of a coordinate axis in Euclidean space is related to time-reversal by a Wick rotation. Let  $r$  be a reflection of the coordinate axis which is to be Wick-rotated. The corresponding element of  $Pin^\pm$  acts on the fermions by a Dirac matrix  $\gamma_d$  which satisfies  $\gamma_d^2 = \pm 1$ . Wick rotation amounts to  $\gamma_d \mapsto i\gamma_d$ , hence  $Pin^+$  corresponds to  $T^2 = (-1)^F$ , while  $Pin^-$  corresponds to  $T^2 = 1$ . This identification will be confirmed by the comparison with the results from the condensed matter literature.

$$T^2 = (-1)^F$$

We propose that interacting fermionic SPT phases protected by time-reversal symmetry  $T$  with  $T^2 = (-1)^F$  are classified by elements of

$$\Omega_{Pin^+}^d(pt) = \text{Hom}(\Omega_d^{Pin^+}(pt), U(1)).$$

We will call this group the  $Pin^+$  cobordism group with  $U(1)$  coefficients.

The  $Pin^+$  bordism groups have been computed by Kirby and Taylor [96]

$$\Omega_1^{Pin^+}(pt) = 0, \quad \Omega_2^{Pin^+}(pt) = \mathbb{Z}_2, \quad \Omega_3^{Pin^+}(pt) = \mathbb{Z}_2, \quad \Omega_4^{Pin^+}(pt) = \mathbb{Z}_{16},$$

$Pin^+$  bordism groups grow quickly with dimension, soon having multiple cyclic factors.

In one space-time dimension, the  $Pin^+$  cobordism group vanishes. This is easily interpreted in physical terms. Recall that without time-reversal symmetry, the ground state can be bosonic or fermionic, and the latter possibility corresponds to a nontrivial fermionic  $d = 1$  SPT phases. However, if time-reversal symmetry  $T$  with  $T^2 = (-1)^F$  is present, fermionic states are doubly-degenerate, and since by definition the ground state of an SPT phase are non-degenerate, the ground state cannot be fermionic.

In two space-time dimensions, there is an isomorphism

$$\Omega_2^{Pin^+}(pt) \rightarrow \Omega_2^{Spin}(pt),$$

see [94]. The isomorphism arises from the fact that a  $Pin^+$  structure on an unoriented manifold induces a spin structure on its orientation double cover. Thus there is a unique nontrivial fermionic SPT phase in  $d = 2$ , and the corresponding effective action is simply the action (4.3) on the orientation double cover:

$$S(q) = \frac{1}{\sqrt{|H^1(\tilde{X}, \mathbb{Z}_2)|}} \sum_{A \in H^1(\tilde{X}, \mathbb{Z}_2)} e^{2\pi i q(A)/2}.$$

The classification of the free fermionic SPTs in  $d = 2$  also predicts a unique nontrivial phase with time-reversal symmetry  $T^2 = (-1)^F$  [34, 84]. It can be realized by a time-reversal-invariant version of the Majorana chain and is characterized by the presence of a pair of dangling Majorana zero modes on the edge.

In three space-time dimensions, a similar map is not an isomorphism, as  $\Omega_3^{Spin} = 0$ . However, there is a map

$$[\cap w_1] : \Omega_3^{Pin^+} \rightarrow \Omega_2^{Spin} \tag{4.4}$$

taking a  $Pin^+$  manifold to a codimension 1 submanifold Poincaré dual to the orientation class  $w_1$ . This submanifold is defined to be minimal for the property that the complement can be consistently oriented. With this choice of partial orientation,

crossing this submanifold reverses the orientation, so it can be thought of as a time-reversal domain wall. For  $Pin^+$  3-manifolds, we have  $w_1^2 = 0$ , so this domain wall is oriented and inherits a Spin structure from the ambient spacetime.

The map (4.4) is an isomorphism [94]. From the physical viewpoint this means that away from the time-reversal domain walls the SPT is trivial and the boundary can be gapped, but on the domain walls there is a  $d = 2$  fermionic SPT, the Majorana chain, so at locations where the domain walls meet the boundary there are Majorana zero modes. This is a special case of a construction of SPT phases discussed in the bosonic case in [46]. One starts with a system with symmetry  $G$  in a trivial phase, breaks the  $G$  symmetry, decorates the resulting domain walls with an SPT in 1 dimension lower, and finally proliferates the domain walls to restore the symmetry  $G$ . One can also do this with defects of higher codimension. A mathematical counterpart of this general construction is the Smith homomorphism discussed below.

The classification of free fermionic SPT phases also predicts a unique nontrivial  $d = 3$  SPT phase. It can be realized by a spin-polarized  $p \pm ip$  superconductor [34, 84]. It is characterized by the presence of a pair of counter-propagating massless Majorana fermions on the edge of the SPT phase.

In four space-time dimensions, the cobordism classification says that fermionic SPT phases are labeled by elements of  $\mathbb{Z}_{16}$ . Free fermionic SPTs in  $d = 4$  are classified by  $\mathbb{Z}$  [34, 84], but with interactions turned on  $\mathbb{Z}$  collapses to  $\mathbb{Z}_{16}$  [86]. The generator of  $\Omega_4^{Pin^+} = \mathbb{Z}_{16}$  is the eta invariant of a Dirac operator [97]. The corresponding free fermionic SPT phase can be realized by a spin-triplet superconductor [34, 84]. It is characterized by the property that on its boundary there is a single massless Majorana fermion.

Two layers of the basic phase can be constructed from the  $d = 2$  phase with time-reversal symmetry  $T^2 = 1$ , via the map

$$[\cap w_1^2]: \Omega_4^{vPin^+} \rightarrow \Omega_2^{vPin^-}.$$

The map sends a the bordism class of a manifold  $X$  on the left hand side to the bordism class of a codimension-2 submanifold of  $X$  representing  $w_1^2(TX)$ . From the physical viewpoint, the order 8 phase with  $T^2 = (-1)^F$  can be obtained from the trivial SPT phase by decorating certain codimension 2 defects (self-intersections of time-reversal domain walls, see the 3d case above) with the order 8  $D = 1$  phase with  $T^2 = 1$ , i.e. the Kitaev chain.

Eight copies of this fermionic SPT phase are equivalent to a bosonic SPT phase with time-reversal symmetry and the effective action  $\int w_1^4$  (the bosonic SPT phase predicted by group cohomology, see [89]). To show this, we need to show  $8\eta = w_1^4$  for every  $Pin^+$  4-manifold. The space  $\mathbb{RP}^4$  generates the  $Pin^+$  bordism group in 4 dimensions, so every such manifold  $X$  is  $Pin^+$  bordant to a disjoint union of  $k$   $\mathbb{RP}^4$ s. Since  $\eta$  is a  $Pin^+$  bordism invariant, it follows  $8\eta(X) = 8k\eta(\mathbb{RP}^4)$ . Now  $w_1^4$  is also a bordism invariant, so  $w_1^4(X) = kw_1^4(\mathbb{RP}^4)$ . Thus, we just need to show  $8\eta(\mathbb{RP}^4) = w_1^4(\mathbb{RP}^4)$ . We know the left hand side is  $-1$  since the bordism group is  $\mathbb{Z}/16$  and  $\eta$  generates the dual group, and it is simple to show  $w_1^4(\mathbb{RP}^4) = -1$  as well. The equivalence of these two phases was also argued in [87].

Note that the eta-invariant cannot be written as an integral over a Lagrangian density  $\mathcal{L}$  naturally associated to a lattice configuration on the underlying manifold  $M$ . In particular, if we have a covering map, we can pullback configurations to the cover. If the Lagrangian density were to simply pull back, then the action would just be multiplied by the number of sheets of the cover. However, for  $M = \mathbb{RP}^4$  the eta-invariant associated to the standard Dirac operator is order 16 but trivial for its orientation double cover,  $S^4$ .

This signals that the effective field theory requires a certain amount of non-locality. It cannot have a description where each  $Pin^+$  structure corresponds to a lattice configuration which respects covering maps of spacetimes up to gauge transformations.

It is interesting to note that the topological  $Pin^+$  bordism group in 4d is  $\mathbb{Z}_8$  rather than  $\mathbb{Z}_{16}$ . There is a manifold homeomorphic to the smooth generator  $\mathbb{RP}^4$  but not smoothly  $Pin^+$  cobordant to it which has a  $\mathbb{Z}_{16}$  invariant equal to 9 as opposed to  $\mathbb{RP}^4$ 's 1 (these numbers are equal mod 8). The eta-invariant distinguishes these two manifolds. Since the classification of topological insulators in 3+1d is known to be at least  $\mathbb{Z}_{16}$ , this example shows that the spacetimes relevant to these systems always carry smooth structure.

$$T^2 = 1$$

We propose that interacting fermionic SPT phases protected by time-reversal symmetry with  $T^2 = 1$  are classified by the  $Pin^-$  cobordism groups with  $U(1)$  coefficients. In low dimensions the  $Pin^-$  bordism groups are [94]

$$\Omega_1^{Pin^-}(pt) = \mathbb{Z}_2, \quad \Omega_2^{Pin^-}(pt) = \mathbb{Z}_8, \quad \Omega_3^{Pin^-}(pt) = 0, \quad \Omega_4^{Pin^-}(pt) = 0,$$

and the cobordism groups are their Pontryagin duals.

In one space-time dimension, fermionic SPT phases are classified by  $\mathbb{Z}_2$ . This is easily interpreted in physical terms: the non-degenerate ground state can be either bosonic or fermionic, without breaking  $T$ .

In two space-time dimensions, a  $Pin^-$  structure can be thought of as a  $\mathbb{Z}_4$ -valued quadratic enhancement of the intersection form which in the oriented ( $Spin$ ) case is even and reduces to our description above[94]. Such a form  $q$  satisfies  $q(x + y) = q(x) + 2x \cap y + q(y) \pmod{4}$ , where  $2x \cap y$  represents the mod 2 intersection of  $x$  and  $y$  mapped to  $\mathbb{Z}_4$ . The bordism group  $\Omega_2^{Pin^-} = \mathbb{Z}_8$  is generated by  $\mathbb{RP}^2$ . The effective action is a generalization of the Arf invariant, the Arf-Brown-Kervaire invariant:

$$S(q) = \frac{1}{\sqrt{|H^1(X, \mathbb{Z}_2)|}} \sum_{A \in H^1(X, \mathbb{Z}_2)} \exp(2\pi i q(A)/4). \quad (4.5)$$

It takes values in  $\mathbb{Z}_8 \in U(1)$ . If  $q(x)$  is even for all  $x$  (that is, if  $q$  is  $\mathbb{Z}_2$ -valued), it reduces to the Arf invariant. This situation occurs when the space-time is orientable.

From the physical viewpoint, the generator of  $\mathbb{Z}_8$  is the Majorana chain, which can be regarded as a time-reversal invariant system with  $T^2 = 1$ . Time-reversal protects the dangling Majorana zero modes from being gapped out in pairs. Instead, interactions can only gap out octets, yielding a  $\mathbb{Z}_8$  classification of phases labeled by the number of dangling modes [85]. Moreover, four copies of the Majorana chain with  $T^2 = 1$  have states on the boundary on which  $T$  acts projectively,  $T^2 = -1$  [85]; hence, four copies of the basic fermionic SPT phases with time-reversal  $T^2 = 1$  are equivalent to the basic bosonic SPT phase in  $d = 2$  with time-reversal symmetry. We can easily see this from the cobordism viewpoint. The generator of the  $Pin^-$  bordism group in  $d = 2$  is  $\mathbb{RP}^2$ , so the fourth power of the generator of the cobordism group is  $-1$  for this spacetime (here we are thinking about  $\mathbb{Z}_8$  as a subgroup of  $U(1)$ ). Meanwhile,  $w_1^2$  is also  $-1$  on  $\mathbb{RP}^2$ . Since both of these are  $Pin^-$ -bordism invariants, they are equal on all  $d = 2$  spacetimes.

As with the eta-invariant discussed above, the Arf-Brown-Kervaire invariant does not admit a local expression. There is a  $\nu Pin^+$  structure on  $\mathbb{RP}^2$  for which the Arf-Brown-Kervaire invariant is a primitive 8th root of unity. However, the corresponding  $Spin$  structure on the orientation double cover  $S^2$  has Arf-Brown-Kervaire invariant 1 (the unique  $Spin$  structure on the 2-sphere extends to a 3-ball).

#### 4.6 Fermionic SPT phases with a unitary $\mathbb{Z}_2$ symmetry

Let  $g$  denote the generator of a unitary  $\mathbb{Z}_2$  symmetry. There are two possibilities: either  $g^2 = 1$  or  $g^2 = (-1)^F$ . In this section we discuss the former possibility only;

the other one is discussed in the next section.

We propose that interacting fermionic SPT phases with unitary  $\mathbb{Z}_2$  symmetry  $g$ ,  $g^2 = 1$ , are classified by

$$\Omega_{Spin,tors}^d(B\mathbb{Z}_2) = \text{Hom}(\Omega_d^{Spin,tors}(B\mathbb{Z}_2), U(1))$$

The analogous group in the bosonic case is  $\Omega_{SO,tors}^d(B\mathbb{Z}_2)$ . In all dimensions there is an isomorphism called the Smith isomorphism

$$\tilde{\Omega}_d^{Spin}(B\mathbb{Z}_2) \rightarrow \Omega_{d-1}^{Pin^-}(pt),$$

where on the left hand side we use the tilde to denote reduced bordism: the kernel of the forgetful map to  $\Omega_d^{Spin}(pt)$ . The torsion part of reduced bordism is dual to SPT phases which can be made trivial after breaking the symmetry. Not all SPT phases are of this sort. One could imagine that after breaking the symmetry the system is reduced to some non-trivial SRE like the Kitaev chain. In general,

$$\Omega_d^{Spin}(BG) = \tilde{\Omega}_d^{Spin}(BG) \oplus \Omega_d^{Spin}(pt),$$

so these effects can be separated consistently and the Smith isomorphism is enough to classify the  $G = \mathbb{Z}_2$  phases. This splitting fails if any elements of  $G$  are orientation reversing or if  $G$  acts projectively on fermions.

The Smith isomorphism is defined as follows. Starting with a Spin manifold  $X$  and some  $A \in H^1(X, \mathbb{Z}_2)$  representing a class on the left hand side, we produce a submanifold  $Y$  Poincaré dual to  $A$ . (That we can do this is a special fact about codimension 1 classes with  $\mathbb{Z}_2$  coefficients. Not all homology classes are represented by submanifolds.) The manifold  $Y$  is not necessarily orientable. The Spin structure on  $TX$  restricts to a Spin structure on  $TY \oplus NY$ , where  $NY$  is the normal bundle of  $Y$  in  $X$ . In fact,  $NY$  is classified by the restriction of  $A$  to  $Y$ . We compute

$$0 = w_1(TX)|_Y = w_1(TY \oplus NY) = w_1(TY) + A,$$

so on  $Y$  the gauge field  $A$  restricts to the orientation class, ie. the  $\mathbb{Z}_2$  symmetry is orientation-reversing for  $Y$ . We also have

$$w_2(TY \oplus NY) = w_2(TY) + w_1(TY)^2,$$

so the Spin structure on  $X$  becomes a  $Pin^-$  structure on  $Y$ .

Physically, the submanifold  $Y$  Poincaré dual to  $A$  represents  $\mathbb{Z}_2$  domain walls. The dual map from the  $Pin^-$  cobordism of a point in  $d - 1$  dimensions to the  $Spin$

cobordism of  $B\mathbb{Z}_2$  in  $d$  dimensions has the following physical meaning. Picking an element of the  $Pin^-$  cobordism group gives us a  $d - 1$ -dimensional fermionic SPT with time-reversal symmetry  $T^2 = 1$ . To obtain a  $d$ -dimensional SPT, we decorate  $\mathbb{Z}_2$  domain walls with this  $d - 1$ -dimensional SPT and then proliferate the walls.

The inverse map can be described via compactification. One takes the  $d$ -dimensional SPT on a spacetime which is a circle bundle over the  $d - 1$ -dimensional (perhaps unorientable) spacetime. This circle bundle is the unit circle bundle of the orientation line plus a trivial line, and is therefore oriented. We give the gauge field nontrivial holonomy around this circle and compactify. The effective field theory in  $d - 1$  dimensions is the  $d - 1$ -dimensional SPT phase with time-reversal symmetry.

Fermionic SPT phases with a unitary  $\mathbb{Z}_2$  symmetry have not been much studied in the physics literature. In one space-time dimension, they are classified by  $\mathbb{Z}_2 \times \mathbb{Z}_2$ , since the ground state can be either bosonic or fermionic, as well as  $g$ -even or  $g$ -odd. In three space-time dimensions, Levin and Gu [88] argued that fermionic SPT phases with  $\mathbb{Z}_2$  symmetry and zero thermal Hall conductance are classified by  $\mathbb{Z}_8$ . Both of these results agree with the cobordism approach.

#### 4.7 Fermionic SPT phases with a general symmetry

A choice of spin structure gives a lift of the oriented frame bundle  $P_{SO(d)}$  to a spin frame bundle  $P_{Spin(d)}$ . Neutral Dirac spinors are sections of the bundle  $S$  associated to this one by the complex spin representation. For Dirac spinors charged under some  $G$  representation  $\rho$ , they are sections of the tensor bundle

$$\psi \in \Gamma(S \otimes_{\mathbb{C}} A^*\rho),$$

where  $A^*\rho$  denotes the vector bundle associated to the gauge bundle by  $\rho$ . Bosonic observables are composed of fermion bilinears which are sections of the tensor square of this bundle or the tensor product of this bundle with its dual. These are composed of integral spin representations of  $SO(d)$  and exterior powers of  $\rho^2$ .

However, the situations where the spacetime is not a spin manifold are still physically important if  $\rho$  is a projective representation. That is, while the spin frame bundle  $P_{Spin(d)}$  or charge bundle  $A^*\rho$  may not exist, the tensor product above does. For example, when  $\rho$  is a half-charge representation of  $G = U(1)$  the choice of a tensor product bundle is the same as a  $Spin^c$  structure with determinant line  $\rho^2$ . One also knows that such a  $Spin^c$  structure is the same as a spin structure on  $TX \oplus A^*\rho^2$ .

One way to deal with this situation is to regard the fermions in  $d$  dimensions as dimensional reduction of fermions in  $d + n$  dimensions. Under such a reduction, the rotation group  $SO(n+d)$  decomposes into  $SO(d) \times SO(n)$  (for the moment we assume that the  $d$ -dimensional theory does not have orientation-reversing symmetries, and accordingly the  $d$ -dimensional space-time is orientable). We imagine that the symmetry group  $G$  is embedded into  $SO(d)$ , and denote by  $\xi$  the  $G$ -representation in which the  $n$ -vector of  $SO(n)$  transforms. We can think of  $\xi$  as a particular  $G$ -bundle over  $BG$ . Spinors in  $d + n$  dimensions are elements of an irreducible module over the Clifford algebra built from  $\mathbb{R}^n \oplus \xi$ .

Consider now the theory on a curved space-time  $X$  equipped with a  $G$ -bundle  $A$ . As usual, we can think of  $A$  as a map from  $X$  to  $BG$ , defined up to homotopy. To define the theory on such a space-time we must specify the bundle in which the fermions take value. This bundle must have the same rank as the spinor of  $SO(d + n)$  and be a module over a bundle of Clifford algebras  $T^*X \oplus A^*\xi$ . Such a bundle is called a spin structure on the  $SO(d + n)$ -bundle  $T^*X \oplus A^*\xi$ .

If some of the symmetries are orientation-reversing, we need to allow  $X$  to be unorientable, so that the structure group of the tangent bundle is  $O(d)$  rather than  $SO(d)$ . But we can compensate for this by embedding  $G$  into  $O(n)$  so that the generators of the Clifford algebra transform as a vector of  $SO(d + n)$ . Then fermions must take values in the irreducible Clifford module over the corresponding bundle of Clifford algebras, as before.

This discussion leads us to the following proposal Given a bosonic symmetry group  $G$ , and its representation  $\xi$ , fermionic SPT phases in  $d$  space-time dimensions with this symmetry structure are classified by

$$\Omega_{Spin}^d(\mathfrak{b}BG, \xi),$$

a cobordism theory dual to the torsion part of the bordism theory of  $d$ -manifolds  $X$  with a map  $A : X \rightarrow \mathfrak{b}BG$  (the gauge field) and a spin structure on  $TX \oplus A^*\xi$ . It is important for continuous groups to use  $\mathfrak{b}BG$  rather than  $BG$  since gauging the  $G$  symmetry means coupling to a flat  $G$  gauge field. Turning on curvature for the gauge field requires a kinetic term which is non-canonical. One model for  $\mathfrak{b}BG$  is to take the classifying space of  $G$  as a discrete group. For finite  $G$  this is of course automatic.

The data  $(G, \xi)$  may seem to depend on some unphysical details, like the embedding of  $G$  into  $SO(n)$ , but one can show that cobordism groups thus defined depend

only on  $w_1(\xi) : G \rightarrow \mathbb{Z}_2$ , which picks out the orientation reversing elements, and  $w_2(\xi) \in H^2(G, \mathbb{Z}_2)$  [98], which determines how  $G$  is extended by fermion parity.

Let us illustrate this with some examples. For  $G = \mathbb{Z}_2$ , first there is the trivial representation, for which this twisted cobordism group is the ordinary ones classifying fermionic SPTs with an internal  $\mathbb{Z}_2$  symmetry acting honestly on the fermions, so the total symmetry group is  $\mathbb{Z}_2 \times \mathbb{Z}_2^F$ .

The other irreducible is the 1d sign representation. For this representation we have  $w_1$  equal to the generator of  $H^1(B\mathbb{Z}_2, \mathbb{Z}_2)$ , this being the determinant of the representation, and  $w_2 = 0$  since this representation is 1 dimensional. We compute

$$w_1(TX \oplus A^*\xi) = w_1(TX) + A^*w_1(\xi) = w_1(TX) + A,$$

so an orientation of  $TX \oplus A^*\xi$  identifies  $A$  with the orientation class of  $X$ . We also have

$$w_2(TX \oplus A^*\xi) = w_2(TX) + w_1(TX)A^*w_1(\xi) = w_2(TX) + w_1(TX)^2,$$

a trivialization of which is a  $Pin^-$  structure on  $TX$ . Thus,

$$\Omega_{Spin}^d(B\mathbb{Z}_2, sign) = \Omega_{Pin^-}^d.$$

Since  $w_1(\xi) \neq 0$  and  $w_2(\xi) = 0$  we interpret this group as classifying fermionic SPTs with an orientation-reversing symmetry such as time reversal which satisfies  $T^2 = 1$ . Note that the same group classifies SPT phases with a reflection symmetry squaring to 1.

We can also consider a sum of two sign representations, for which we have  $w_1(\xi) = 0$  and  $w_2(\xi) \neq 0$ . This gives a bordism theory of oriented manifolds with  $A^2 = w_2(TX)$ . This symmetry structure is that associated to an orientation preserving symmetry such as particle-hole symmetry which squares to the fermion parity.

The sum of three sign representations has both  $w_1(\xi)$  and  $w_2(\xi)$  nonzero. The cohomology of  $B\mathbb{Z}_2$  implies also  $w_2(\xi) = w_1(\xi)^2$ . With this we compute

$$w_1(TX \oplus A^*\xi) = w_1(TX) + A$$

and

$$w_2(TX \oplus A^*\xi) = w_2(TX) + A^2 + A^2 = w_2(TX).$$

The first implies that  $A$  equals the orientation class of  $X$ . The second says that a spin structure on  $TX \oplus A^*\xi$  is the same as a  $Pin^+$  structure on  $TX$ . Thus

$$\Omega_{Spin}^d(B\mathbb{Z}_2, 3 \times sign) = \Omega_{Pin^+}^d.$$

Therefore fermionic SPT phases with an orientation reversing  $\mathbb{Z}_2$  symmetry squaring to the fermion parity are classified by  $Pin^+$  cobordism.

For  $G = U(1)$  there are no continuous representations with  $w_1 \neq 0$  and  $w_2 \neq 0$  for a continuous representation precisely when the sum of charges is odd. In this case  $A^*w_2(\xi)$  is the mod 2 reduction of the gauge curvature  $F_A$ . A spin structure on  $w_2(TX \oplus A^*\xi)$  is therefore the same thing as a  $Spin^c$  structure with determinant line  $F_A$ . Note that these are not the  $Spin^c$  cobordism groups studied in most of the mathematical literature since we require the determinant line to be flat.

For  $G = U(1) \times \mathbb{Z}_2$  we now have representations where the  $\mathbb{Z}_2$  is orientation reversing. For example, consider  $\xi = \text{charge } 1 \otimes \text{trivial} \oplus \text{trivial} \otimes \text{sign}$ . For this representation,  $w_1(\xi)$  is the map to  $\mathbb{Z}_2$  which is trivial on  $U(1)$  and the identity on  $\mathbb{Z}_2$ . We also find

$$w_2(TX \oplus A^*\xi) = w_2(TX) + w_1(TX)^2 + F_A.$$

If we instead used three copies of the sign representation, we would have

$$w_2(TX \oplus A^*\tilde{\xi}) = w_2(TX) + F_A.$$

It may first appear that these give different cobordism theories, but note that  $w_1(TX)^2$  lifts to an integral class, so a redefinition of the  $U(1)$  field produces an equivalence between the two bordism groups. This is the same redefinition used in [87] to show that the  $T^2 = 1$  and  $T^2 = (-1)^F$  classifications agree, a result verified here in cobordism. This is also reflected in the uniqueness of the  $Pin^c(d)$  group and we find that both types of phase are classified by  $Pin^c$  bordism with flat determinant line.

Now consider  $G = U(1) \rtimes \mathbb{Z}_2$  with  $\mathbb{Z}_2$  acting by conjugation. This group can be thought of as  $SO(2) \rtimes \mathbb{Z}_2 = O(2)$ . Consider first the standard 2d representation  $\xi$ . For this,  $w_1(\xi)$  is the determinant  $O(2) \rightarrow \mathbb{Z}_2$  and  $w_2(\xi)$  is the obstruction to finding a section of

$$Pin^+(2) \rightarrow O(2),$$

ie. it is the class in group cohomology  $H^2(BO(2), \mathbb{Z}_2)$  classifying  $Pin^+(2)$ . The ring  $H^*(BO(2), \mathbb{Z}_2)$  is generated by the universal Stiefel-Whitney classes  $w_1$  and  $w_2$ , and  $w_2(\xi)$  is the universal  $w_2$ . This representation corresponds to  $T^2 = 1$  since  $T^2 = 1$  in  $Pin^+(2)$ .

One can also consider  $T^2 = (-1)^F$  by using the representation  $\tilde{\xi} = \xi + 2 \times \text{sign}$ . For this,  $w_1(\tilde{\xi}) = w_1(\xi)$ , but  $w_2(\tilde{\xi})$  is the universal  $w_2 + w_1^2$ , which differs from the

other representation, demonstrating that these two classifications differ when time reversal does not commute with  $U(1)$ .

#### 4.8 Concluding remarks

We have seen that cobordism correctly predicts the known classification of interacting fermionic SPT phases in  $D \leq 3$  with  $\mathbb{Z}_2$  symmetry, either unitary or anti-unitary. We find that for  $0 \leq D \leq 3$ , all phases are realized by free fermions. However, in higher dimensions new phenomena occur. First of all, while the classification of free fermionic SPT phases with a fixed symmetry exhibits mod 8 periodicity in dimension [34], in the interacting case there is no periodicity. Second, the deviations from the free fermionic classification occur for high enough  $D$ , but the precise point depends on the symmetry group. For example, for SPT phases with time-reversal symmetry  $T$ ,  $T^2 = (-1)^F$ , deviations start at  $D = 3$ . For SPT phases with no symmetry beyond  $(-1)^F$  deviations start at  $D = 6$ . (In  $D = 6$  the free fermionic classification predicts  $\mathbb{Z}$ , but in the interacting case it is  $\mathbb{Z} \times \mathbb{Z}$  because there are two different gravitational Chern-Simons terms possible based on the Pontryagin numbers  $p_1^2$  and  $p_2$ , respectively.)

Third, while in low dimensions the effect of interactions is to truncate the free fermionic classification, in high enough dimension inherently interacting fermionic SPT phases appear. For example, in  $D = 7$  free fermionic SPT phases with time-reversal symmetry  $T$ ,  $T^2 = (-1)^F$ , are classified by  $\mathbb{Z}$ , while the cobordism approach predicts  $\mathbb{Z}_2 \times \mathbb{Z}_{32}$ . The latter group is not a quotient of the former, so truncation alone cannot explain the discrepancy. The most likely interpretation is that  $\mathbb{Z}_{32}$  is a truncation of  $\mathbb{Z}$ , while the  $\mathbb{Z}_2$  factor corresponds to an inherently interacting fermionic SPT phase. Similarly, in  $D = 6$  there should exist inherently interacting fermionic SPT phases with only fermion parity as a symmetry.

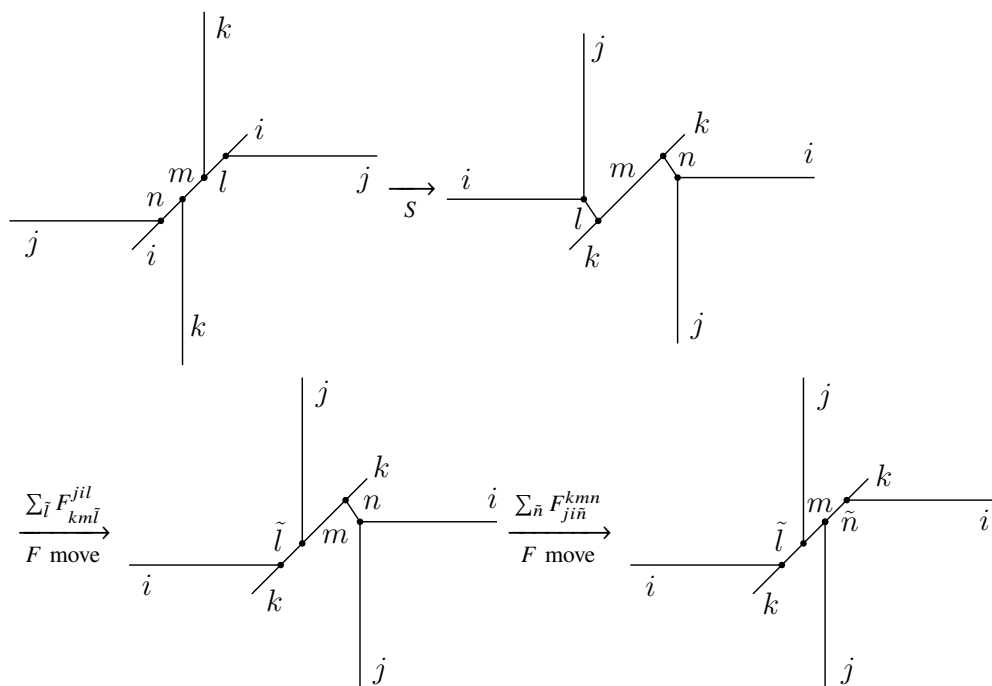
We have found that the correct classification requires the use of smooth manifolds rather than topological manifolds. It would be interesting to determine whether there is some physical difference between the smooth and piecewise linear categories.

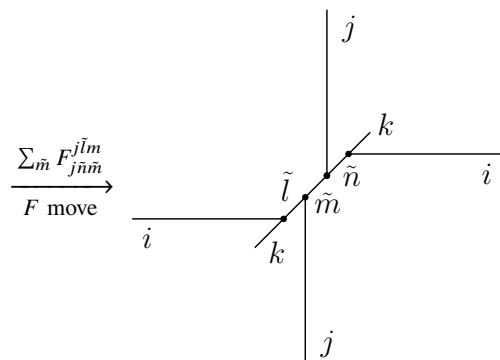
We find also that the fermionic SPT effective action has a degree of non-locality that was not present in the case of bosonic SPTs. For  $D = 1$ , the effective action can be written in terms of a sum over an auxiliary  $\mathbb{Z}_2$  gauge field. It is tempting to interpret it as a gauge field which couples to the fermion parity, but this needs to be tested. We leave this and the determination of possible boundary behaviors of fermionic SPT phases to further work.

## Appendix A

## 3D MODULAR TRANSFORMATIONS FOR WALKER-WANG MODELS ON THE MINIMAL LATTICE

In this appendix, we calculate the matrix representation of the  $S$  and  $T$  transformations in the ground space of a Walker-Wang model defined on the minimal lattice. For simplicity, we will use a labeling of the minimal lattice by the input anyons to represent the amplitude of the associated string-net configuration in the ground state wave function. The set of all string-net configurations constitute a basis for the ground state Hilbert space. To compute the  $S$  and  $T$  matrices, we apply the corresponding transformations to a particular basis vector, and express the resulting vector as a superposition of the basis vectors by applying the  $F$  and  $R$  moves. The coefficients in front of the superposition are nothing but the matrix elements of  $S$  and  $T$ .

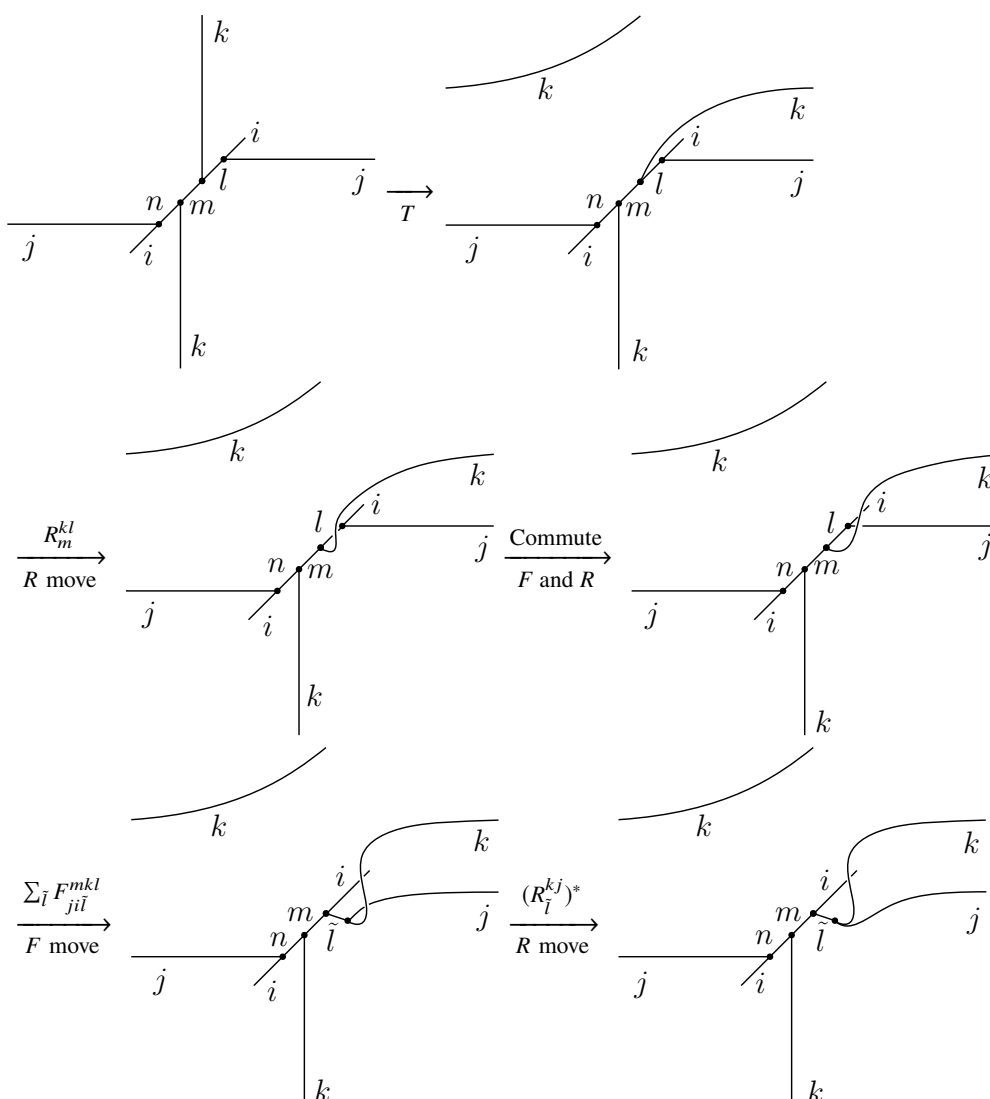
A.1  $S$  matrix

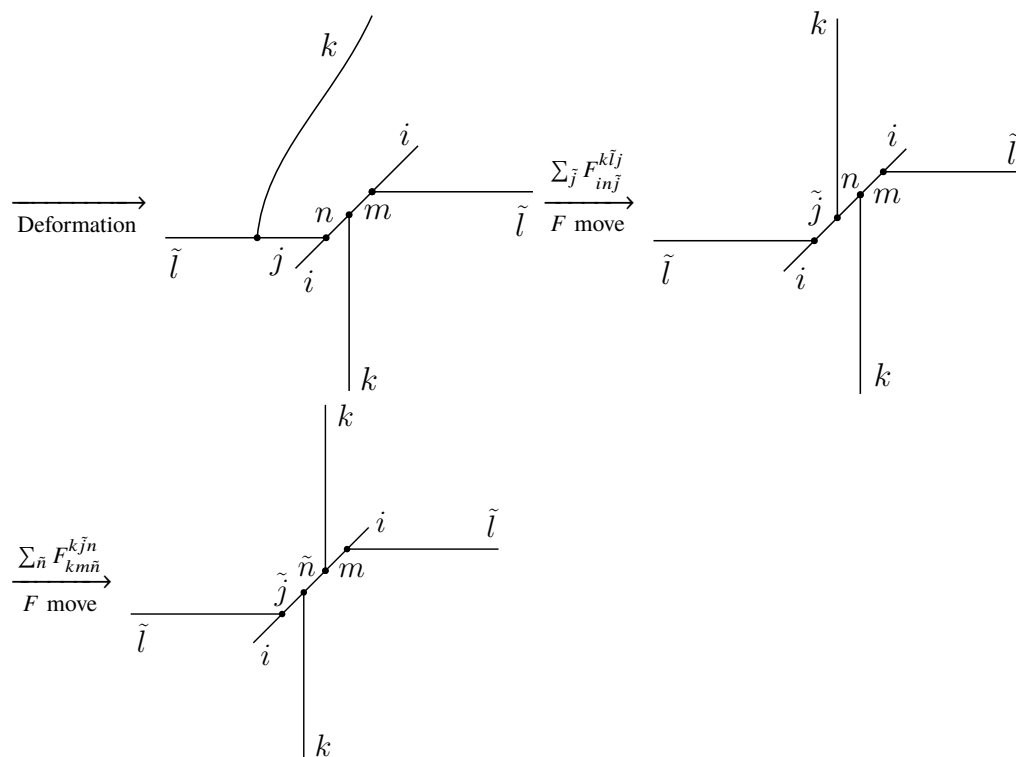


Collecting the coefficients from each step, we obtain

$$S_{(i,j,k,l,m,n)}^{(k,i,j,\tilde{n},\tilde{m},\tilde{l})} = F_{kml}^{jil} F_{ji\tilde{n}}^{kmn} F_{j\tilde{n}\tilde{m}}^{j\tilde{l}m}. \quad (\text{A.1})$$

## A.2 T matrix





Collecting the coefficients from each step, we obtain

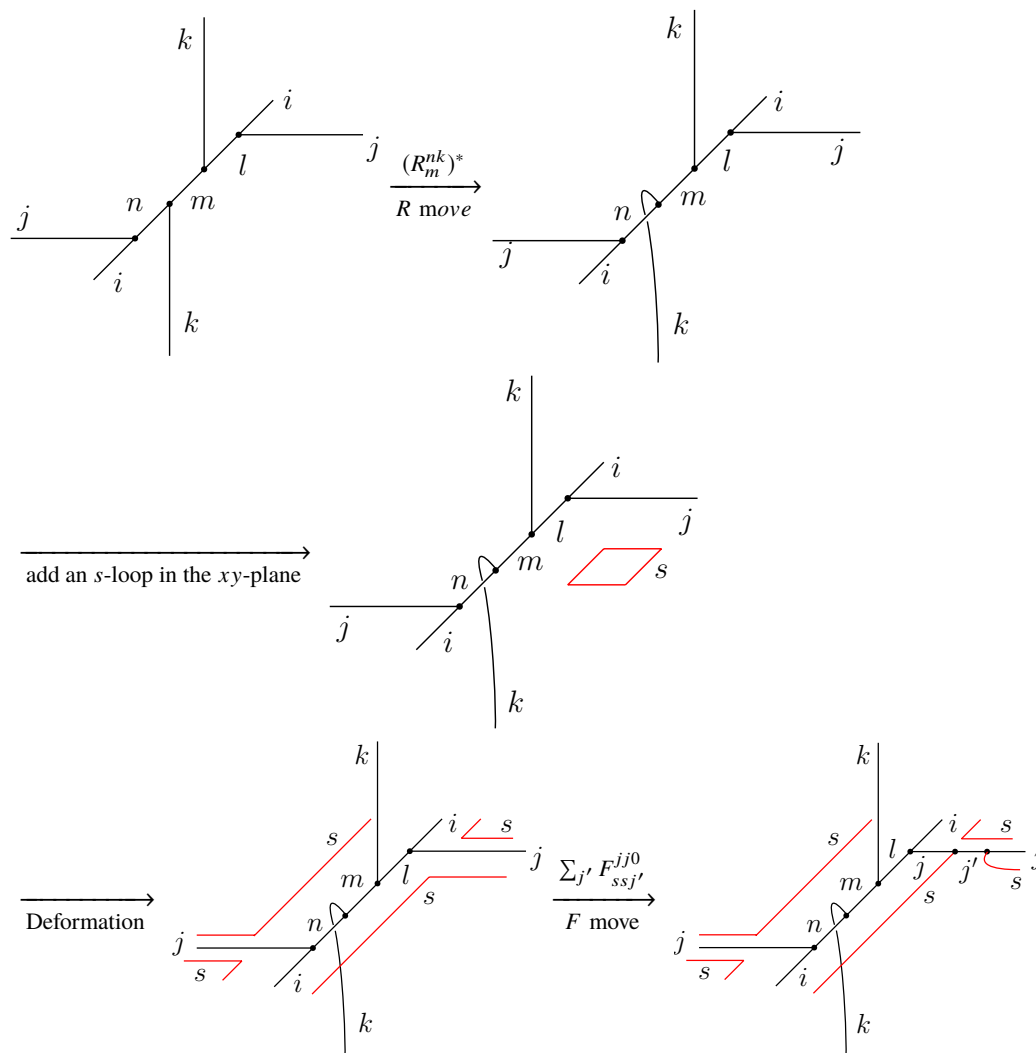
$$T_{(i,j,k,l,m,n)}^{(i,\tilde{l},k,m,\tilde{n},\tilde{j})} = R_m^{kl} F_{j\tilde{l}}^{mkl} (R_{\tilde{l}}^{kj})^* F_{in\tilde{j}}^{k\tilde{l}j} F_{km\tilde{n}}^{k\tilde{j}n}. \quad (\text{A.2})$$

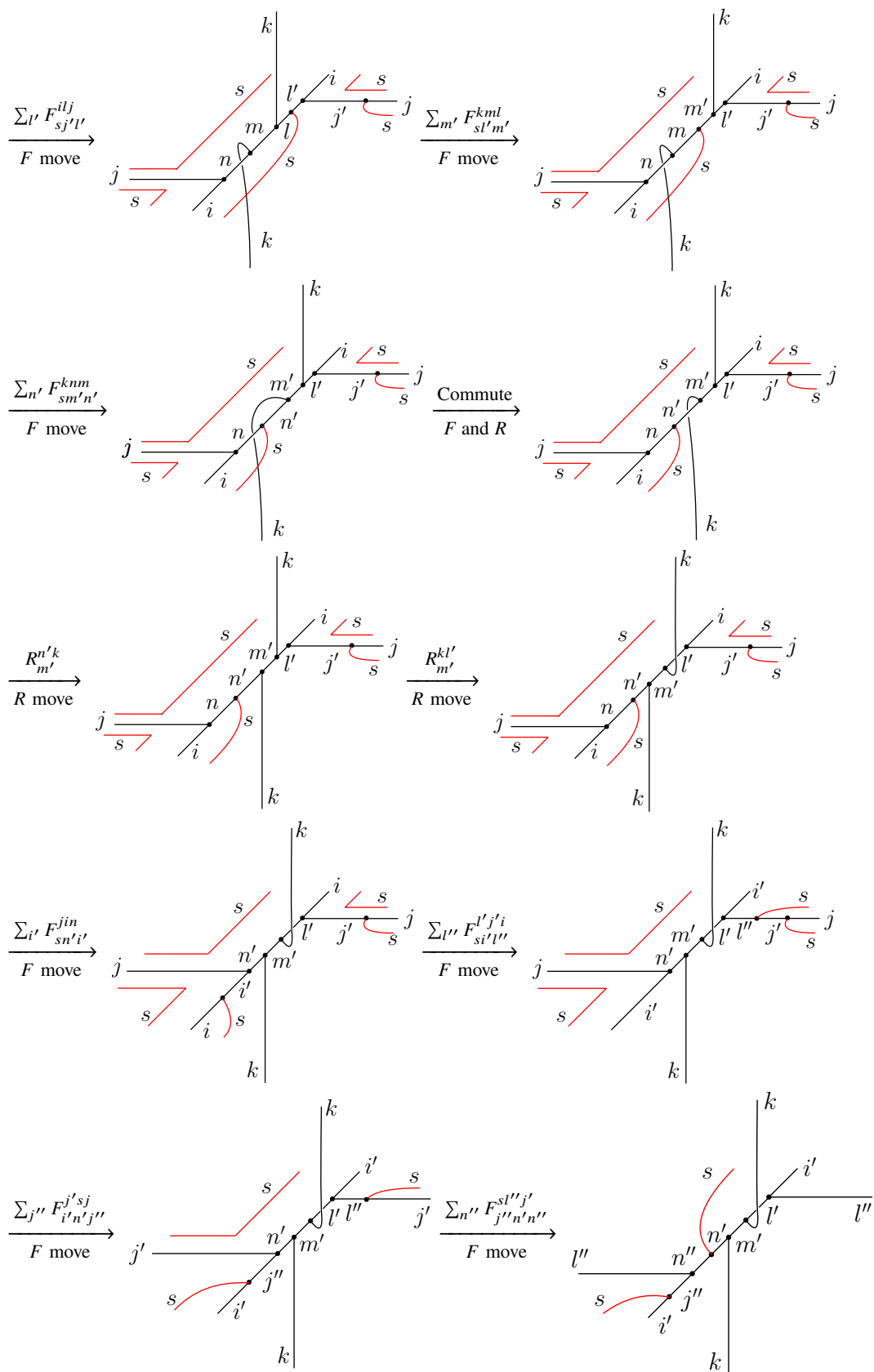
Appendix B

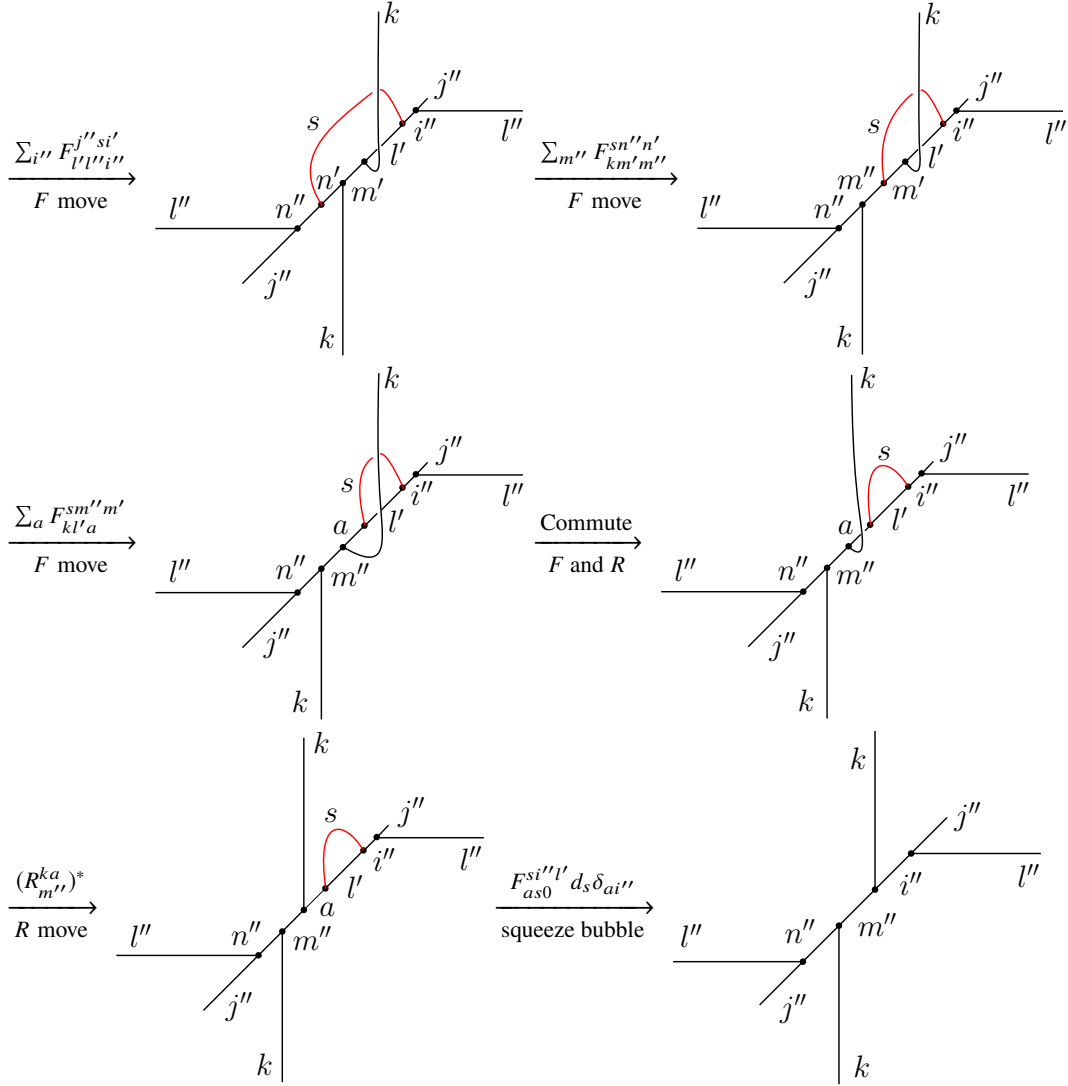
## HAMILTONIAN FOR WALKER-WANG MODELS ON THE MINIMAL LATTICE

In this appendix, we calculate the plaquette operators of a Walker-Wang model defined on the minimal lattice. For simplicity, we will calculate  $B_p^s$  for a particular anyon label  $s$ , and the full plaquette operator can be obtained by summing over  $s$  weighted by the quantum dimension of  $s$ :  $B_p = \sum_s d_s B_p^s$ .

### B.1 Plaquette operator in the $xy$ -plane



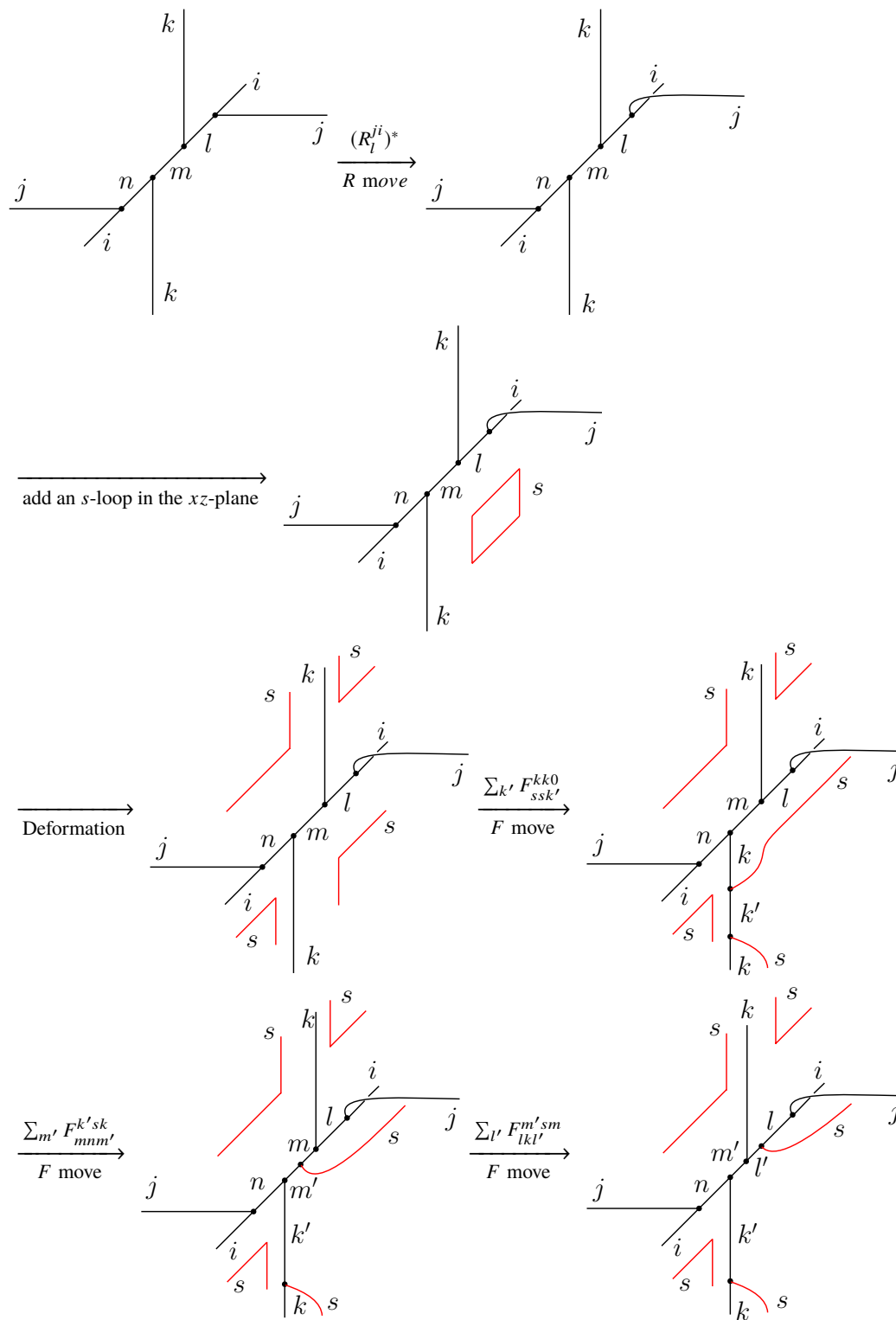


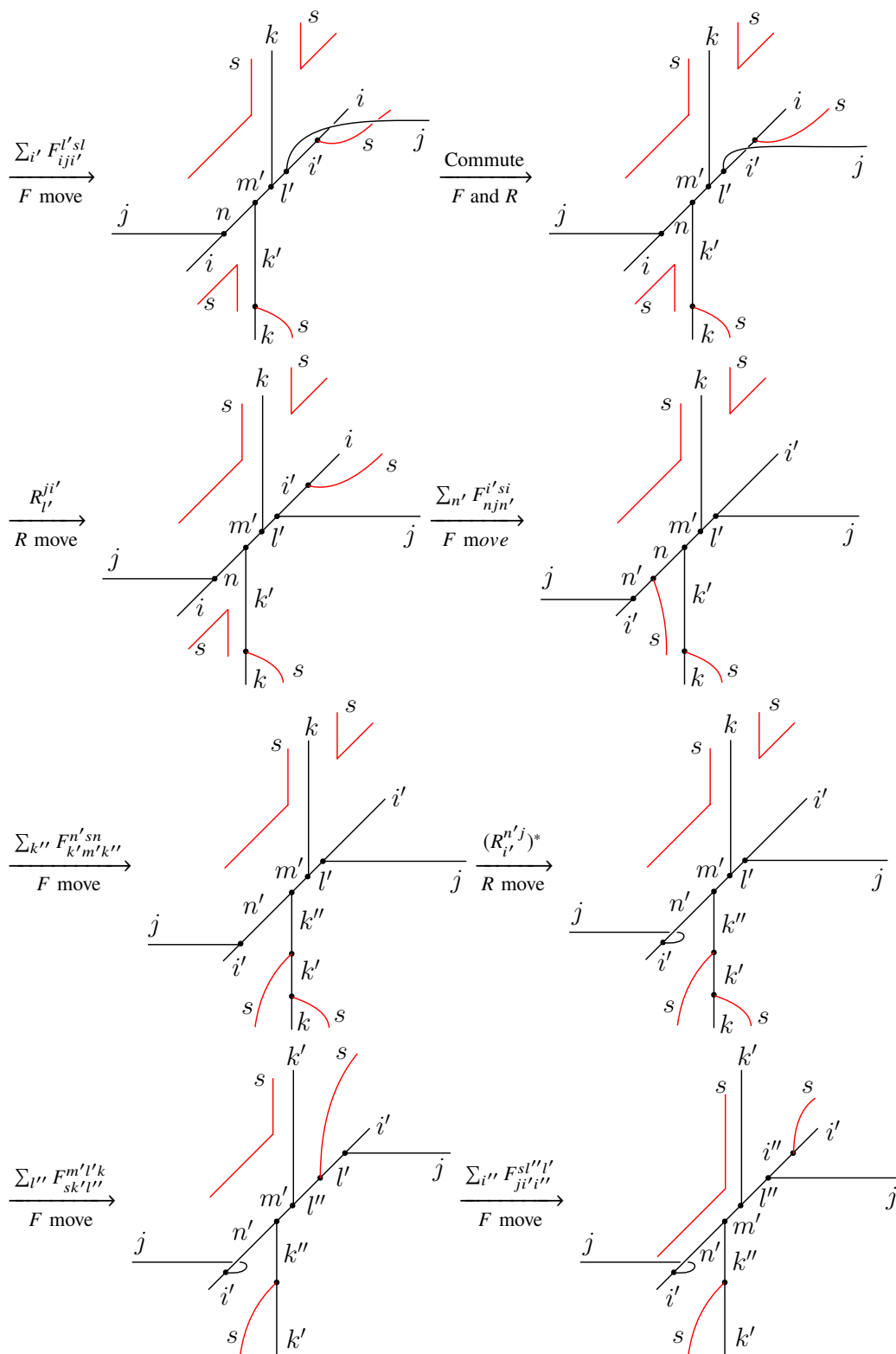


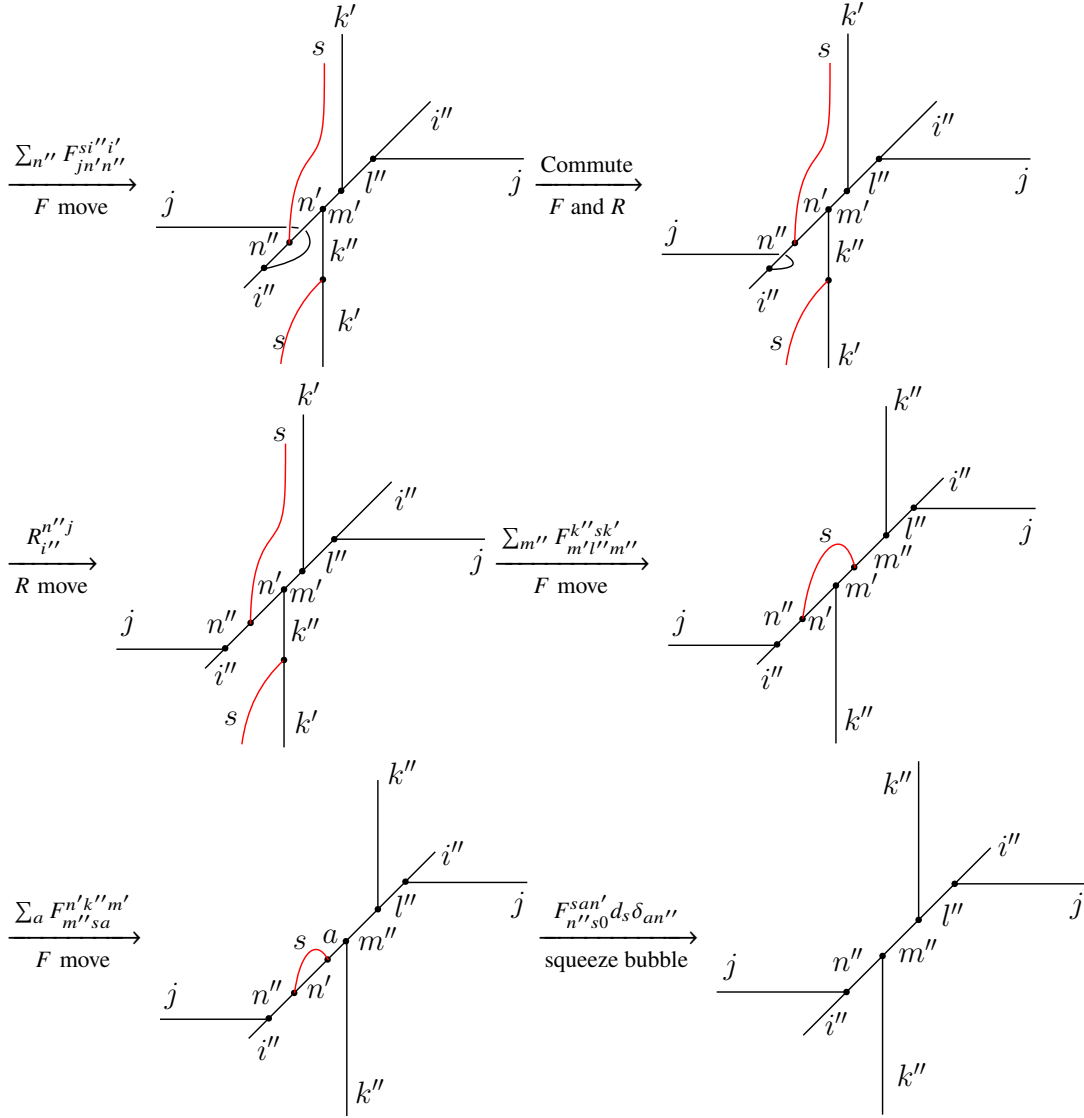
Collecting the coefficients from each step, we obtain

$$\begin{aligned}
 (B_{xy}^s)_{(i,j,k,l,m,n)}^{(j'',l'',k,i'',m'',n'')} &= \sum_{j',l',m',n',i'} (R_m^{nk})^* F_{ssj'}^{jj0} \times \\
 &F_{sj'l'}^{ilj} F_{sl'm'}^{kml} F_{sm'n'}^{knm} R_{m'}^{n'k} R_{m'}^{kl'} F_{sn'i'}^{jin} F_{si'l'}^{l'j'i} F_{i'n'j''}^{j'sj} F_{j''n'n''}^{sl''j'} \times \\
 &F_{l'l'i''}^{j''si''} F_{km''m''}^{sn''n''} F_{kl'i''}^{sm''m''} (R_{m''}^{ki''})^* F_{i''s0}^{si''l'} d_s.
 \end{aligned} \tag{B.1}$$

## B.2 Plaquette operator in the $xz$ -plane



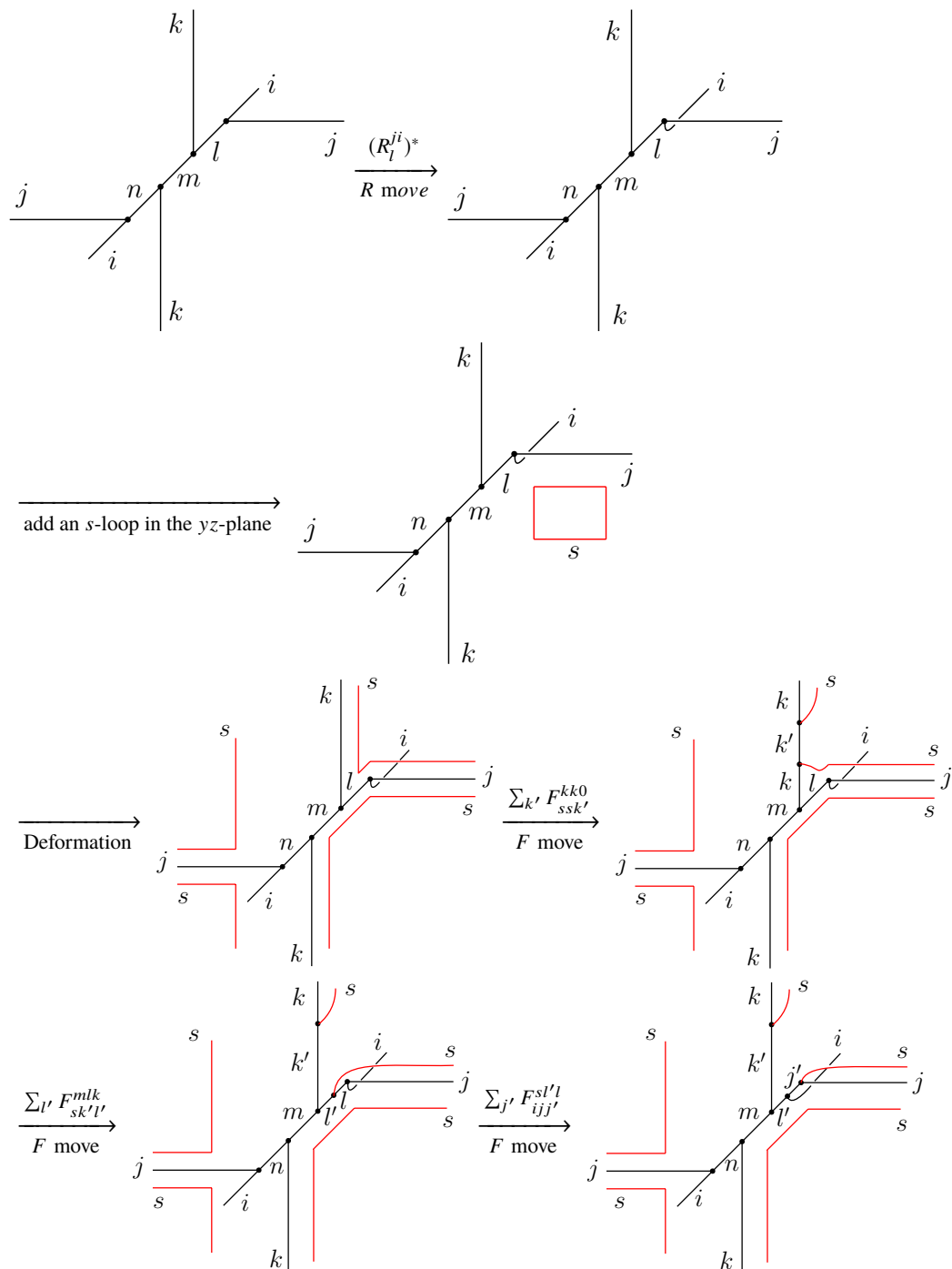


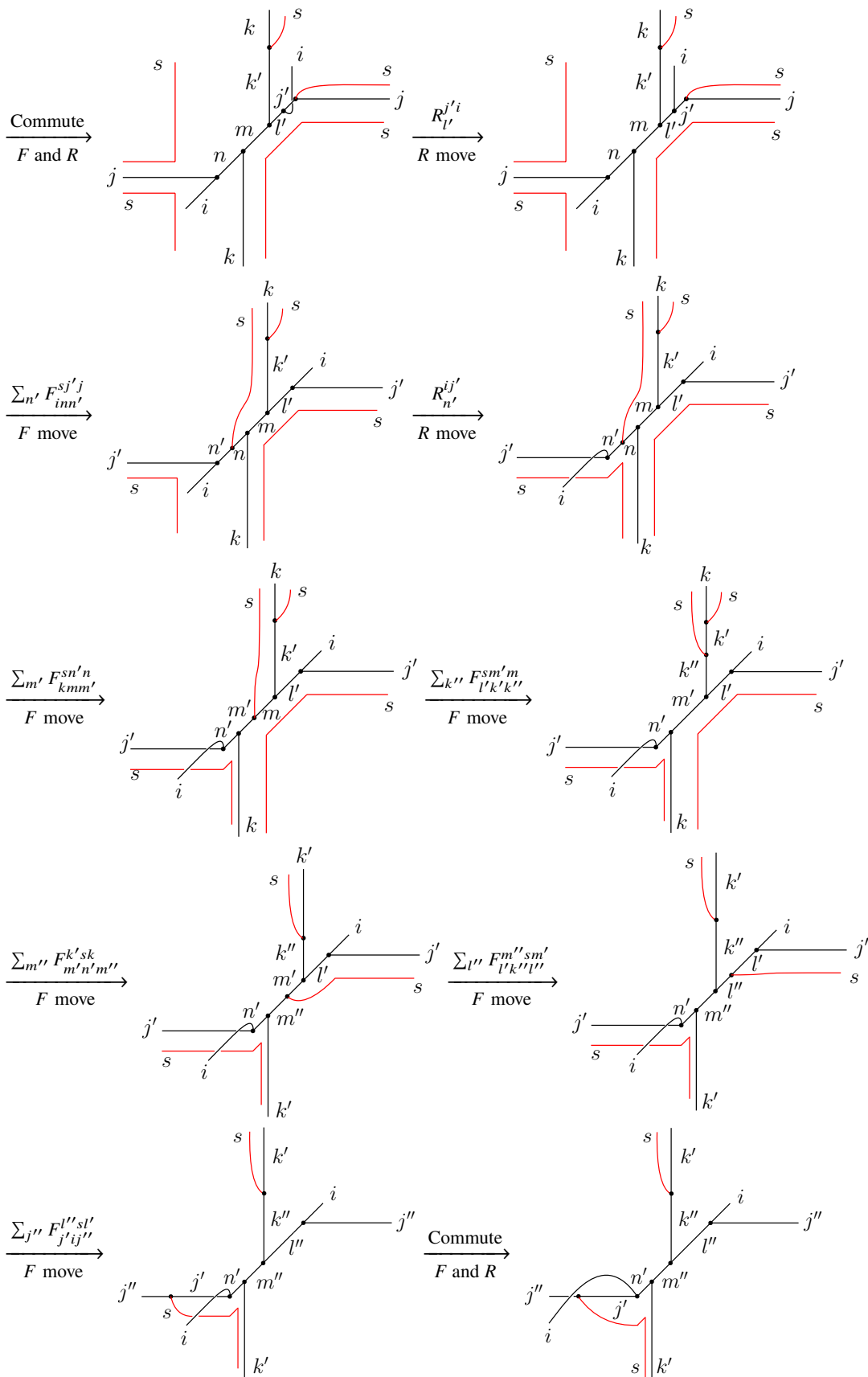


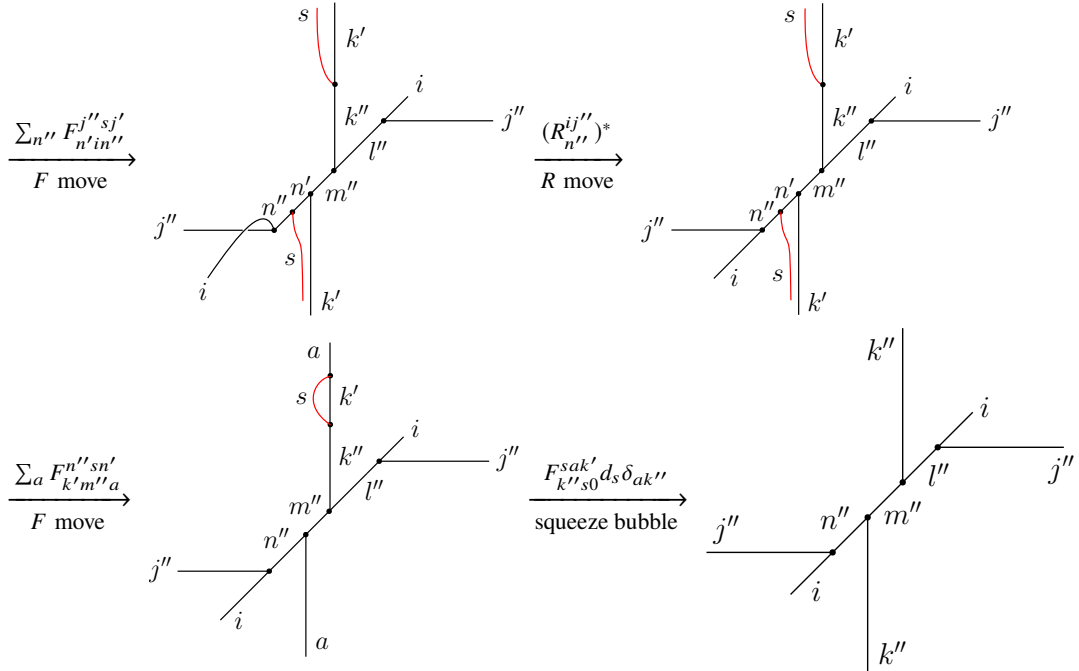
Collecting the coefficients from each step, we obtain

$$\begin{aligned}
 (B_{xz}^s)_{(i,j,k,l,m,n)}^{(i'',j,k'',l'',m'',n'')} &= \sum_{k',m',l',i',n'} (R_l^{j_i})^* F_{ssk'}^{kk0} \times \\
 &F_{mnm'}^{k'sk} F_{lkl'}^{m'sm} F_{iji'}^{l'sl} R_{l'}^{ji'} F_{n'jn'}^{i'si} F_{k'm'k''}^{n'sn} (R_{i'}^{n'j})^* F_{sk'l''}^{m'l'k} F_{ji'i''}^{sl'l'} \times \\
 &F_{jn'n''}^{si'i'} R_{i''}^{n''j} F_{m'l''m''}^{k''sk'} F_{m''sn''}^{n'k''m'} F_{n''s0}^{sn''n'} d_s.
 \end{aligned} \tag{B.2}$$

### B.3 Plaquette operator in the $yz$ -plane







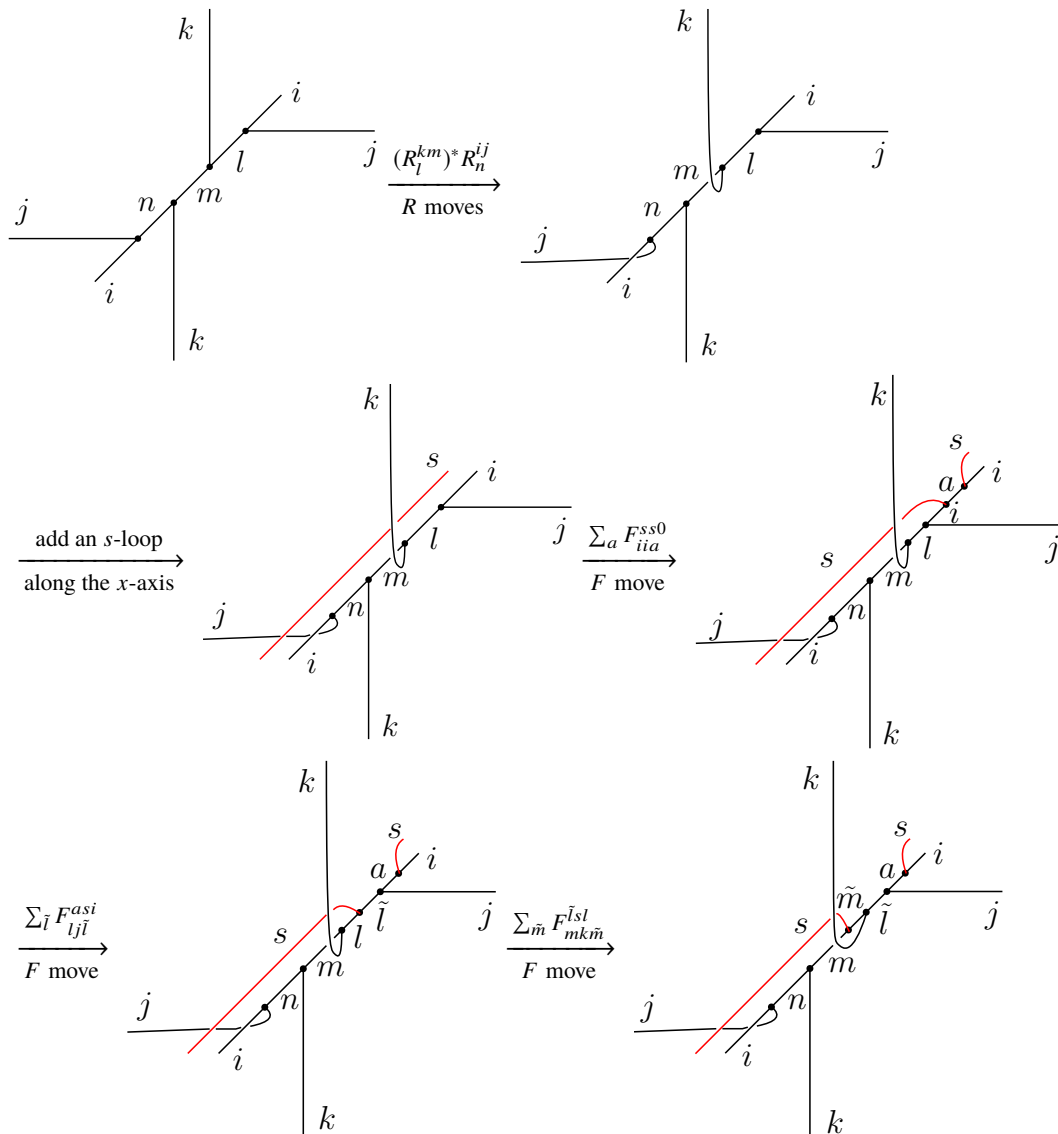
Collecting the coefficients from each step, we obtain

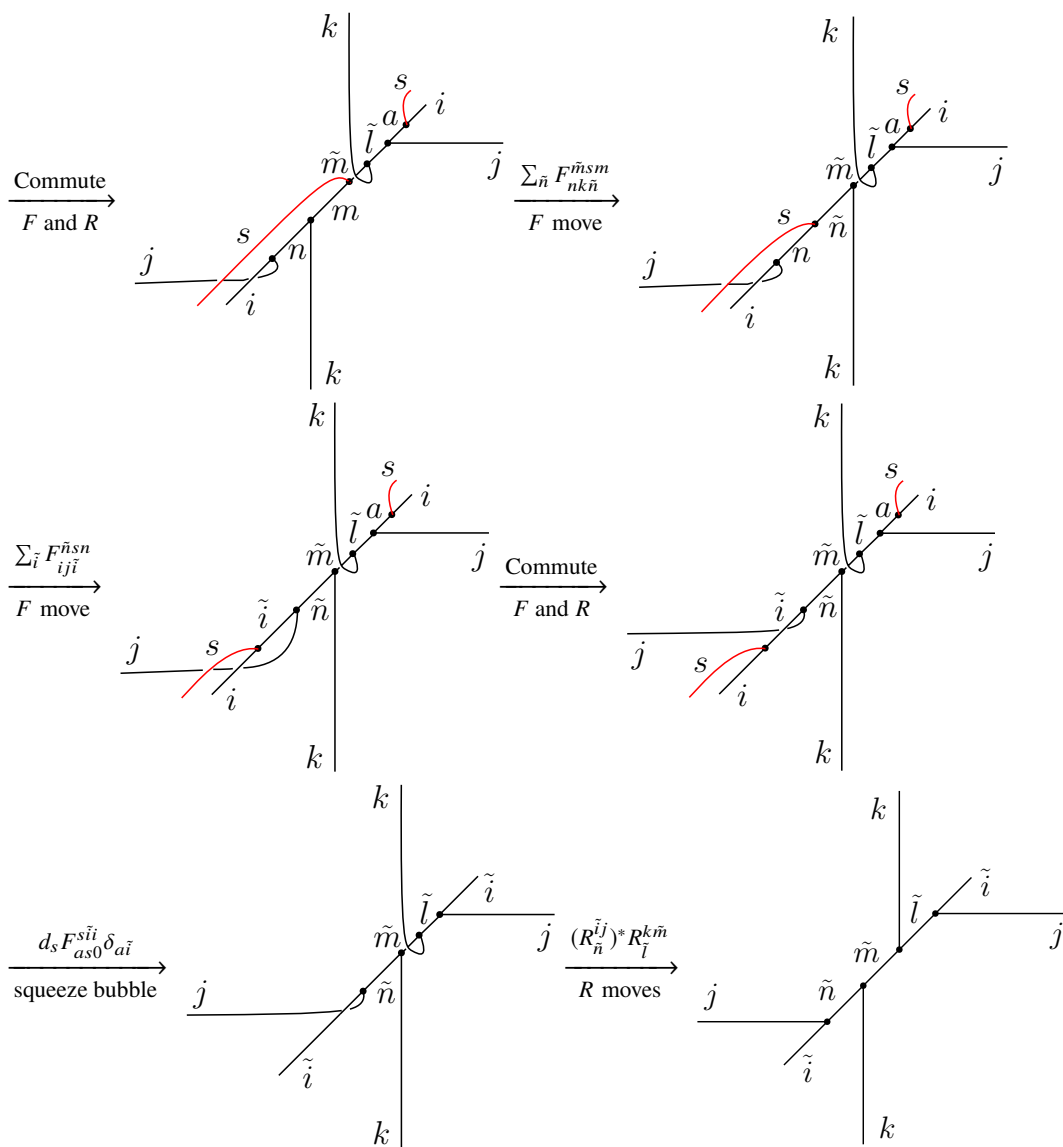
$$\begin{aligned}
 (B_{yz}^s)_{(i,j,k,l,m,n)}^{(i,j'',k'',l'',m'',n'')} &= \sum_{k',l',j',n',m'} (R_l^i)^* F_{ssk'}^{kk0} \times \\
 &F_{sk'l'}^{mlk} F_{ijj'}^{sl'l} R_{l'}^{j'i} F_{inn'}^{sj'j} R_{n'}^{ij'} F_{kmm'}^{sn'n} F_{l'k'k''}^{sm'm} F_{m'n'm''}^{k'sk} F_{l'k''l''}^{m''sm'} \times \\
 &F_{j'ij''}^{l''sl'} F_{n'in''}^{j''s_j'} (R_{n''}^{ij''})^* F_{k'm''k''}^{n''sn'} F_{k''s0}^{sk''k'} d_s.
 \end{aligned} \tag{B.3}$$

## Appendix C

## STRING OPERATORS FOR WALKER-WANG MODELS ON THE MINIMAL LATTICE

In this appendix, we calculate the string operators of a Walker-Wang model defined on the minimal lattice. The string is labeled by  $s$ , where  $s$  is a generic anyon label in the input anyon theory  $\mathcal{A}$ .

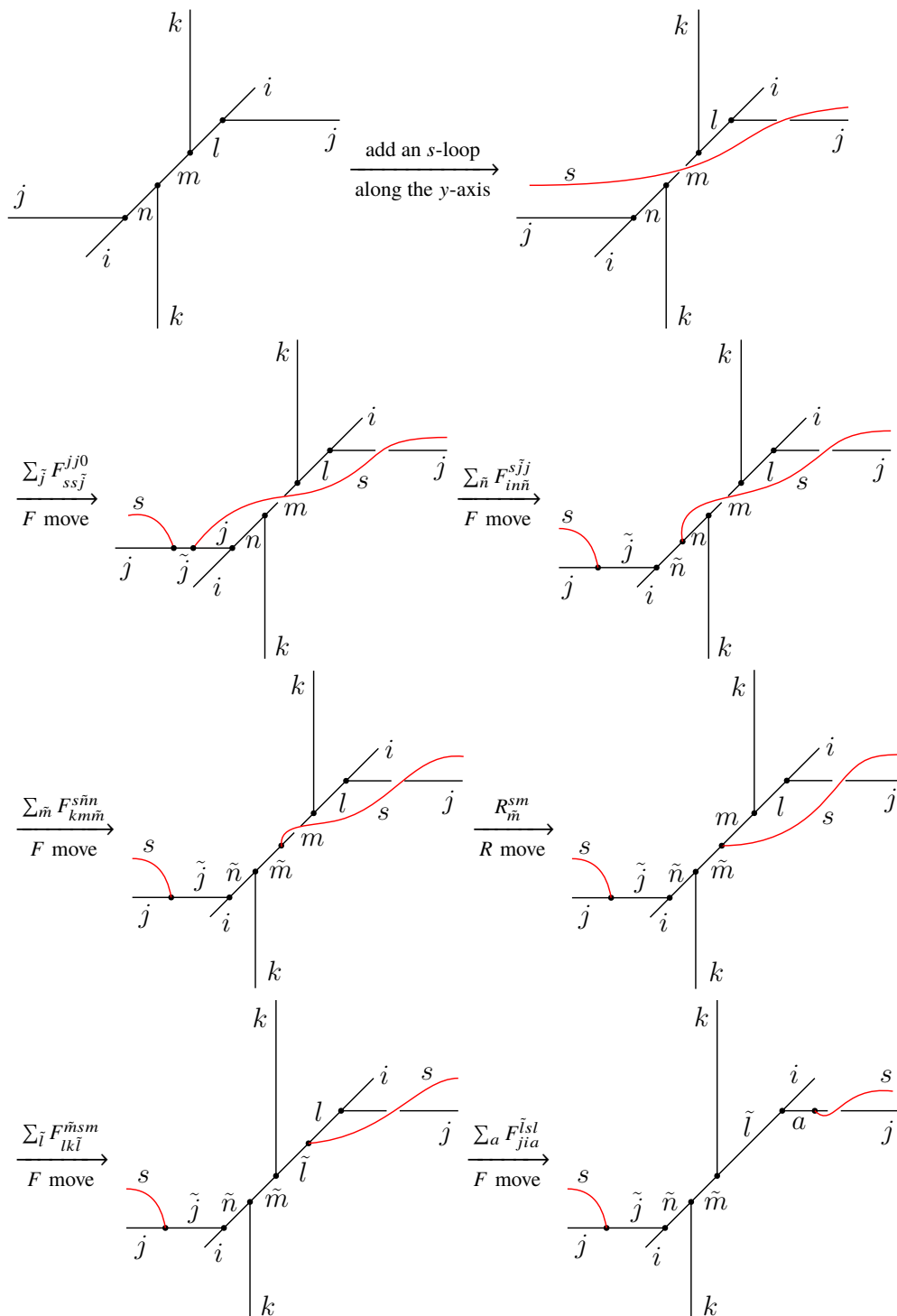
C.1 String operator along the  $x$ -direction

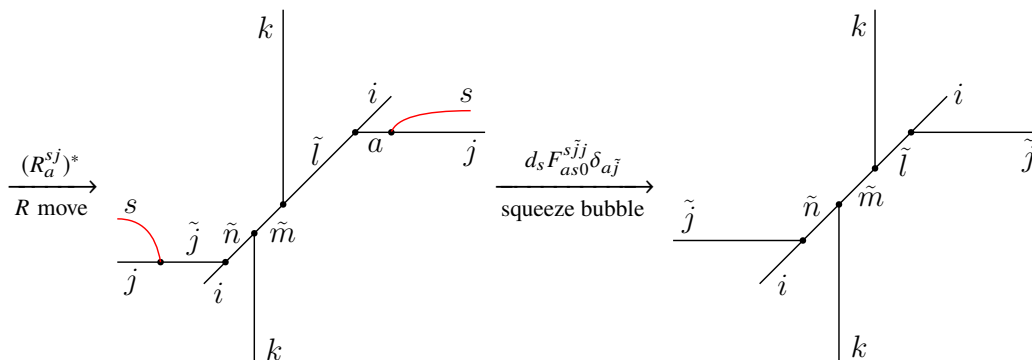


Collecting the coefficients from each step, we obtain

$$\begin{aligned}
 (W_x^s)_{(i,j,k,l,m,n)}^{(\tilde{i},\tilde{j},\tilde{k},\tilde{l},\tilde{m},\tilde{n})} &= (R_{\tilde{l}}^{km})^* R_{\tilde{n}}^{ij} F_{i\tilde{i}\tilde{i}}^{ss0} F_{l\tilde{j}\tilde{l}}^{\tilde{i}si} F_{m\tilde{k}\tilde{m}}^{\tilde{l}sl} F_{nk\tilde{n}}^{\tilde{m}sm} \times \\
 &F_{ij\tilde{i}}^{\tilde{n}sn} d_s F_{is0}^{\tilde{s}ii} (R_{\tilde{n}}^{\tilde{i}j})^* R_{\tilde{l}}^{k\tilde{m}}.
 \end{aligned} \tag{C.1}$$

## C.2 String operator along the y-direction

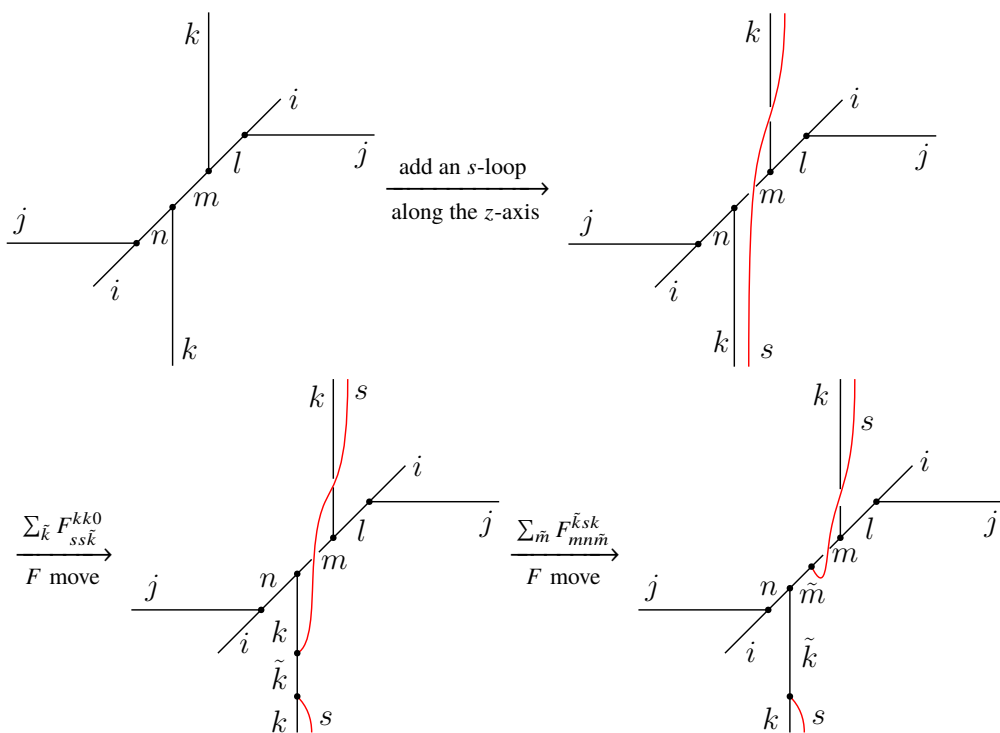


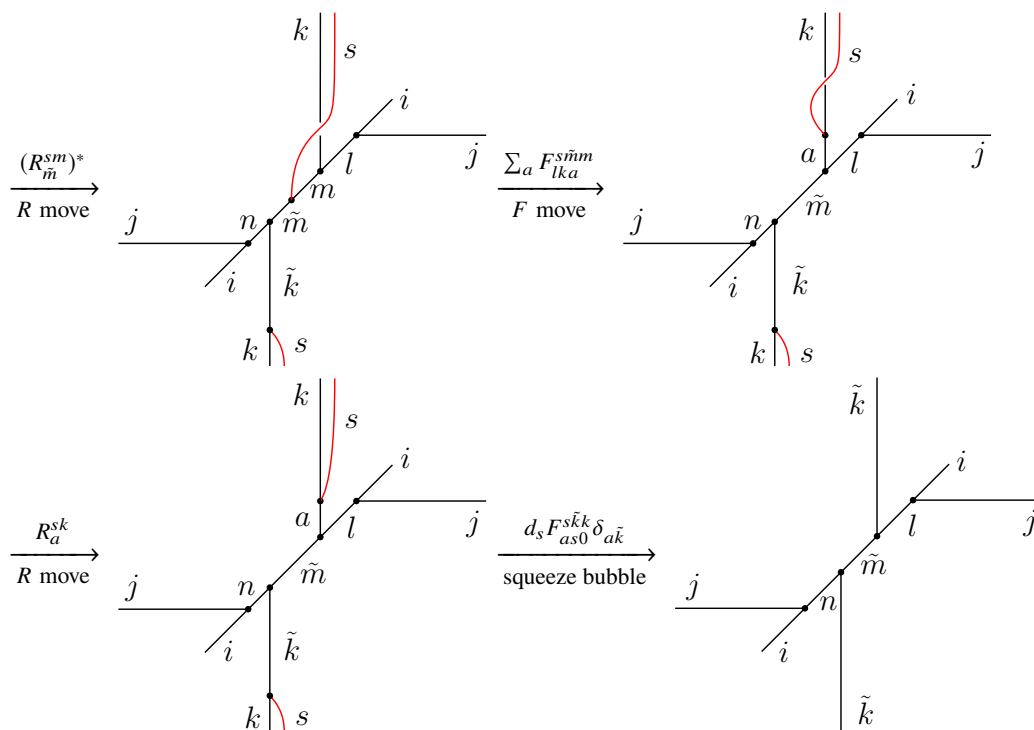


Collecting the coefficients from each step, we obtain

$$(W_y^s)_{(i,j,k,l,m,n)}^{(i,\tilde{j},k,\tilde{l},\tilde{m},\tilde{n})} = F_{ss\tilde{j}}^{jj0} F_{in\tilde{n}}^{s\tilde{j}j} F_{km\tilde{m}}^{s\tilde{n}n} R_{\tilde{m}}^{sm} F_{lk\tilde{l}}^{\tilde{m}sm} \times F_{ji\tilde{j}}^{\tilde{l}sl} (R_{\tilde{j}}^{sj})^* d_s F_{\tilde{j}s0}^{s\tilde{j}j}. \quad (\text{C.2})$$

### C.3 String operator along the $z$ -direction





Collecting the coefficients from each step, we obtain

$$(W_z^s)_{(i,j,k,l,m,n)}^{(i,j,\tilde{k},l,\tilde{m},n)} = F_{s\tilde{k}}^{kk0} F_{m\tilde{m}}^{\tilde{k}sk} (R_{\tilde{m}}^{sm})^* F_{l\tilde{k}}^{s\tilde{m}m} R_{\tilde{k}}^{sk} d_s F_{\tilde{k}s0}^{s\tilde{k}k}. \quad (\text{C.3})$$

*Appendix D*

**MES BASIS AND CANONICAL FORM FOR  $S$  AND  $T$   
MATRICES**

In this appendix, we explain the necessary steps involved in transforming the 16 by 16 blocks  $S_{a,b}$  and  $T_{a,b}$  in Section 2.4 from the simultaneous eigenstates of  $W_y^s$  and  $W_z^s$  to the simultaneous eigenstates of  $W_y^s$  and  $V_y^s$  (the MES basis). We can focus on the 4-dimensional eigenspaces of the pair  $(W_y^1, W_y^2)$  with fixed eigenvalues  $(w_y^1, w_y^2)$ , where  $w_y^1, w_y^2 = \pm 1$ . Within each eigenspace, the problem is simplified to a basis transformation from the simultaneous eigenstates of  $W_z^s$  to the simultaneous eigenstates of  $V_y^s$ . We denote the former (respectively, latter) by  $\{|w_z^1, w_z^2\rangle\}$  (respectively,  $\{|v_y^1, v_y^2\rangle\}$ ), where  $w_z^1, w_z^2 = \pm 1$ , and  $v_y^1, v_y^2 = \pm$ . Due to the Aharonov-Bohm interaction between charges and fluxes, the string operators satisfy the following commutation and anticommutation relations:

$$\begin{aligned} \{W_z^1, V_y^1\} &= 0, & [W_z^1, V_y^2] &= 0, \\ \{W_z^2, V_y^2\} &= 0, & [W_z^2, V_y^1] &= 0. \end{aligned} \tag{D.1}$$

One can prove from these relations that the most general unitary change of basis from  $\{|w_z^1, w_z^2\rangle\}$  to  $\{|v_y^1, v_y^2\rangle\}$  is of the form

$$\begin{aligned} |+, +\rangle &= \delta(|1, 1\rangle + \alpha |1, -1\rangle + \beta |-1, 1\rangle + \gamma |-1, -1\rangle), \\ |+, -\rangle &= \delta(|1, 1\rangle - \alpha |1, -1\rangle + \beta |-1, 1\rangle - \gamma |-1, -1\rangle), \\ |-, +\rangle &= \delta(|1, 1\rangle + \alpha |1, -1\rangle - \beta |-1, 1\rangle - \gamma |-1, -1\rangle), \\ |-, -\rangle &= \delta(|1, 1\rangle - \alpha |1, -1\rangle - \beta |-1, 1\rangle + \gamma |-1, -1\rangle), \end{aligned} \tag{D.2}$$

where  $\alpha, \beta, \gamma$ , and  $\delta$  are independent  $U(1)$  phases. We can then rewrite  $S_{a,b}$  and  $T_{a,b}$  in the transformed basis and try to match them with the  $S$  and  $T$  matrices of the 2D  $\mathbb{Z}_2 \times \mathbb{Z}_2$  gauge theories. We find that by choosing the  $U(1)$  phases appropriately, we can match each  $S_{a,b}$  and  $T_{a,b}$  to the  $S$  and  $T$  matrices of precisely one of the eight 2D  $\mathbb{Z}_2 \times \mathbb{Z}_2$  gauge theories. The results are listed in Table 2.2.

For concreteness, we present below the explicit form of  $S_{a,b}$  and  $T_{a,b}$  ( $a, b = \pm 1$ ) in the MES basis for the Walker-Wang models with input data  $\text{Rep}_s(Q_8)$  and  $\text{Rep}_s(D_4)$ . Data for models that permute the charge labels of  $D_4$  are omitted due to their

similarity to those in the  $\text{Rep}_s(D_4)$  case. The basis vectors in  $\{|w_y^1, w_y^2, v_y^1, v_y^2\rangle\}$  are listed from large to small according to the number  $v_y^1 + 2v_y^2 + 4w_y^1 + 8w_y^2$ .

For the Walker-Wang model with input  $\text{Rep}_s(Q_8)$ , the data are the following:

$$S_{1,1} = S_{-1,1} = S_{1,-1} = S_{-1,-1} = \frac{1}{4} \begin{pmatrix} 1 & 1 & 1 & 1 & 1 & 1 & 1 & 1 & 1 & 1 & 1 & 1 & 1 & 1 & 1 \\ 1 & 1 & 1 & 1 & -1 & -1 & -1 & -1 & 1 & 1 & 1 & 1 & -1 & -1 & -1 & -1 \\ 1 & 1 & 1 & 1 & 1 & 1 & 1 & 1 & -1 & -1 & -1 & -1 & -1 & -1 & -1 & -1 \\ 1 & 1 & 1 & 1 & -1 & -1 & -1 & -1 & -1 & -1 & -1 & -1 & 1 & 1 & 1 & 1 \\ 1 & -1 & 1 & -1 & 1 & -1 & 1 & -1 & 1 & -1 & 1 & -1 & 1 & -1 & 1 & -1 \\ 1 & -1 & 1 & -1 & -1 & 1 & -1 & 1 & 1 & -1 & 1 & -1 & -1 & 1 & -1 & 1 \\ 1 & -1 & 1 & -1 & 1 & -1 & 1 & -1 & -1 & 1 & -1 & 1 & -1 & 1 & -1 & 1 \\ \frac{1}{4} & 1 & -1 & 1 & -1 & -1 & 1 & -1 & 1 & -1 & 1 & -1 & 1 & 1 & -1 & 1 & -1 \\ \frac{1}{4} & 1 & 1 & -1 & -1 & 1 & 1 & -1 & -1 & 1 & 1 & -1 & -1 & 1 & 1 & -1 & -1 \\ 1 & 1 & -1 & -1 & -1 & -1 & 1 & 1 & 1 & 1 & -1 & -1 & -1 & -1 & 1 & 1 \\ 1 & 1 & -1 & -1 & 1 & 1 & -1 & -1 & -1 & -1 & 1 & 1 & -1 & -1 & 1 & 1 \\ 1 & 1 & -1 & -1 & -1 & -1 & 1 & 1 & -1 & -1 & 1 & 1 & 1 & 1 & -1 & -1 \\ 1 & -1 & -1 & 1 & 1 & -1 & -1 & 1 & 1 & -1 & -1 & 1 & 1 & -1 & -1 & 1 \\ 1 & -1 & -1 & 1 & -1 & 1 & 1 & -1 & 1 & -1 & -1 & 1 & -1 & 1 & 1 & -1 \\ 1 & -1 & -1 & 1 & 1 & -1 & -1 & 1 & -1 & 1 & 1 & -1 & -1 & 1 & 1 & -1 \\ 1 & -1 & -1 & 1 & -1 & 1 & 1 & -1 & -1 & 1 & 1 & -1 & 1 & -1 & -1 & 1 \end{pmatrix} \quad (\text{D.3})$$

$$T_{1,1} = T_{-1,1} = T_{1,-1} = T_{-1,-1} =$$











*Appendix E*

**PROOF THAT THE  $X_p$  TERMS COMMUTE WITH EACH OTHER**

The Hamiltonian defined in Section 3.3 is a sum of commuting projectors. It is straightforward to see that all terms in  $H_{\text{tunnel}}$  commute with each other, and every term in  $H_{\text{tunnel}}$  commutes with every term in  $H_{\text{decorate}}$ . In this section, we prove that all terms in  $H_{\text{tunnel}}$  commute with each other.

Proving that any pair of plaquette operators  $\tau_{p_1}^x X_{p_1}$  and  $\tau_{p_2}^x X_{p_2}$  commute is equivalent to proving that for any state in the Hilbert space, the state obtained by applying the two plaquette operators sequentially is independent of the order. Namely,

$$\tau_{p_1}^x X_{p_1} \tau_{p_2}^x X_{p_2} |\Psi\rangle = \tau_{p_2}^x X_{p_2} \tau_{p_1}^x X_{p_1} |\Psi\rangle. \quad (\text{E.1})$$

For non-adjacent  $p_1$  and  $p_2$ , these two terms involve different spins and Majorana modes and the plaquette operators have even fermion parity, so they commute trivially. However, for adjacent  $p_1$  and  $p_2$ , some of the Majorana modes that the two plaquette operators act on are the same, and it is not obvious that they should commute. Since  $X_p$  by construction, guarantees that the Majorana configurations match the plaquette spin configurations, and the plaquette spin configuration is independent of the order in which we apply the plaquette operators, the final configuration of the Majorana modes are actually the same, but the fermionic state can differ by a complex phase, i.e., the plaquette operators commute up to a complex phase. As we will argue below, such complex phases are actually all equal to zero, and the plaquette operators commute exactly.

Recall that  $P_p^{\{\mu_{p,q}\}}$  projects onto the spin configuration of  $\{\mu_p, \mu_q\}$  and  $\Pi_p$  projects onto the fermionic subspace that conforms to such spin configuration, so we only need to consider those states whose fermion configurations satisfy the decoration rules specified by the spin configurations. We denote such states by  $|\Psi_{\{\mu_{p,q}\}}\rangle \otimes |\tau_1, \tau_2, \dots\rangle$ , where  $\tau_1$  and  $\tau_2$  denote the spins on  $p_1$  and  $p_2$ , respectively. We compute

$$\begin{aligned} & \tau_{p_1}^x X_{p_1} |\Psi_{\{\mu_{p,q}\}}\rangle \otimes |\tau_1, \tau_2, \dots, \tau_N\rangle \\ &= X_{p_1}^{\{\mu_{p,q}\}} |\Psi_{\{\mu_{p,q}\}}\rangle \otimes |\tau'_1, \tau_2, \dots, \tau_N\rangle \\ &\propto |\Psi_{\{\mu_p^1, \mu_q\}}\rangle \otimes |\tau'_1, \tau_2, \dots, \tau_N\rangle. \end{aligned} \quad (\text{E.2})$$

$|\Psi_{\{\mu_{p,q}\}}\rangle$  and  $|\Psi_{\{\mu_p^1, \mu_q^1\}}\rangle$  have the same Majorana configuration apart from those around the plaquette  $p_1$ , which we denote by  $\gamma_1^{\sigma_1}, \gamma_2^{\sigma_2}, \dots, \gamma_{2n}^{\sigma_{2n}}$ . More explicitly, we assume  $is_{2i-1,2i}\gamma_{2i-1}^{\sigma_{2i-1}}\gamma_{2i}^{\sigma_{2i}}|\Psi_{\{\mu_{p,q}\}}\rangle = |\Psi_{\{\mu_{p,q}\}}\rangle$ , and  $is_{2i,2i+1}\gamma_{2i}^{\sigma_{2i}}\gamma_{2i+1}^{\sigma_{2i+1}}|\Psi_{\{\mu_p^1, \mu_q^1\}}\rangle = |\Psi_{\{\mu_p^1, \mu_q^1\}}\rangle$ . In this case, the expression of  $V_p^{\{\mu_{p,q}\}}$  is exactly of the form in (3.10):

$$V_{p_1}^{\{\mu_{p_1,q}\}} = 2^{-\frac{n+1}{2}} (1 + is_{2,3}\gamma_2^{\sigma_2(\{\mu_{p_1,q}\})}\gamma_3^{\sigma_3(\{\mu_{p_1,q}\})})(1 + is_{4,5}\gamma_4^{\sigma_4(\{\mu_{p_1,q}\})}\gamma_5^{\sigma_5(\{\mu_{p_1,q}\})}) \dots (1 + is_{2n,1}\gamma_{2n}^{\sigma_{2n}(\{\mu_{p_1,q}\})}\gamma_1^{\sigma_1(\{\mu_{p_1,q}\})}) \quad (\text{E.3})$$

Note that the choice of  $\{\sigma_i(\{\mu_{p_1,q}\})\}$  depends on the spin configuration. This becomes important when considering two adjacent plaquettes. For adjacent plaquettes  $p_1$  and  $p_2$ , we consider first flipping the spin in  $p_1$  and then the spin in  $p_2$

$$\begin{aligned} & \tau_{p_2}^x X_{p_2} \tau_{p_1}^x X_{p_1} |\Psi_{\{\mu_{p,q}\}}\rangle \otimes |\tau_1, \tau_2, \dots\rangle \\ &= X_{p_2}^{\{\mu_p^1, \mu_q^1\}} X_{p_1}^{\{\mu_{p,q}\}} |\Psi_{\{\mu_{p,q}\}}\rangle \otimes |\tau'_1, \tau'_2, \dots\rangle. \end{aligned} \quad (\text{E.4})$$

Next, we reverse the order of the two plaquette operators

$$\begin{aligned} & \tau_{p_1}^x X_{p_1} \tau_{p_2}^x X_{p_2} |\Psi_{\{\mu_{p,q}\}}\rangle \otimes |\tau_1, \tau_2, \dots\rangle \\ &= X_{p_1}^{\{\mu_p^2, \mu_q^2\}} X_{p_2}^{\{\mu_{p,q}\}} |\Psi_{\{\mu_{p,q}\}}\rangle \otimes |\tau'_1, \tau'_2, \dots\rangle. \end{aligned} \quad (\text{E.5})$$

Proving  $\tau_{p_1}^x X_{p_1}$  and  $\tau_{p_2}^x X_{p_2}$  commute is then equivalent to proving that the final states in (E.4) and (E.5) are the same, which is equivalent to proving that

$$X_{p_1}^{\{\mu_p^2, \mu_q^2\}} X_{p_2}^{\{\mu_{p,q}\}} P = X_{p_2}^{\{\mu_p^1, \mu_q^1\}} X_{p_1}^{\{\mu_{p,q}\}} P, \quad (\text{E.6})$$

where  $P$  is the Majorana projector on the Majorana configuration of  $|\Psi_{\{\mu_{p,q}\}}\rangle$  that satisfies the identity  $P|\Psi_{\{\mu_{p,q}\}}\rangle = |\Psi_{\{\mu_{p,q}\}}\rangle$ . We will prove (E.6) in detail.

We denote by  $\{\mu_{p,q}\}$  and  $\{\mu_{p,q}^f\}$  the arbitrary initial and final spin configurations, respectively. Let  $\{\mu_{p,q}^{1,2}\}$  be the corresponding intermediate spin configuration after flipping the spin  $\tau_{p_{1,2}}$ .  $p_1$  and  $p_2$  share two triangles and one short bond. In the relation (E.6), projectors that do not cover the Majorana modes on the shared triangles commute trivially, whereas those that do may not commute. Since the configuration of the Majorana modes on the shared triangles depends on the spin configuration around them, we enumerate all possible cases in Fig. E.1 and show that (E.6) indeed holds.

**Case I:**  $\tau_{p_1}^z = \tau_{p_2}^z$

Without loss of generality, we assume that  $\tau_{p_1}^z = \tau_{p_2}^z = -1$ . See Fig. E.2 for an example configuration. The proof demonstrated in this section applies similarly to all configurations with  $\tau_{p_1}^z = \tau_{p_2}^z$ .

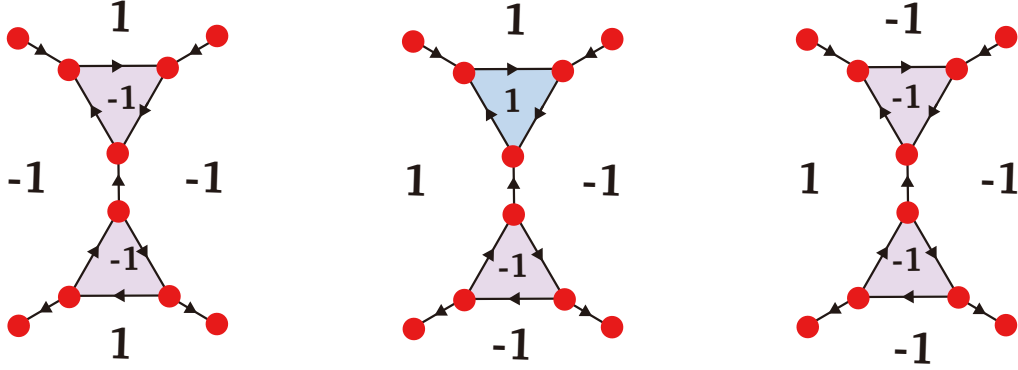


Figure E.1: The three relevant spin configurations. Although there are in total  $2^4 = 16$  kinds of spin configurations around the shared triangles, the proof of Eq. E.6 proceeds in a similar way for some of them. We find that the three cases shown here represent the three essentially different classes.

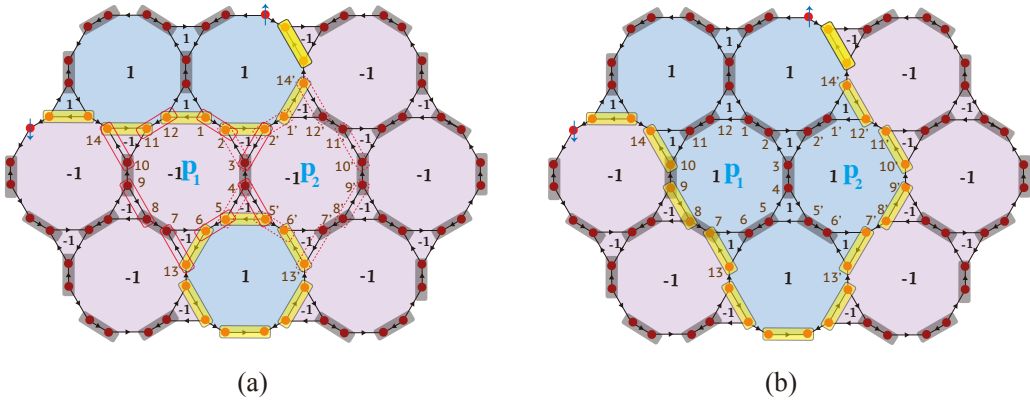


Figure E.2: The spin configuration and the corresponding Majorana configuration for case I.

$$\begin{aligned}
P = & 2^{-24} (1 + is_{12,1} \gamma_{12}^\downarrow \gamma_1^\uparrow) (1 + is_{2,2} \gamma_2^\uparrow \gamma_2^\downarrow) (1 + is_{1,2} \gamma_1^\downarrow \gamma_2^\downarrow) (1 + is_{3,4} \gamma_3^\uparrow \gamma_4^\uparrow) \\
& (1 + is_{3,4} \gamma_3^\downarrow \gamma_4^\downarrow) (1 + is_{5,5} \gamma_5^\downarrow \gamma_5^\uparrow) (1 + is_{6,13} \gamma_6^\uparrow \gamma_{13}^\downarrow) (1 + is_{5,6} \gamma_5^\downarrow \gamma_6^\downarrow) \\
& (1 + is_{7,8} \gamma_7^\uparrow \gamma_8^\uparrow) (1 + is_{7,8} \gamma_7^\downarrow \gamma_8^\downarrow) (1 + is_{9,10} \gamma_9^\uparrow \gamma_{10}^\uparrow) (1 + is_{9,10} \gamma_9^\downarrow \gamma_{10}^\downarrow) \\
& (1 + is_{14,11} \gamma_{14}^\uparrow \gamma_{11}^\downarrow) (1 + is_{11,12} \gamma_{11}^\uparrow \gamma_{12}^\uparrow) (1 + is_{1,14} \gamma_1^\downarrow \gamma_{14}^\uparrow) (1 + is_{2,1} \gamma_2^\uparrow \gamma_1^\uparrow) \\
& (1 + is_{12,11} \gamma_{12}^\uparrow \gamma_{11}^\uparrow) (1 + is_{12,11} \gamma_{12}^\downarrow \gamma_{11}^\downarrow) (1 + is_{10,9} \gamma_{10}^\uparrow \gamma_9^\uparrow) (1 + is_{10,9} \gamma_{10}^\downarrow \gamma_9^\downarrow) \\
& (1 + is_{8,7} \gamma_8^\uparrow \gamma_7^\uparrow) (1 + is_{8,7} \gamma_8^\downarrow \gamma_7^\downarrow) (1 + is_{13,6} \gamma_{13}^\uparrow \gamma_6^\downarrow) (1 + is_{5,6} \gamma_5^\uparrow \gamma_6^\uparrow). \quad (\text{E.7})
\end{aligned}$$

$$\begin{aligned}
X_{p_1}^{\{d_{vw}\}} = & 2^{-9} (1 + is_{1,2} \gamma_1^\uparrow \gamma_2^\uparrow) (1 + is_{2,3} \gamma_2^\downarrow \gamma_3^\uparrow) (1 + is_{4,5} \gamma_4^\uparrow \gamma_5^\downarrow) (1 + is_{5,6} \gamma_5^\uparrow \gamma_6^\uparrow) \\
& (1 + is_{13,7} \gamma_{13}^\downarrow \gamma_7^\uparrow) (1 + is_{8,9} \gamma_8^\uparrow \gamma_9^\downarrow) (1 + is_{10,14} \gamma_{10}^\downarrow \gamma_{14}^\uparrow) (1 + is_{11,12} \gamma_{11}^\downarrow \gamma_{12}^\downarrow), \quad (\text{E.8})
\end{aligned}$$

$$X_{p_2}^{\{d_{vw}^1\}} = 2^{-4}(1 + is_{2',1'}\gamma_2^\downarrow\gamma_1^\downarrow)(1 + is_{14',12'}\gamma_{14}^\uparrow\gamma_{12}^\downarrow)(1 + is_{11',10'}\gamma_{11}^\downarrow\gamma_{10}^\uparrow) \\ (1 + is_{9',8'}\gamma_9^\uparrow\gamma_8^\downarrow)(1 + is_{7',13'}\gamma_7^\downarrow\gamma_{13}^\uparrow)(1 + is_{6',5'}\gamma_6^\downarrow\gamma_5^\downarrow)(1 + is_{4,3}\gamma_4^\uparrow\gamma_3^\uparrow). \quad (\text{E.9})$$

$$X_{p_2}^{\{d_{vw}\}} = 2^{-\frac{9}{2}}(1 + is_{2',1'}\gamma_2^\downarrow\gamma_1^\downarrow)(1 + is_{14',12'}\gamma_{14}^\uparrow\gamma_{12}^\downarrow)(1 + is_{11',10'}\gamma_{11}^\downarrow\gamma_{10}^\uparrow) \\ (1 + is_{9',8'}\gamma_9^\uparrow\gamma_8^\downarrow)(1 + is_{7',13'}\gamma_7^\downarrow\gamma_{13}^\uparrow)(1 + is_{6',5'}\gamma_6^\downarrow\gamma_5^\downarrow)(1 + is_{5,4}\gamma_5^\uparrow\gamma_4^\downarrow) \\ (1 + is_{3,2}\gamma_3^\downarrow\gamma_2^\uparrow), \quad (\text{E.10})$$

$$X_{p_1}^{\{d_{vw}^2\}} = 2^{-4}(1 + is_{1,2}\gamma_1^\uparrow\gamma_2^\uparrow)(1 + is_{3,4}\gamma_3^\downarrow\gamma_4^\downarrow)(1 + is_{5,6}\gamma_5^\uparrow\gamma_6^\uparrow)(1 + is_{13,7}\gamma_{13}^\downarrow\gamma_7^\uparrow) \\ (1 + is_{8,9}\gamma_8^\uparrow\gamma_9^\downarrow)(1 + is_{10,14}\gamma_{10}^\downarrow\gamma_{14}^\uparrow)(1 + is_{11,12}\gamma_{11}^\downarrow\gamma_{12}^\downarrow). \quad (\text{E.11})$$

Therefore, to show that  $X_{p_2}^{\{d_{vw}^1\}} X_{p_1}^{\{d_{vw}\}} P = X_{p_1}^{\{d_{vw}^2\}} X_{p_2}^{\{d_{vw}\}} P$ , it suffices to prove

$$\Gamma_{\text{ext}}(1 + is_{3,4}\gamma_3^\uparrow\gamma_4^\uparrow)(1 + is_{2,3}\gamma_2^\downarrow\gamma_3^\uparrow)(1 + is_{4,5}\gamma_4^\uparrow\gamma_5^\downarrow)P = 4\Gamma_{\text{ext}}P, \quad (\text{E.12})$$

$$\Gamma_{\text{ext}}(1 + is_{3,4}\gamma_3^\downarrow\gamma_4^\downarrow)(1 + is_{2,3}\gamma_2^\uparrow\gamma_3^\downarrow)(1 + is_{4,5}\gamma_4^\downarrow\gamma_5^\uparrow)P = 4\Gamma_{\text{ext}}P, \quad (\text{E.13})$$

where we define

$$\Gamma_{\text{ext}} = 2^{-\frac{17}{2}}(1 + is_{2',1'}\gamma_2^\downarrow\gamma_1^\downarrow)(1 + is_{14',12'}\gamma_{14}^\uparrow\gamma_{12}^\downarrow)(1 + is_{11',10'}\gamma_{11}^\downarrow\gamma_{10}^\uparrow) \\ (1 + is_{9',8'}\gamma_9^\uparrow\gamma_8^\downarrow)(1 + is_{7',13'}\gamma_7^\downarrow\gamma_{13}^\uparrow)(1 + is_{6',5'}\gamma_6^\downarrow\gamma_5^\downarrow)(1 + is_{1,2}\gamma_1^\uparrow\gamma_2^\uparrow) \\ (1 + is_{5,6}\gamma_5^\uparrow\gamma_6^\uparrow)(1 + is_{13,7}\gamma_{13}^\downarrow\gamma_7^\uparrow)(1 + is_{8,9}\gamma_8^\uparrow\gamma_9^\downarrow)(1 + is_{10,14}\gamma_{10}^\downarrow\gamma_{14}^\uparrow) \\ (1 + is_{11,12}\gamma_{11}^\downarrow\gamma_{12}^\downarrow). \quad (\text{E.14})$$

To prove Eq. (E.12), we can first pull out the projector  $(1 + is_{3,4}\gamma_3^\uparrow\gamma_4^\uparrow)$  from  $P$  and write  $P = (1 + is_{3,4}\gamma_3^\uparrow\gamma_4^\uparrow)\tilde{P}$ . Then we make use of the identity

$$(1 + is_{3,4}\gamma_3^\uparrow\gamma_4^\uparrow)(1 + is_{2,3}\gamma_2^\downarrow\gamma_3^\uparrow)(1 + is_{4,5}\gamma_4^\uparrow\gamma_5^\downarrow)(1 + is_{3,4}\gamma_3^\uparrow\gamma_4^\uparrow) \\ = 2(1 + is_{2',3}s_{3,4}s_{4,5}\gamma_2^\downarrow\gamma_5^\downarrow)(1 + is_{3,4}\gamma_3^\uparrow\gamma_4^\uparrow) \quad (\text{E.15})$$

to simplify the left-hand side of Eq. (E.12). We get

$$\Gamma_{\text{ext}}(1 + is_{3,4}\gamma_3^\uparrow\gamma_4^\uparrow)(1 + is_{2,3}\gamma_2^\downarrow\gamma_3^\uparrow)(1 + is_{4,5}\gamma_4^\uparrow\gamma_5^\downarrow)P \\ = \Gamma_{\text{ext}}2(1 + is_{2',3}s_{3,4}s_{4,5}\gamma_2^\downarrow\gamma_5^\downarrow)P. \quad (\text{E.16})$$

We can use the following trick to further simplify the left-hand side of Eq. (E.16). We can pull out fermion bilinears of the form  $is_{vw}\gamma_v^{s_v}\gamma_w^{s_w}$  from both  $P$  and  $\Gamma_{\text{ext}}$ , both containing projectors that set these bilinears to 1. More specifically,

$$\Gamma_{\text{ext}}(is_{2',3}s_{3,4}s_{4,5}\gamma_2^\downarrow\gamma_5^\downarrow)P$$

$$\begin{aligned}
&= \Gamma_{\text{ext}} \left( i s_{2',3} s_{3,4} s_{4,5'} (i s_{1',2'} \gamma_1^\downarrow \gamma_2^\downarrow) \gamma_2^\downarrow \gamma_5^\downarrow \right) P \\
&= \Gamma_{\text{ext}} (-s_{1',2'} s_{2',3} s_{3,4} s_{4,5'} \gamma_1^\downarrow \gamma_5^\downarrow) P \\
&= \Gamma_{\text{ext}} \left( -s_{1',2'} s_{2',3} s_{3,4} s_{4,5'} \gamma_1^\downarrow \gamma_5^\downarrow (i s_{14',1'} \gamma_{14'}^\uparrow \gamma_1^\downarrow) \right) P \\
&= \Gamma_{\text{ext}} (-i s_{14',1'} s_{1',2'} s_{2',3} s_{3,4} s_{4,5'} \gamma_5^\downarrow \gamma_{14'}^\uparrow) P \\
&= \Gamma_{\text{ext}} \left( -i s_{14',1'} s_{1',2'} s_{2',3} s_{3,4} s_{4,5'} \gamma_5^\downarrow (i s_{12',14'} \gamma_{12'}^\downarrow \gamma_{14'}^\uparrow) \gamma_{14'}^\uparrow \right) P \\
&= \Gamma_{\text{ext}} (s_{12',14'} s_{14',1'} s_{1',2'} s_{2',3} s_{3,4} s_{4,5'} \gamma_5^\downarrow \gamma_{12'}^\downarrow) P \\
&= \Gamma_{\text{ext}} \left( s_{12',14'} s_{14',1'} s_{1',2'} s_{2',3} s_{3,4} s_{4,5'} \gamma_5^\downarrow \gamma_{12'}^\downarrow (i s_{11',12'} \gamma_{11'}^\downarrow \gamma_{12'}^\downarrow) \right) P \\
&= \Gamma_{\text{ext}} (-i s_{11',12'} s_{12',14'} s_{14',1'} s_{1',2'} s_{2',3} s_{3,4} s_{4,5'} \gamma_5^\downarrow \gamma_{11'}^\downarrow) P \\
&= \Gamma_{\text{ext}} \left( -i s_{11',12'} s_{12',14'} s_{14',1'} s_{1',2'} s_{2',3} s_{3,4} s_{4,5'} \gamma_5^\downarrow (i s_{10',11'} \gamma_{10'}^\uparrow \gamma_{11'}^\downarrow) \gamma_{11'}^\downarrow \right) P \\
&= \Gamma_{\text{ext}} (s_{10',11'} s_{11',12'} s_{12',14'} s_{14',1'} s_{1',2'} s_{2',3} s_{3,4} s_{4,5'} \gamma_5^\downarrow \gamma_{10'}^\uparrow) P \\
&= \Gamma_{\text{ext}} \left( s_{10',11'} s_{11',12'} s_{12',14'} s_{14',1'} s_{1',2'} s_{2',3} s_{3,4} s_{4,5'} \gamma_5^\downarrow \gamma_{10'}^\uparrow (i s_{9',10'} \gamma_9^\uparrow \gamma_{10'}^\uparrow) \right) P \\
&= \Gamma_{\text{ext}} (-i s_{9',10'} s_{10',11'} s_{11',12'} s_{12',14'} s_{14',1'} s_{1',2'} s_{2',3} s_{3,4} s_{4,5'} \gamma_5^\downarrow \gamma_9^\uparrow) P \\
&= \Gamma_{\text{ext}} \left( -i s_{9',10'} s_{10',11'} s_{11',12'} s_{12',14'} s_{14',1'} s_{1',2'} s_{2',3} s_{3,4} s_{4,5'} \gamma_5^\downarrow (i s_{8',9'} \gamma_8^\downarrow \gamma_9^\uparrow) \gamma_9^\uparrow \right) P \\
&= \Gamma_{\text{ext}} (s_{8',9'} s_{9',10'} s_{10',11'} s_{11',12'} s_{12',14'} s_{14',1'} s_{1',2'} s_{2',3} s_{3,4} s_{4,5'} \gamma_5^\downarrow \gamma_8^\downarrow) P \\
&= \Gamma_{\text{ext}} \left( s_{8',9'} s_{9',10'} s_{10',11'} s_{11',12'} s_{12',14'} s_{14',1'} s_{1',2'} s_{2',3} s_{3,4} s_{4,5'} \gamma_5^\downarrow \gamma_8^\downarrow (i s_{7',8'} \gamma_7^\downarrow \gamma_8^\downarrow) \right) P \\
&= \Gamma_{\text{ext}} (-i s_{7',8'} s_{8',9'} s_{9',10'} s_{10',11'} s_{11',12'} s_{12',14'} s_{14',1'} s_{1',2'} s_{2',3} s_{3,4} s_{4,5'} \gamma_5^\downarrow \gamma_7^\downarrow) P \\
&= \Gamma_{\text{ext}} \left( -i s_{7',8'} s_{8',9'} s_{9',10'} s_{10',11'} s_{11',12'} s_{12',14'} s_{14',1'} s_{1',2'} s_{2',3} s_{3,4} s_{4,5'} \gamma_5^\downarrow \right. \\
&\quad \left. (i s_{13',7'} \gamma_{13'}^\uparrow \gamma_7^\downarrow) \gamma_7^\downarrow \right) P \\
&= \Gamma_{\text{ext}} (s_{13',7'} s_{7',8'} s_{8',9'} s_{9',10'} s_{10',11'} s_{11',12'} s_{12',14'} s_{14',1'} s_{1',2'} s_{2',3} s_{3,4} s_{4,5'} \gamma_5^\downarrow \gamma_{13'}^\uparrow) P \\
&= \Gamma_{\text{ext}} \left( s_{13',7'} s_{7',8'} s_{8',9'} s_{9',10'} s_{10',11'} s_{11',12'} s_{12',14'} s_{14',1'} s_{1',2'} s_{2',3} s_{3,4} s_{4,5'} \gamma_5^\downarrow \gamma_{13'}^\uparrow \right. \\
&\quad \left. (i s_{6',13'} \gamma_6^\downarrow \gamma_{13'}^\uparrow) \right) P \\
&= \Gamma_{\text{ext}} (-i s_{6',13'} s_{13',7'} s_{7',8'} s_{8',9'} s_{9',10'} s_{10',11'} s_{11',12'} s_{12',14'} s_{14',1'} s_{1',2'} s_{2',3} s_{3,4} s_{4,5'} \\
&\quad \gamma_5^\downarrow \gamma_6^\downarrow) P
\end{aligned}$$

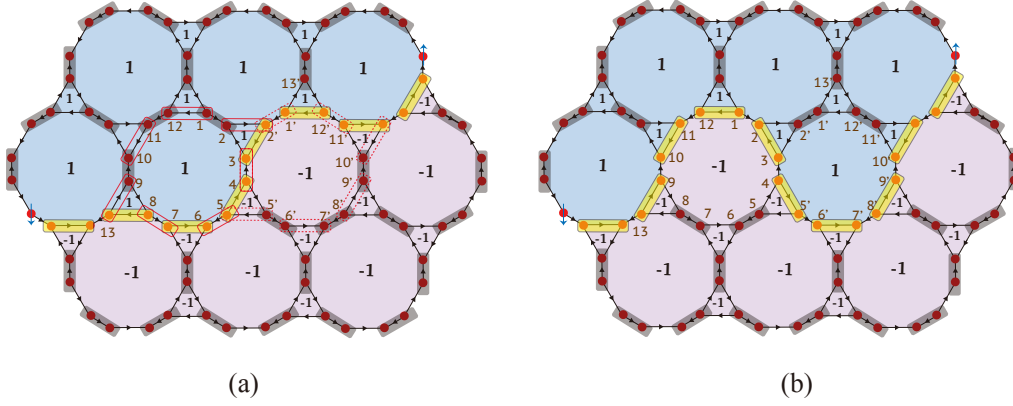


Figure E.3: The spin configuration and the corresponding Majorana configuration for case II(a).

$$\begin{aligned}
&= \Gamma_{\text{ext}} \left( -is_{6',13'}s_{13',7'}s_{7',8'}s_{8',9'}s_{9',10'}s_{10',11'}s_{11',12'}s_{12',14'}s_{14',1'}s_{1',2'}s_{2',3}s_{3,4}s_{4,5'} \right. \\
&\quad \left. (is_{5',6'}\gamma_5^\downarrow\gamma_6^\downarrow)\gamma_5^\downarrow\gamma_6^\downarrow \right) P \\
&= \Gamma_{\text{ext}}(-s_{5',6'}s_{6',13'}s_{13',7'}s_{7',8'}s_{8',9'}s_{9',10'}s_{10',11'}s_{11',12'}s_{12',14'}s_{14',1'}s_{1',2'}s_{2',3}s_{3,4}s_{4,5'})P \\
&= \Gamma_{\text{ext}}P. \tag{E.17}
\end{aligned}$$

Thus,  $\Gamma_{\text{ext}}2(1 + is_{2',3}s_{3,4}s_{4,5'}\gamma_2^\downarrow\gamma_5^\downarrow)P = 4\Gamma_{\text{ext}}P$ , which implies Eq. (E.12). Eq. (E.13) can be proved similarly, and Eqs. (E.12) and (E.13) together implies that

$$X_{p_2}^{\{d_{vw}^\downarrow\}} X_{p_1}^{\{d_{vw}\}} P = X_{p_1}^{\{d_{vw}^\downarrow\}} X_{p_2}^{\{d_{vw}\}} P. \tag{E.18}$$

**Case II:**  $\tau_{p_1}^z = -\tau_{p_2}^z$

Without loss of generality, we assume that  $\tau_{p_1}^z = 1$ ,  $\tau_{p_2}^z = -1$ . Unlike the previous case, further subtleties may arise depending on the spin configuration of the two plaquettes bordering both  $p_1$  and  $p_2$ . We therefore discuss them separately. We first consider the case where the two plaquettes bordering both  $p_1$  and  $p_2$  are in opposite spin configurations. See Fig. E.3 for an example configuration. The proof demonstrated below applies all configurations of this type.

$$\begin{aligned}
P &= 2^{-23}(1 + is_{1,2}\gamma_1^\uparrow\gamma_2^\uparrow)(1 + is_{1,2}\gamma_1^\downarrow\gamma_2^\downarrow)(1 + is_{2',3}\gamma_2^\downarrow\gamma_3^\uparrow)(1 + is_{3,4}\gamma_3^\downarrow\gamma_4^\downarrow) \\
&\quad (1 + is_{4,5}\gamma_4^\uparrow\gamma_5^\downarrow)(1 + is_{6,7}\gamma_6^\downarrow\gamma_7^\uparrow)(1 + is_{5,6}\gamma_5^\uparrow\gamma_6^\downarrow)(1 + is_{8,13}\gamma_8^\uparrow\gamma_{13}^\downarrow)(1 + is_{7,8}\gamma_7^\downarrow\gamma_8^\downarrow) \\
&\quad (1 + is_{9,10}\gamma_9^\uparrow\gamma_{10}^\uparrow)(1 + is_{9,10}\gamma_9^\downarrow\gamma_{10}^\downarrow)(1 + is_{11,12}\gamma_{11}^\uparrow\gamma_{12}^\uparrow)(1 + is_{11,12}\gamma_{11}^\downarrow\gamma_{12}^\downarrow) \\
&\quad (1 + is_{5',6'}\gamma_5^\uparrow\gamma_6^\uparrow)(1 + is_{5',6'}\gamma_5^\downarrow\gamma_6^\downarrow)(1 + is_{7',8'}\gamma_7^\uparrow\gamma_8^\uparrow)(1 + is_{7',8'}\gamma_7^\downarrow\gamma_8^\downarrow) \\
&\quad (1 + is_{9',10'}\gamma_9^\uparrow\gamma_{10'}^\uparrow)(1 + is_{9',10'}\gamma_9^\downarrow\gamma_{10'}^\downarrow)(1 + is_{13',11'}\gamma_{13}^\downarrow\gamma_{11}^\uparrow)(1 + is_{11',12'}\gamma_{11}^\downarrow\gamma_{12'}^\downarrow)
\end{aligned}$$

$$(1 + is_{12',1'}\gamma_{12'}^\uparrow\gamma_{1'}^\downarrow)(1 + is_{1',2'}\gamma_{1'}^\uparrow\gamma_{2'}^\uparrow). \quad (\text{E.19})$$

$$\begin{aligned} X_{p_1}^{\{d_{vw}\}} &= 2^{-4}(1 + is_{12,1}\gamma_{12}^\downarrow\gamma_1^\uparrow)(1 + is_{2,2'}\gamma_2^\uparrow\gamma_{2'}^\downarrow)(1 + is_{3,4}\gamma_3^\uparrow\gamma_4^\uparrow)(1 + is_{5,6}\gamma_5^\downarrow\gamma_6^\downarrow) \\ &\quad (1 + is_{7,8}\gamma_7^\uparrow\gamma_8^\uparrow)(1 + is_{13,9}\gamma_{13}^\downarrow\gamma_9^\uparrow)(1 + is_{10,11}\gamma_{10}^\uparrow\gamma_{11}^\downarrow), \end{aligned} \quad (\text{E.20})$$

$$\begin{aligned} X_{p_2}^{\{d_{vw}^1\}} &= 2^{-4}(1 + is_{1',2'}\gamma_{1'}^\downarrow\gamma_{2'}^\downarrow)(1 + is_{2,3}\gamma_2^\uparrow\gamma_3^\downarrow)(1 + is_{4,5'}\gamma_4^\downarrow\gamma_{5'}^\uparrow)(1 + is_{6',7'}\gamma_{6'}^\uparrow\gamma_{7'}^\downarrow) \\ &\quad (1 + is_{8',9'}\gamma_{8'}^\downarrow\gamma_{9'}^\uparrow)(1 + is_{10',13'}\gamma_{10'}^\uparrow\gamma_{13'}^\downarrow)(1 + is_{11',12'}\gamma_{11'}^\uparrow\gamma_{12'}^\uparrow). \end{aligned} \quad (\text{E.21})$$

$$\begin{aligned} X_{p_2}^{\{d_{vw}\}} &= 2^{-4}(1 + is_{1',2'}\gamma_{1'}^\downarrow\gamma_{2'}^\downarrow)(1 + is_{3,4}\gamma_3^\uparrow\gamma_4^\uparrow)(1 + is_{5,5'}\gamma_5^\downarrow\gamma_{5'}^\uparrow)(1 + is_{6',7'}\gamma_{6'}^\uparrow\gamma_{7'}^\downarrow) \\ &\quad (1 + is_{8',9'}\gamma_{8'}^\downarrow\gamma_{9'}^\uparrow)(1 + is_{10',13'}\gamma_{10'}^\uparrow\gamma_{13'}^\downarrow)(1 + is_{11',12'}\gamma_{11'}^\uparrow\gamma_{12'}^\uparrow), \end{aligned} \quad (\text{E.22})$$

$$\begin{aligned} X_{p_1}^{\{d_{vw}^2\}} &= 2^{-4}(1 + is_{2,3}\gamma_2^\uparrow\gamma_3^\downarrow)(1 + is_{4,5'}\gamma_4^\downarrow\gamma_{5'}^\uparrow)(1 + is_{5,6}\gamma_5^\downarrow\gamma_6^\downarrow)(1 + is_{7,8}\gamma_7^\uparrow\gamma_8^\uparrow) \\ &\quad (1 + is_{13,9}\gamma_{13}^\downarrow\gamma_9^\uparrow)(1 + is_{10,11}\gamma_{10}^\uparrow\gamma_{11}^\downarrow)(1 + is_{12,1}\gamma_{12}^\downarrow\gamma_1^\uparrow). \end{aligned} \quad (\text{E.23})$$

Therefore, to show that  $X_{p_2}^{\{d_{vw}^1\}} X_{p_1}^{\{d_{vw}\}} P = X_{p_1}^{\{d_{vw}^2\}} X_{p_2}^{\{d_{vw}\}} P$ , it suffices to prove

$$X_{p_2}^{\{d_{vw}^1\}} \tilde{X}_{p_1}^{\{d_{vw}\}} 2^{-1}(1 + is_{2,2'}\gamma_2^\uparrow\gamma_{2'}^\downarrow)P = X_{p_2}^{\{d_{vw}^1\}} \tilde{X}_{p_1}^{\{d_{vw}\}} P, \quad (\text{E.24})$$

$$X_{p_1}^{\{d_{vw}^2\}} \tilde{X}_{p_2}^{\{d_{vw}\}} 2^{-1}(1 + is_{5,5'}\gamma_5^\downarrow\gamma_{5'}^\uparrow)P = X_{p_1}^{\{d_{vw}^2\}} \tilde{X}_{p_2}^{\{d_{vw}\}} P, \quad (\text{E.25})$$

where we define

$$\begin{aligned} \tilde{X}_{p_1}^{\{d_{vw}\}} &= 2^{-3}(1 + is_{12,1}\gamma_{12}^\downarrow\gamma_1^\uparrow)(1 + is_{3,4}\gamma_3^\uparrow\gamma_4^\uparrow)(1 + is_{5,6}\gamma_5^\downarrow\gamma_6^\downarrow)(1 + is_{7,8}\gamma_7^\uparrow\gamma_8^\uparrow) \\ &\quad (1 + is_{13,9}\gamma_{13}^\downarrow\gamma_9^\uparrow)(1 + is_{10,11}\gamma_{10}^\uparrow\gamma_{11}^\downarrow), \end{aligned} \quad (\text{E.26})$$

$$\begin{aligned} \tilde{X}_{p_2}^{\{d_{vw}\}} &= 2^{-3}(1 + is_{1',2'}\gamma_{1'}^\downarrow\gamma_{2'}^\downarrow)(1 + is_{3,4}\gamma_3^\uparrow\gamma_4^\uparrow)(1 + is_{6',7'}\gamma_{6'}^\uparrow\gamma_{7'}^\downarrow)(1 + is_{8',9'}\gamma_{8'}^\downarrow\gamma_{9'}^\uparrow) \\ &\quad (1 + is_{10',13'}\gamma_{10'}^\uparrow\gamma_{13'}^\downarrow)(1 + is_{11',12'}\gamma_{11'}^\uparrow\gamma_{12'}^\uparrow). \end{aligned} \quad (\text{E.27})$$

We can use the following trick to simplify the left-hand side of Eq. (E.24) (respectively, Eq. (E.25)). We can pull out fermion bilinears of the form  $is_{vw}\gamma_v^{Sv}\gamma_w^{Sw}$  from both  $P$  and  $\tilde{X}_{p_1}^{\{d_{vw}\}}$  (respectively,  $\tilde{X}_{p_2}^{\{d_{vw}\}}$ ), both containing projectors that set these bilinears to 1. More specifically,

$$\begin{aligned} &X_{p_2}^{\{d_{vw}^1\}} \tilde{X}_{p_1}^{\{d_{vw}\}} (is_{2,2'}\gamma_2^\uparrow\gamma_{2'}^\downarrow)P \\ &= X_{p_2}^{\{d_{vw}^1\}} \tilde{X}_{p_1}^{\{d_{vw}\}} \left( is_{2,2'}\gamma_2^\uparrow\gamma_{2'}^\downarrow (is_{1,2}\gamma_1^\uparrow\gamma_2^\uparrow) \right) P \\ &= X_{p_2}^{\{d_{vw}^1\}} \tilde{X}_{p_1}^{\{d_{vw}\}} (-s_{1,2}s_{2,2'}\gamma_2^\downarrow\gamma_1^\uparrow)P \\ &= X_{p_2}^{\{d_{vw}^1\}} \tilde{X}_{p_1}^{\{d_{vw}\}} (-s_{1,2}s_{2,2'}\gamma_2^\downarrow\gamma_1^\uparrow)P \\ &= X_{p_2}^{\{d_{vw}^1\}} \tilde{X}_{p_1}^{\{d_{vw}\}} \left( -s_{1,2}s_{2,2'}\gamma_2^\downarrow (is_{12,1}\gamma_{12}^\downarrow\gamma_1^\uparrow)\gamma_1^\uparrow \right) P \end{aligned}$$

$$\begin{aligned}
&= X_{p_2}^{\{d_{vw}^1\}} \tilde{X}_{p_1}^{\{d_{vw}\}} (-i s_{12,1} s_{1,2} s_{2,2'} \gamma_2^\downarrow \gamma_{12}^\downarrow) P \\
&= X_{p_2}^{\{d_{vw}^1\}} \tilde{X}_{p_1}^{\{d_{vw}\}} \left( -i s_{12,1} s_{1,2} s_{2,2'} \gamma_2^\downarrow \gamma_{12}^\downarrow (i s_{11,12} \gamma_{11}^\downarrow \gamma_{12}^\downarrow) \right) P \\
&= X_{p_2}^{\{d_{vw}^1\}} \tilde{X}_{p_1}^{\{d_{vw}\}} (-s_{11,12} s_{12,1} s_{1,2} s_{2,2'} \gamma_2^\downarrow \gamma_{11}^\downarrow) P \\
&= X_{p_2}^{\{d_{vw}^1\}} \tilde{X}_{p_1}^{\{d_{vw}\}} \left( -s_{11,12} s_{12,1} s_{1,2} s_{2,2'} \gamma_2^\downarrow (i s_{10,11} \gamma_{10}^\uparrow \gamma_{11}^\downarrow) \gamma_{11}^\downarrow \right) P \\
&= X_{p_2}^{\{d_{vw}^1\}} \tilde{X}_{p_1}^{\{d_{vw}\}} (-i s_{10,11} s_{11,12} s_{12,1} s_{1,2} s_{2,2'} \gamma_2^\downarrow \gamma_{10}^\uparrow) P \\
&= X_{p_2}^{\{d_{vw}^1\}} \tilde{X}_{p_1}^{\{d_{vw}\}} \left( -i s_{10,11} s_{11,12} s_{12,1} s_{1,2} s_{2,2'} \gamma_2^\downarrow \gamma_{10}^\uparrow (i s_{9,10} \gamma_9^\uparrow \gamma_{10}^\uparrow) \right) P \\
&= X_{p_2}^{\{d_{vw}^1\}} \tilde{X}_{p_1}^{\{d_{vw}\}} (-s_{9,10} s_{10,11} s_{11,12} s_{12,1} s_{1,2} s_{2,2'} \gamma_2^\downarrow \gamma_9^\uparrow) P \\
&= X_{p_2}^{\{d_{vw}^1\}} \tilde{X}_{p_1}^{\{d_{vw}\}} \left( -s_{9,10} s_{10,11} s_{11,12} s_{12,1} s_{1,2} s_{2,2'} \gamma_2^\downarrow (i s_{13,9} \gamma_{13}^\downarrow \gamma_9^\uparrow) \gamma_9^\uparrow \right) P \\
&= X_{p_2}^{\{d_{vw}^1\}} \tilde{X}_{p_1}^{\{d_{vw}\}} (-i s_{13,9} s_{9,10} s_{10,11} s_{11,12} s_{12,1} s_{1,2} s_{2,2'} \gamma_2^\downarrow \gamma_{13}^\downarrow) P \\
&= X_{p_2}^{\{d_{vw}^1\}} \tilde{X}_{p_1}^{\{d_{vw}\}} \left( -i s_{13,9} s_{9,10} s_{10,11} s_{11,12} s_{12,1} s_{1,2} s_{2,2'} \gamma_2^\downarrow \gamma_{13}^\downarrow (i s_{8,13} \gamma_8^\uparrow \gamma_{13}^\downarrow) \right) P \\
&= X_{p_2}^{\{d_{vw}^1\}} \tilde{X}_{p_1}^{\{d_{vw}\}} (-s_{8,13} s_{13,9} s_{9,10} s_{10,11} s_{11,12} s_{12,1} s_{1,2} s_{2,2'} \gamma_2^\downarrow \gamma_8^\uparrow) P \\
&= X_{p_2}^{\{d_{vw}^1\}} \tilde{X}_{p_1}^{\{d_{vw}\}} \left( -s_{8,13} s_{13,9} s_{9,10} s_{10,11} s_{11,12} s_{12,1} s_{1,2} s_{2,2'} \gamma_2^\downarrow (i s_{7,8} \gamma_7^\uparrow \gamma_8^\uparrow) \gamma_8^\uparrow \right) P \\
&= X_{p_2}^{\{d_{vw}^1\}} \tilde{X}_{p_1}^{\{d_{vw}\}} (-i s_{7,8} s_{8,13} s_{13,9} s_{9,10} s_{10,11} s_{11,12} s_{12,1} s_{1,2} s_{2,2'} \gamma_2^\downarrow \gamma_7^\uparrow) P \\
&= X_{p_2}^{\{d_{vw}^1\}} \tilde{X}_{p_1}^{\{d_{vw}\}} \left( -i s_{7,8} s_{8,13} s_{13,9} s_{9,10} s_{10,11} s_{11,12} s_{12,1} s_{1,2} s_{2,2'} \gamma_2^\downarrow \gamma_7^\uparrow (i s_{6,7} \gamma_6^\downarrow \gamma_7^\uparrow) \right) P \\
&= X_{p_2}^{\{d_{vw}^1\}} \tilde{X}_{p_1}^{\{d_{vw}\}} (-s_{6,7} s_{7,8} s_{8,13} s_{13,9} s_{9,10} s_{10,11} s_{11,12} s_{12,1} s_{1,2} s_{2,2'} \gamma_2^\downarrow \gamma_6^\downarrow) P \\
&= X_{p_2}^{\{d_{vw}^1\}} \tilde{X}_{p_1}^{\{d_{vw}\}} \left( -s_{6,7} s_{7,8} s_{8,13} s_{13,9} s_{9,10} s_{10,11} s_{11,12} s_{12,1} s_{1,2} s_{2,2'} \gamma_2^\downarrow (i s_{5,6} \gamma_5^\downarrow \gamma_6^\downarrow) \gamma_6^\downarrow \right) P \\
&= X_{p_2}^{\{d_{vw}^1\}} \tilde{X}_{p_1}^{\{d_{vw}\}} (-i s_{5,6} s_{6,7} s_{7,8} s_{8,13} s_{13,9} s_{9,10} s_{10,11} s_{11,12} s_{12,1} s_{1,2} s_{2,2'} \gamma_2^\downarrow \gamma_5^\downarrow) P \\
&= X_{p_2}^{\{d_{vw}^1\}} \tilde{X}_{p_1}^{\{d_{vw}\}} \left( -i s_{5,6} s_{6,7} s_{7,8} s_{8,13} s_{13,9} s_{9,10} s_{10,11} s_{11,12} s_{12,1} s_{1,2} s_{2,2'} \gamma_2^\downarrow \gamma_5^\downarrow \right. \\
&\quad \left. (i s_{4,5} \gamma_4^\uparrow \gamma_5^\downarrow) \right) P \\
&= X_{p_2}^{\{d_{vw}^1\}} \tilde{X}_{p_1}^{\{d_{vw}\}} (-s_{4,5} s_{5,6} s_{6,7} s_{7,8} s_{8,13} s_{13,9} s_{9,10} s_{10,11} s_{11,12} s_{12,1} s_{1,2} s_{2,2'} \gamma_2^\downarrow \gamma_4^\uparrow) P \\
&= X_{p_2}^{\{d_{vw}^1\}} \tilde{X}_{p_1}^{\{d_{vw}\}} \left( -s_{4,5} s_{5,6} s_{6,7} s_{7,8} s_{8,13} s_{13,9} s_{9,10} s_{10,11} s_{11,12} s_{12,1} s_{1,2} s_{2,2'} \gamma_2^\downarrow \right. \\
&\quad \left. (i s_{3,4} \gamma_3^\uparrow \gamma_4^\uparrow) \gamma_4^\uparrow \right) P \\
&= X_{p_2}^{\{d_{vw}^1\}} \tilde{X}_{p_1}^{\{d_{vw}\}} (-i s_{3,4} s_{4,5} s_{5,6} s_{6,7} s_{7,8} s_{8,13} s_{13,9} s_{9,10} s_{10,11} s_{11,12} s_{12,1} s_{1,2} s_{2,2'} \gamma_2^\downarrow \gamma_3^\uparrow) P
\end{aligned}$$

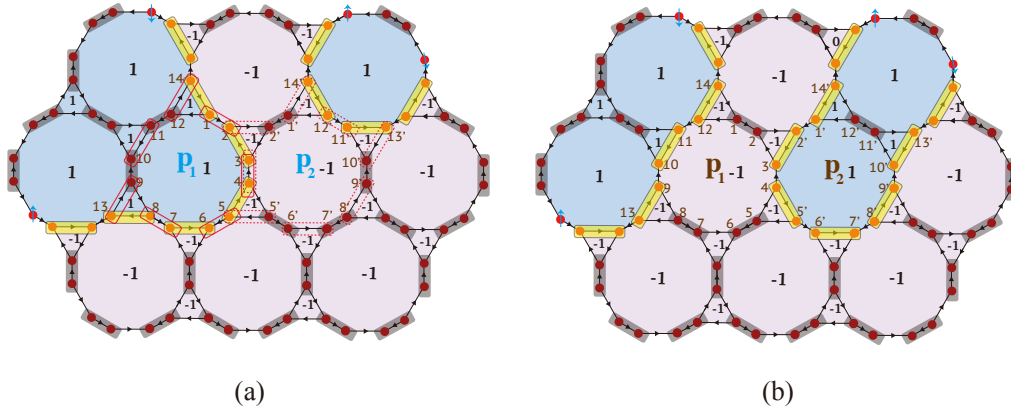


Figure E.4: The spin configuration and the corresponding Majorana configuration for case II(b).

$$\begin{aligned}
&= X_{p_2}^{\{d_{vw}^1\}} \tilde{X}_{p_1}^{\{d_{vw}\}} \left( -i s_{3,4} s_{4,5} s_{5,6} s_{6,7} s_{7,8} s_{8,13} s_{13,9} s_{9,10} s_{10,11} s_{11,12} s_{12,1} s_{1,2} s_{2,2'} \gamma_2^\downarrow \gamma_3^\uparrow \right. \\
&\quad \left. (i s_{2',3} \gamma_2^\downarrow \gamma_3^\uparrow) \right) P \\
&= X_{p_2}^{\{d_{vw}^1\}} \tilde{X}_{p_1}^{\{d_{vw}\}} (-s_{2',3} s_{3,4} s_{4,5} s_{5,6} s_{6,7} s_{7,8} s_{8,13} s_{13,9} s_{9,10} s_{10,11} s_{11,12} s_{12,1} s_{1,2} s_{2,2'}) P \\
&= X_{p_2}^{\{d_{vw}^1\}} \tilde{X}_{p_1}^{\{d_{vw}\}} P. \tag{E.28}
\end{aligned}$$

Hence, Eq. (E.24) holds. Similarly, one can show that

$$X_{p_1}^{\{d_{vw}^2\}} \tilde{X}_{p_2}^{\{d_{vw}\}} (i s_{5,5'} \gamma_5^\downarrow \gamma_{5'}^\uparrow) P = X_{p_1}^{\{d_{vw}^2\}} \tilde{X}_{p_2}^{\{d_{vw}\}} P, \tag{E.29}$$

which implies Eq. (E.25). Combining Eqs. (E.24) and (E.25), we conclude that

$$X_{p_2}^{\{d_{vw}^1\}} X_{p_1}^{\{d_{vw}\}} P = X_{p_1}^{\{d_{vw}^2\}} X_{p_2}^{\{d_{vw}\}} P. \tag{E.30}$$

Next, we consider the case where the two plaquettes bordering both  $p_1$  and  $p_2$  are in the same spin configuration while  $p_1$  and  $p_2$  are initially in different spin states. See Fig. E.4 for an example configuration. The proof demonstrated below applies all configurations of this type.

$$\begin{aligned}
P &= 2^{-24} (1 + i s_{14,1} \gamma_{14}^\uparrow \gamma_1^\downarrow) (1 + i s_{2,3} \gamma_2^\downarrow \gamma_3^\uparrow) (1 + i s_{1,2} \gamma_1^\uparrow \gamma_2^\downarrow) (1 + i s_{3,4} \gamma_3^\downarrow \gamma_4^\uparrow) \\
&\quad (1 + i s_{4,5} \gamma_4^\uparrow \gamma_5^\downarrow) (1 + i s_{6,7} \gamma_6^\downarrow \gamma_7^\uparrow) (1 + i s_{5,6} \gamma_5^\uparrow \gamma_6^\downarrow) (1 + i s_{8,13} \gamma_8^\uparrow \gamma_{13}^\downarrow) \\
&\quad (1 + i s_{7,8} \gamma_7^\downarrow \gamma_8^\uparrow) (1 + i s_{9,10} \gamma_9^\uparrow \gamma_{10}^\downarrow) (1 + i s_{9,10} \gamma_9^\downarrow \gamma_{10}^\uparrow) (1 + i s_{11,12} \gamma_{11}^\uparrow \gamma_{12}^\downarrow) \\
&\quad (1 + i s_{11,12} \gamma_{11}^\downarrow \gamma_{12}^\uparrow) (1 + i s_{1',2'} \gamma_{1'}^\uparrow \gamma_{2'}^\downarrow) (1 + i s_{1',2'} \gamma_{1'}^\downarrow \gamma_{2'}^\uparrow) (1 + i s_{5',6'} \gamma_{5'}^\uparrow \gamma_{6'}^\downarrow) \\
&\quad (1 + i s_{5',6'} \gamma_{5'}^\downarrow \gamma_{6'}^\uparrow) (1 + i s_{7',8'} \gamma_{7'}^\uparrow \gamma_{8'}^\downarrow) (1 + i s_{7',8'} \gamma_{7'}^\downarrow \gamma_{8'}^\uparrow) (1 + i s_{9',10'} \gamma_{9'}^\uparrow \gamma_{10'}^\downarrow)
\end{aligned}$$

$$(1 + is_{9',10'}\gamma_9^\downarrow\gamma_{10'}^\downarrow)(1 + is_{13',11'}\gamma_{13'}^\downarrow\gamma_{11'}^\uparrow)(1 + is_{12',14'}\gamma_{12'}^\uparrow\gamma_{14'}^\downarrow) \\ (1 + is_{11',12'}\gamma_{11'}^\downarrow\gamma_{12'}^\downarrow). \quad (\text{E.31})$$

$$X_{p_1}^{\{d_{vw}\}} = 2^{-4}(1 + is_{1,2}\gamma_1^\downarrow\gamma_2^\downarrow)(1 + is_{3,4}\gamma_3^\uparrow\gamma_4^\uparrow)(1 + is_{5,6}\gamma_5^\downarrow\gamma_6^\downarrow)(1 + is_{7,8}\gamma_7^\uparrow\gamma_8^\uparrow) \\ (1 + is_{13,9}\gamma_{13}^\downarrow\gamma_9^\uparrow)(1 + is_{10,11}\gamma_{10}^\uparrow\gamma_{11}^\downarrow)(1 + is_{12,14}\gamma_{12}^\downarrow\gamma_{14}^\uparrow), \quad (\text{E.32})$$

$$X_{p_2}^{\{d_{vw}^1\}} = 2^{-4}(1 + is_{14',1'}\gamma_{14'}^\downarrow\gamma_{1'}^\uparrow)(1 + is_{2',3}\gamma_{2'}^\uparrow\gamma_3^\downarrow)(1 + is_{4,5'}\gamma_4^\downarrow\gamma_{5'}^\uparrow)(1 + is_{6',7'}\gamma_{6'}^\uparrow\gamma_{7'}^\downarrow) \\ (1 + is_{8',9'}\gamma_{8'}^\downarrow\gamma_{9'}^\uparrow)(1 + is_{10',13'}\gamma_{10'}^\uparrow\gamma_{13'}^\downarrow)(1 + is_{11',12'}\gamma_{11'}^\uparrow\gamma_{12'}^\uparrow). \quad (\text{E.33})$$

$$X_{p_2}^{\{d_{vw}^2\}} = 2^{-\frac{9}{2}}(1 + is_{14',1'}\gamma_{14'}^\downarrow\gamma_{1'}^\uparrow)(1 + is_{2',2}\gamma_{2'}^\uparrow\gamma_2^\downarrow)(1 + is_{3,4}\gamma_3^\uparrow\gamma_4^\uparrow)(1 + is_{5,5'}\gamma_5^\downarrow\gamma_{5'}^\uparrow) \\ (1 + is_{6',7'}\gamma_{6'}^\uparrow\gamma_{7'}^\downarrow)(1 + is_{8',9'}\gamma_{8'}^\downarrow\gamma_{9'}^\uparrow)(1 + is_{10',13'}\gamma_{10'}^\uparrow\gamma_{13'}^\downarrow)(1 + is_{11',12'}\gamma_{11'}^\uparrow\gamma_{12'}^\uparrow), \quad (\text{E.34})$$

$$X_{p_1}^{\{d_{vw}^2\}} = 2^{-\frac{9}{2}}(1 + is_{1,2}\gamma_1^\downarrow\gamma_2^\downarrow)(1 + is_{2',3}\gamma_{2'}^\uparrow\gamma_3^\downarrow)(1 + is_{4,5'}\gamma_4^\downarrow\gamma_{5'}^\uparrow)(1 + is_{5,6}\gamma_5^\downarrow\gamma_6^\downarrow) \\ (1 + is_{7,8}\gamma_7^\uparrow\gamma_8^\uparrow)(1 + is_{13,9}\gamma_{13}^\downarrow\gamma_9^\uparrow)(1 + is_{10,11}\gamma_{10}^\uparrow\gamma_{11}^\downarrow)(1 + is_{12,14}\gamma_{12}^\downarrow\gamma_{14}^\uparrow). \quad (\text{E.35})$$

Therefore, to show that  $X_{p_2}^{\{d_{vw}^1\}}X_{p_1}^{\{d_{vw}\}}P = X_{p_1}^{\{d_{vw}^2\}}X_{p_2}^{\{d_{vw}\}}P$ , it suffices to prove

$$X_{p_1}^{\{d_{vw}^2\}}\tilde{X}_{p_2}^{\{d_{vw}\}}2^{-1}(1 + is_{5,5'}\gamma_5^\downarrow\gamma_{5'}^\uparrow)P = X_{p_1}^{\{d_{vw}^2\}}\tilde{\tilde{X}}_{p_2}^{\{d_{vw}\}}P, \quad (\text{E.36})$$

where we define

$$\tilde{\tilde{X}}_{p_2}^{\{d_{vw}\}} = 2^{-\frac{7}{2}}(1 + is_{14',1'}\gamma_{14'}^\downarrow\gamma_{1'}^\uparrow)(1 + is_{3,4}\gamma_3^\uparrow\gamma_4^\uparrow)(1 + is_{6',7'}\gamma_{6'}^\uparrow\gamma_{7'}^\downarrow) \\ (1 + is_{8',9'}\gamma_{8'}^\downarrow\gamma_{9'}^\uparrow)(1 + is_{10',13'}\gamma_{10'}^\uparrow\gamma_{13'}^\downarrow)(1 + is_{11',12'}\gamma_{11'}^\uparrow\gamma_{12'}^\uparrow), \quad (\text{E.37})$$

and

$$\tilde{X}_{p_2}^{\{d_{vw}\}} = \tilde{\tilde{X}}_{p_2}^{\{d_{vw}\}}(1 + is_{2',2}\gamma_{2'}^\uparrow\gamma_2^\downarrow). \quad (\text{E.38})$$

We can use the following trick to simplify the left-hand side of Eq. (E.36). We can pull out fermion bilinears of the form  $is_{vw}\gamma_v^{s_v}\gamma_w^{s_w}$  from both  $P$  and  $\tilde{X}_{p_2}^{\{d_{vw}\}}$ , both containing projectors that set these bilinears to 1. More specifically,

$$X_{p_1}^{\{d_{vw}^2\}}\tilde{X}_{p_2}^{\{d_{vw}\}}(is_{5,5'}\gamma_5^\downarrow\gamma_{5'}^\uparrow)P \\ = X_{p_1}^{\{d_{vw}^2\}}\tilde{X}_{p_2}^{\{d_{vw}\}}\left(is_{5,5'}\gamma_5^\downarrow\gamma_{5'}^\uparrow(is_{5',6'}\gamma_{5'}^\uparrow\gamma_{6'}^\uparrow)\right)P \\ = X_{p_1}^{\{d_{vw}^2\}}\tilde{X}_{p_2}^{\{d_{vw}\}}(-s_{5,5'}s_{5',6'}\gamma_5^\downarrow\gamma_{6'}^\uparrow)P$$

$$\begin{aligned}
&= X_{p_1}^{\{d_{vw}^2\}} \tilde{X}_{p_2}^{\{d_{vw}\}} \left( -s_{5,5'} s_{5',6'} \gamma_5^\downarrow (i s_{6',7'} \gamma_6^\uparrow \gamma_7^\downarrow) \gamma_6^\uparrow \right) P \\
&= X_{p_1}^{\{d_{vw}^2\}} \tilde{X}_{p_2}^{\{d_{vw}\}} (i s_{5,5'} s_{5',6'} s_{6',7'} \gamma_5^\downarrow \gamma_7^\downarrow) P \\
&= X_{p_1}^{\{d_{vw}^2\}} \tilde{X}_{p_2}^{\{d_{vw}\}} \left( i s_{5,5'} s_{5',6'} s_{6',7'} \gamma_5^\downarrow \gamma_7^\downarrow (i s_{7',8'} \gamma_7^\downarrow \gamma_8^\downarrow) \right) P \\
&= X_{p_1}^{\{d_{vw}^2\}} \tilde{X}_{p_2}^{\{d_{vw}\}} (-s_{5,5'} s_{5',6'} s_{6',7'} s_{7',8'} \gamma_5^\downarrow \gamma_8^\downarrow) P \\
&= X_{p_1}^{\{d_{vw}^2\}} \tilde{X}_{p_2}^{\{d_{vw}\}} \left( -s_{5,5'} s_{5',6'} s_{6',7'} s_{7',8'} \gamma_5^\downarrow (i s_{8',9'} \gamma_8^\downarrow \gamma_9^\uparrow) \gamma_8^\downarrow \right) P \\
&= X_{p_1}^{\{d_{vw}^2\}} \tilde{X}_{p_2}^{\{d_{vw}\}} (i s_{5,5'} s_{5',6'} s_{6',7'} s_{7',8'} s_{8',9'} \gamma_5^\downarrow \gamma_9^\uparrow) P \\
&= X_{p_1}^{\{d_{vw}^2\}} \tilde{X}_{p_2}^{\{d_{vw}\}} \left( i s_{5,5'} s_{5',6'} s_{6',7'} s_{7',8'} s_{8',9'} \gamma_5^\downarrow \gamma_9^\uparrow (i s_{9',10'} \gamma_9^\uparrow \gamma_{10'}^\uparrow) \right) P \\
&= X_{p_1}^{\{d_{vw}^2\}} \tilde{X}_{p_2}^{\{d_{vw}\}} (-s_{5,5'} s_{5',6'} s_{6',7'} s_{7',8'} s_{8',9'} s_{9',10'} \gamma_5^\downarrow \gamma_{10'}^\uparrow) P \\
&= X_{p_1}^{\{d_{vw}^2\}} \tilde{X}_{p_2}^{\{d_{vw}\}} \left( -s_{5,5'} s_{5',6'} s_{6',7'} s_{7',8'} s_{8',9'} s_{9',10'} \gamma_5^\downarrow (i s_{10',13'} \gamma_{10'}^\uparrow \gamma_{13'}^\downarrow) \gamma_{10'}^\uparrow \right) P \\
&= X_{p_1}^{\{d_{vw}^2\}} \tilde{X}_{p_2}^{\{d_{vw}\}} (i s_{5,5'} s_{5',6'} s_{6',7'} s_{7',8'} s_{8',9'} s_{9',10'} s_{10',13'} \gamma_5^\downarrow \gamma_{13'}^\downarrow) P \\
&= X_{p_1}^{\{d_{vw}^2\}} \tilde{X}_{p_2}^{\{d_{vw}\}} \left( i s_{5,5'} s_{5',6'} s_{6',7'} s_{7',8'} s_{8',9'} s_{9',10'} s_{10',13'} \gamma_5^\downarrow \gamma_{13'}^\downarrow (i s_{13',11'} \gamma_{13'}^\downarrow \gamma_{11'}^\uparrow) \right) P \\
&= X_{p_1}^{\{d_{vw}^2\}} \tilde{X}_{p_2}^{\{d_{vw}\}} (-s_{5,5'} s_{5',6'} s_{6',7'} s_{7',8'} s_{8',9'} s_{9',10'} s_{10',13'} s_{13',11'} \gamma_5^\downarrow \gamma_{11'}^\uparrow) P \\
&= X_{p_1}^{\{d_{vw}^2\}} \tilde{X}_{p_2}^{\{d_{vw}\}} \left( -s_{5,5'} s_{5',6'} s_{6',7'} s_{7',8'} s_{8',9'} s_{9',10'} s_{10',13'} s_{13',11'} \gamma_5^\downarrow \right. \\
&\quad \left. (i s_{11',12'} \gamma_{11'}^\uparrow \gamma_{12'}^\uparrow) \gamma_{11'}^\uparrow \right) P \\
&= X_{p_1}^{\{d_{vw}^2\}} \tilde{X}_{p_2}^{\{d_{vw}\}} (i s_{5,5'} s_{5',6'} s_{6',7'} s_{7',8'} s_{8',9'} s_{9',10'} s_{10',13'} s_{13',11'} s_{11',12'} \gamma_5^\downarrow \gamma_{12'}^\uparrow) P \\
&= X_{p_1}^{\{d_{vw}^2\}} \tilde{X}_{p_2}^{\{d_{vw}\}} \left( i s_{5,5'} s_{5',6'} s_{6',7'} s_{7',8'} s_{8',9'} s_{9',10'} s_{10',13'} s_{13',11'} s_{11',12'} \gamma_5^\downarrow \gamma_{12'}^\uparrow \right. \\
&\quad \left. (i s_{12',14'} \gamma_{12'}^\uparrow \gamma_{14'}^\downarrow) \right) P \\
&= X_{p_1}^{\{d_{vw}^2\}} \tilde{X}_{p_2}^{\{d_{vw}\}} (-s_{5,5'} s_{5',6'} s_{6',7'} s_{7',8'} s_{8',9'} s_{9',10'} s_{10',13'} s_{13',11'} s_{11',12'} s_{12',14'} \gamma_5^\downarrow \gamma_{14'}^\downarrow) P \\
&= X_{p_1}^{\{d_{vw}^2\}} \tilde{X}_{p_2}^{\{d_{vw}\}} \left( -s_{5,5'} s_{5',6'} s_{6',7'} s_{7',8'} s_{8',9'} s_{9',10'} s_{10',13'} s_{13',11'} s_{11',12'} s_{12',14'} \gamma_5^\downarrow \right. \\
&\quad \left. (i s_{14',1'} \gamma_{14'}^\downarrow \gamma_{1'}^\uparrow) \gamma_{14'}^\downarrow \right) P \\
&= X_{p_1}^{\{d_{vw}^2\}} \tilde{X}_{p_2}^{\{d_{vw}\}} (i s_{5,5'} s_{5',6'} s_{6',7'} s_{7',8'} s_{8',9'} s_{9',10'} s_{10',13'} s_{13',11'} s_{11',12'} s_{12',14'} s_{14',1'} \\
&\quad \gamma_5^\downarrow \gamma_{1'}^\uparrow) P
\end{aligned}$$

$$\begin{aligned}
&= X_{p_1}^{\{d_{vw}^2\}} \tilde{X}_{p_2}^{\{d_{vw}\}} \left( i s_{5,5',5',6',6',7',7',8',8',9',9',10',10',13',13',11',11',12',12',14',14',1' \right. \\
&\quad \left. \gamma_5^\downarrow \gamma_1^\uparrow (i s_{1',2',2',1',1',2',2'}) \right) P \\
&= X_{p_1}^{\{d_{vw}^2\}} \tilde{X}_{p_2}^{\{d_{vw}\}} (-s_{5,5',5',6',6',7',7',8',8',9',9',10',10',13',13',11',11',12',12',14',14',1' \\
&\quad s_{1',2',2',5',5'}) P \\
&= X_{p_1}^{\{d_{vw}^2\}} \tilde{X}_{p_2}^{\{d_{vw}\}} (-s_{5,5',5',6',6',7',7',8',8',9',9',10',10',13',13',11',11',12',12',14',14',1' \\
&\quad s_{1',2',2',5',5'}^\downarrow (i s_{2',2',2',2',2',2'}) \gamma_2^\uparrow) P \\
&= X_{p_1}^{\{d_{vw}^2\}} \tilde{X}_{p_2}^{\{d_{vw}\}} (i s_{5,5',5',6',6',7',7',8',8',9',9',10',10',13',13',11',11',12',12',14',14',1' \\
&\quad s_{1',2',2',2',2',2',2'}) P \\
&= X_{p_1}^{\{d_{vw}^2\}} \tilde{X}_{p_2}^{\{d_{vw}\}} \left( i s_{5,5',5',6',6',7',7',8',8',9',9',10',10',13',13',11',11',12',12',14',14',1' \right. \\
&\quad \left. s_{1',2',2',2',2',2',2'}^\downarrow \gamma_2^\downarrow (i s_{2,3,3,2,2,2}) \gamma_3^\uparrow \right) P \\
&= X_{p_1}^{\{d_{vw}^2\}} \tilde{X}_{p_2}^{\{d_{vw}\}} (-s_{5,5',5',6',6',7',7',8',8',9',9',10',10',13',13',11',11',12',12',14',14',1' \\
&\quad s_{1',2',2',2',2',2',2',2',2',2',2',2'}) P \\
&= X_{p_1}^{\{d_{vw}^2\}} \tilde{X}_{p_2}^{\{d_{vw}\}} \left( -s_{5,5',5',6',6',7',7',8',8',9',9',10',10',13',13',11',11',12',12',14',14',1' \right. \\
&\quad \left. s_{1',2',2',2',2',2',2',2',2',2',2',2'}^\downarrow (i s_{3,4,4,3,3,3}) \gamma_3^\uparrow \right) P \\
&= X_{p_1}^{\{d_{vw}^2\}} \tilde{X}_{p_2}^{\{d_{vw}\}} (i s_{5,5',5',6',6',7',7',8',8',9',9',10',10',13',13',11',11',12',12',14',14',1' \\
&\quad s_{1',2',2',2',2',2',2',2',2',2',2',2'}^\downarrow \gamma_4^\uparrow) P \\
&= X_{p_1}^{\{d_{vw}^2\}} \tilde{X}_{p_2}^{\{d_{vw}\}} \left( i s_{5,5',5',6',6',7',7',8',8',9',9',10',10',13',13',11',11',12',12',14',14',1' \right. \\
&\quad \left. s_{1',2',2',2',2',2',2',2',2',2',2',2'}^\downarrow \gamma_4^\uparrow (i s_{4,5,5,4,4,4}) \gamma_5^\downarrow \right) P \\
&= X_{p_1}^{\{d_{vw}^2\}} \tilde{X}_{p_2}^{\{d_{vw}\}} (-s_{5,5',5',6',6',7',7',8',8',9',9',10',10',13',13',11',11',12',12',14',14',1' \\
&\quad s_{1',2',2',2',2',2',2',2',2',2',2',2'}) P \\
&= X_{p_1}^{\{d_{vw}^2\}} \tilde{X}_{p_2}^{\{d_{vw}\}} P. \tag{E.39}
\end{aligned}$$

Therefore,

$$X_{p_1}^{\{d_{vw}^2\}} \tilde{X}_{p_2}^{\{d_{vw}\}} 2^{-1} (1 + i s_{5,5'} \gamma_5^\downarrow \gamma_5^\uparrow) P = X_{p_1}^{\{d_{vw}^2\}} \tilde{X}_{p_2}^{\{d_{vw}\}} P. \tag{E.40}$$

Next, we show that

$$X_{p_1}^{\{d_{vw}^2\}} \tilde{X}_{p_2}^{\{d_{vw}\}} P = X_{p_1}^{\{d_{vw}^2\}} \tilde{X}_{p_2}^{\{d_{vw}\}} P. \tag{E.41}$$

One subtlety is that now  $X_{p_1}^{\{d_{vw}^2\}}$  commutes with  $\tilde{X}_{p_2}^{\{d_{vw}\}}$ , so that on the left-hand side of  $is_{2',2}\gamma_2^\uparrow\gamma_2^\downarrow$ , we can pull fermion bilinears from both  $\tilde{X}_{p_2}^{\{d_{vw}\}}$  and  $X_{p_1}^{\{d_{vw}^2\}}$ . We compute

$$\begin{aligned}
& X_{p_1}^{\{d_{vw}^2\}} \tilde{X}_{p_2}^{\{d_{vw}\}} (is_{2',2}\gamma_2^\uparrow\gamma_2^\downarrow)P \\
&= X_{p_1}^{\{d_{vw}^2\}} \tilde{X}_{p_2}^{\{d_{vw}\}} \left( is_{2',2}\gamma_2^\uparrow\gamma_2^\downarrow (is_{2',1'}\gamma_2^\uparrow\gamma_1^\uparrow) \right) P \\
&= X_{p_1}^{\{d_{vw}^2\}} \tilde{X}_{p_2}^{\{d_{vw}\}} (s_{2',2}s_{2',1'}\gamma_2^\downarrow\gamma_1^\uparrow)P \\
&= X_{p_1}^{\{d_{vw}^2\}} \tilde{X}_{p_2}^{\{d_{vw}\}} \left( s_{2',2}s_{2',1'}\gamma_2^\downarrow (is_{1',14'}\gamma_1^\uparrow\gamma_{14'}^\downarrow)\gamma_1^\uparrow \right) P \\
&= X_{p_1}^{\{d_{vw}^2\}} \tilde{X}_{p_2}^{\{d_{vw}\}} (-is_{2',2}s_{2',1'}s_{1',14'}\gamma_2^\downarrow\gamma_{14'}^\downarrow)P \\
&= X_{p_1}^{\{d_{vw}^2\}} \tilde{X}_{p_2}^{\{d_{vw}\}} \left( -is_{2',2}s_{2',1'}s_{1',14'}\gamma_2^\downarrow\gamma_{14'}^\downarrow (is_{14',12'}\gamma_{14'}^\downarrow\gamma_{12'}^\uparrow) \right) P \\
&= X_{p_1}^{\{d_{vw}^2\}} \tilde{X}_{p_2}^{\{d_{vw}\}} (s_{2',2}s_{2',1'}s_{1',14'}s_{14',12'}\gamma_2^\downarrow\gamma_{12'}^\uparrow)P \\
&= X_{p_1}^{\{d_{vw}^2\}} \tilde{X}_{p_2}^{\{d_{vw}\}} \left( s_{2',2}s_{2',1'}s_{1',14'}s_{14',12'}\gamma_2^\downarrow (is_{12',11'}\gamma_{12'}^\uparrow\gamma_{11'}^\uparrow)\gamma_{12'}^\uparrow \right) P \\
&= X_{p_1}^{\{d_{vw}^2\}} \tilde{X}_{p_2}^{\{d_{vw}\}} (-is_{2',2}s_{2',1'}s_{1',14'}s_{14',12'}s_{12',11'}\gamma_2^\downarrow\gamma_{11'}^\uparrow)P \\
&= X_{p_1}^{\{d_{vw}^2\}} \tilde{X}_{p_2}^{\{d_{vw}\}} \left( -is_{2',2}s_{2',1'}s_{1',14'}s_{14',12'}s_{12',11'}\gamma_2^\downarrow\gamma_{11'}^\uparrow (is_{11',13'}\gamma_{11'}^\uparrow\gamma_{13'}^\downarrow) \right) P \\
&= X_{p_1}^{\{d_{vw}^2\}} \tilde{X}_{p_2}^{\{d_{vw}\}} (s_{2',2}s_{2',1'}s_{1',14'}s_{14',12'}s_{12',11'}s_{11',13'}\gamma_2^\downarrow\gamma_{13'}^\downarrow)P \\
&= X_{p_1}^{\{d_{vw}^2\}} \tilde{X}_{p_2}^{\{d_{vw}\}} \left( s_{2',2}s_{2',1'}s_{1',14'}s_{14',12'}s_{12',11'}s_{11',13'}\gamma_2^\downarrow (is_{13',10'}\gamma_{13'}^\downarrow\gamma_{10'}^\uparrow)\gamma_{13'}^\downarrow \right) P \\
&= X_{p_1}^{\{d_{vw}^2\}} \tilde{X}_{p_2}^{\{d_{vw}\}} (-is_{2',2}s_{2',1'}s_{1',14'}s_{14',12'}s_{12',11'}s_{11',13'}s_{13',10'}\gamma_2^\downarrow\gamma_{10'}^\uparrow)P \\
&= X_{p_1}^{\{d_{vw}^2\}} \tilde{X}_{p_2}^{\{d_{vw}\}} \left( -is_{2',2}s_{2',1'}s_{1',14'}s_{14',12'}s_{12',11'}s_{11',13'}s_{13',10'}\gamma_2^\downarrow\gamma_{10'}^\uparrow \right. \\
&\quad \left. (is_{10',9'}\gamma_{10'}^\uparrow\gamma_{9'}^\uparrow) \right) P \\
&= X_{p_1}^{\{d_{vw}^2\}} \tilde{X}_{p_2}^{\{d_{vw}\}} (s_{2',2}s_{2',1'}s_{1',14'}s_{14',12'}s_{12',11'}s_{11',13'}s_{13',10'}s_{10',9'}\gamma_2^\downarrow\gamma_{9'}^\uparrow)P \\
&= X_{p_1}^{\{d_{vw}^2\}} \tilde{X}_{p_2}^{\{d_{vw}\}} \left( s_{2',2}s_{2',1'}s_{1',14'}s_{14',12'}s_{12',11'}s_{11',13'}s_{13',10'}s_{10',9'}\gamma_2^\downarrow \right. \\
&\quad \left. (is_{9',8'}\gamma_{9'}^\uparrow\gamma_{8'}^\downarrow)\gamma_{9'}^\uparrow \right) P \\
&= X_{p_1}^{\{d_{vw}^2\}} \tilde{X}_{p_2}^{\{d_{vw}\}} (-is_{2',2}s_{2',1'}s_{1',14'}s_{14',12'}s_{12',11'}s_{11',13'}s_{13',10'}s_{10',9'}s_{9',8'}\gamma_2^\downarrow\gamma_{8'}^\downarrow)P \\
&= X_{p_1}^{\{d_{vw}^2\}} \tilde{X}_{p_2}^{\{d_{vw}\}} \left( -is_{2',2}s_{2',1'}s_{1',14'}s_{14',12'}s_{12',11'}s_{11',13'}s_{13',10'}s_{10',9'}s_{9',8'}\gamma_2^\downarrow\gamma_{8'}^\downarrow \right.
\end{aligned}$$

$$\begin{aligned}
& \left. (is_{8',7'}\gamma_8^\downarrow\gamma_7^\downarrow) \right) P \\
&= X_{p_1}^{\{d_{vw}^2\}} \tilde{X}_{p_2}^{\{d_{vw}\}} (s_{2',2}s_{2',1'}s_{1',14'}s_{14',12'}s_{12',11'}s_{11',13'}s_{13',10'}s_{10',9'}s_{9',8'}s_{8',7'}\gamma_2^\downarrow\gamma_7^\downarrow) P \\
&= X_{p_1}^{\{d_{vw}^2\}} \tilde{X}_{p_2}^{\{d_{vw}\}} \left( s_{2',2}s_{2',1'}s_{1',14'}s_{14',12'}s_{12',11'}s_{11',13'}s_{13',10'}s_{10',9'}s_{9',8'}s_{8',7'}\gamma_2^\downarrow \right. \\
&\quad \left. (is_{7',6'}\gamma_7^\downarrow\gamma_6^\uparrow)\gamma_7^\downarrow \right) P \\
&= X_{p_1}^{\{d_{vw}^2\}} \tilde{X}_{p_2}^{\{d_{vw}\}} (-is_{2',2}s_{2',1'}s_{1',14'}s_{14',12'}s_{12',11'}s_{11',13'}s_{13',10'}s_{10',9'}s_{9',8'}s_{8',7'} \\
&\quad s_{7',6'}\gamma_2^\downarrow\gamma_6^\uparrow) P \\
&= X_{p_1}^{\{d_{vw}^2\}} \tilde{X}_{p_2}^{\{d_{vw}\}} \left( -is_{2',2}s_{2',1'}s_{1',14'}s_{14',12'}s_{12',11'}s_{11',13'}s_{13',10'}s_{10',9'}s_{9',8'}s_{8',7'} \right. \\
&\quad \left. s_{7',6'}\gamma_2^\downarrow\gamma_6^\uparrow (is_{6',5'}\gamma_6^\uparrow\gamma_5^\uparrow) \right) P \\
&= X_{p_1}^{\{d_{vw}^2\}} \tilde{X}_{p_2}^{\{d_{vw}\}} (s_{2',2}s_{2',1'}s_{1',14'}s_{14',12'}s_{12',11'}s_{11',13'}s_{13',10'}s_{10',9'}s_{9',8'}s_{8',7'}s_{7',6'} \\
&\quad s_{6',5'}\gamma_2^\downarrow\gamma_5^\uparrow) P \\
&= X_{p_1}^{\{d_{vw}^2\}} \tilde{X}_{p_2}^{\{d_{vw}\}} \left( s_{2',2}s_{2',1'}s_{1',14'}s_{14',12'}s_{12',11'}s_{11',13'}s_{13',10'}s_{10',9'}s_{9',8'}s_{8',7'}s_{7',6'} \right. \\
&\quad \left. s_{6',5'}\gamma_2^\downarrow (is_{5',4'}\gamma_5^\uparrow\gamma_4^\downarrow)\gamma_5^\uparrow \right) P \\
&= X_{p_1}^{\{d_{vw}^2\}} \tilde{X}_{p_2}^{\{d_{vw}\}} (-is_{2',2}s_{2',1'}s_{1',14'}s_{14',12'}s_{12',11'}s_{11',13'}s_{13',10'}s_{10',9'}s_{9',8'}s_{8',7'} \\
&\quad s_{7',6'}s_{6',5'}s_{5',4'}\gamma_2^\downarrow\gamma_4^\downarrow) P \\
&= X_{p_1}^{\{d_{vw}^2\}} \tilde{X}_{p_2}^{\{d_{vw}\}} \left( -is_{2',2}s_{2',1'}s_{1',14'}s_{14',12'}s_{12',11'}s_{11',13'}s_{13',10'}s_{10',9'}s_{9',8'}s_{8',7'} \right. \\
&\quad \left. s_{7',6'}s_{6',5'}s_{5',4'}\gamma_2^\downarrow\gamma_4^\downarrow (is_{4,3}\gamma_4^\downarrow\gamma_3^\downarrow) \right) P \\
&= X_{p_1}^{\{d_{vw}^2\}} \tilde{X}_{p_2}^{\{d_{vw}\}} (s_{2',2}s_{2',1'}s_{1',14'}s_{14',12'}s_{12',11'}s_{11',13'}s_{13',10'}s_{10',9'}s_{9',8'}s_{8',7'}s_{7',6'} \\
&\quad s_{6',5'}s_{5',4'}s_{4,3}\gamma_2^\downarrow\gamma_3^\downarrow) P \\
&= X_{p_1}^{\{d_{vw}^2\}} \tilde{X}_{p_2}^{\{d_{vw}\}} (s_{2',2}s_{2',1'}s_{1',14'}s_{14',12'}s_{12',11'}s_{11',13'}s_{13',10'}s_{10',9'}s_{9',8'}s_{8',7'}s_{7',6'} \\
&\quad s_{6',5'}s_{5',4'}s_{4,3}\gamma_2^\downarrow (is_{3,2'}\gamma_3^\downarrow\gamma_2^\uparrow)\gamma_3^\downarrow) P \\
&= X_{p_1}^{\{d_{vw}^2\}} \tilde{X}_{p_2}^{\{d_{vw}\}} (-is_{2',2}s_{2',1'}s_{1',14'}s_{14',12'}s_{12',11'}s_{11',13'}s_{13',10'}s_{10',9'}s_{9',8'}s_{8',7'}s_{7',6'} \\
&\quad s_{6',5'}s_{5',4'}s_{4,3}s_{3,2'}\gamma_2^\downarrow\gamma_2^\uparrow) P \\
&= X_{p_1}^{\{d_{vw}^2\}} \tilde{X}_{p_2}^{\{d_{vw}\}} (is_{2',2}\gamma_2^\downarrow\gamma_2^\uparrow) P \\
&= X_{p_1}^{\{d_{vw}^2\}} \tilde{X}_{p_2}^{\{d_{vw}\}} (-is_{2',2}\gamma_2^\uparrow\gamma_2^\downarrow) P. \tag{E.42}
\end{aligned}$$

Hence

$$X_{p_1}^{\{d_{vw}^2\}} \tilde{X}_{p_2}^{\{d_{vw}\}} (is_{2',2} \gamma_2^\uparrow \gamma_2^\downarrow) P = 0, \quad (\text{E.43})$$

which establishes Eq. (E.41). Eqs. (E.40) and (E.41) together implies Eq. (E.36), and we conclude that

$$X_{p_2}^{\{d_{vw}^1\}} X_{p_1}^{\{d_{vw}\}} P = X_{p_1}^{\{d_{vw}^2\}} X_{p_2}^{\{d_{vw}\}} P. \quad (\text{E.44})$$

*Appendix F*

## QUANTIZATION OF THE GRAVITATIONAL CHERN-SIMONS ACTION

In this appendix we discuss the quantization of the coefficient of the gravitational Chern-Simons action. For all topological facts used here, the reader may consult [99]. Let  $X$  be an oriented 3-manifold whose tangent bundle is equipped with a connection  $\omega$ . We can take  $\omega$  to be a Levi-Civita connection for some Riemannian metric on  $X$ , so  $\omega$  can be thought of as an  $SO(3)$  connection.

We define the gravitational Chern-Simons action to be

$$S_{grav}(\omega) = \frac{\kappa}{192\pi} \int_M \text{Tr}(\omega d\omega + \frac{2}{3}\omega^3).$$

The choice of the normalization coefficient will be explained shortly. This formula is only schematic, since  $\omega$  is not a globally-defined 1-form, in general. A more precise definition requires choosing a compact oriented 4-manifold  $M$  whose boundary is  $X$  (this is always possible, since  $\Omega_3^{SO}(pt) = 0$ ). We also extend  $\omega$  to  $X$  and define

$$S_{grav}^X(\omega) = \frac{k}{192\pi} \int_X \text{Tr} R \wedge R.$$

We need to ensure that  $\exp(iS_{grav}^X(\omega))$  does not depend on the choice of  $X$  or the way  $\omega$  is extended from  $M$  to  $X$ . If we choose another  $X'$  with the same boundary  $M$ , the difference between the two ways of defining the gravitational Chern-Simons action is

$$\frac{k}{192\pi} \int_{X' \cup \bar{X}} \text{Tr} R(\omega) \wedge R(\omega),$$

where  $\bar{X}$  is  $X$  with orientation reversed, and  $R(\omega)$  is the curvature 2-form of  $\omega$ . This expression can be rewritten as

$$\frac{\pi k}{24} p_1(X' \cup \bar{X}) = \frac{\pi k}{8} \sigma(X' \cup \bar{X}). \quad (\text{F.1})$$

Here  $p_1(Y)$  denotes the first Pontryagin number of a closed oriented 4-manifold  $Y$ ,  $\sigma(Y)$  denotes its signature, and we used the Hirzebruch signature theorem  $p_1(Y) = 3\sigma(Y)$ . Since the signature is an integer, we conclude that  $\exp(iS_{grav}(\omega))$  is well-defined provided  $k$  is an integer multiple of 16. This determines the quantization of the thermal Hall conductivity for  $d = 3$  bosonic SPTs with time-reversal symmetry.

Now suppose  $M$  is given a spin structure. We can exploit it to define  $\exp(iS_{grav})$  for arbitrary integral  $k$ . We merely require the spin structure to extend to  $X$ . It is always possible to find such an  $X$ , since  $\Omega_3^{Spin}(pt) = 0$ . The difference between  $S_{grav}^X(\omega)$  and  $S_{grav}^{X'}(\omega)$  is again given by (F.1). Since now  $X' \cup \bar{X}$  is a closed spin 4-manifold, we can appeal to the Rohlin theorem which says that the signature of a closed spin 4-manifold is divisible by 16, and conclude that  $\exp(iS_{grav}(\omega))$  is well-defined if  $k$  is integral. This determines the quantization of the thermal Hall conductivity for  $d = 3$  fermionic SPTs with time-reversal symmetry. Note that in the fermionic case the quantum of conductivity is 16 times smaller than in the bosonic case.

## BIBLIOGRAPHY

- [1] D. C. Tsui, H. L. Stormer, and A. C. Gossard. Two-dimensional magneto-transport in the extreme quantum limit. *Phys. Rev. Lett.*, 48:1559–1562, May 1982. doi: 10.1103/PhysRevLett.48.1559. URL <https://link.aps.org/doi/10.1103/PhysRevLett.48.1559>.
- [2] R. B. Laughlin. Anomalous quantum hall effect: An incompressible quantum fluid with fractionally charged excitations. *Phys. Rev. Lett.*, 50:1395–1398, May 1983. doi: 10.1103/PhysRevLett.50.1395. URL <https://link.aps.org/doi/10.1103/PhysRevLett.50.1395>.
- [3] Xie Chen, Zheng-Cheng Gu, and Xiao-Gang Wen. Local unitary transformation, long-range quantum entanglement, wave function renormalization, and topological order. *Phys. Rev. B*, 82:155138, Oct 2010. doi: 10.1103/PhysRevB.82.155138. URL <https://link.aps.org/doi/10.1103/PhysRevB.82.155138>.
- [4] Xiao-Gang Wen. Quantum orders and symmetric spin liquids. *Phys. Rev. B*, 65:165113, Apr 2002. doi: 10.1103/PhysRevB.65.165113. URL <https://link.aps.org/doi/10.1103/PhysRevB.65.165113>.
- [5] Andrew M. Essin and Michael Hermele. Classifying fractionalization: Symmetry classification of gapped  $F_2$  spin liquids in two dimensions. *Phys. Rev. B*, 87:104406, Mar 2013. doi: 10.1103/PhysRevB.87.104406. URL <https://link.aps.org/doi/10.1103/PhysRevB.87.104406>.
- [6] Andrej Mesaros and Ying Ran. Classification of symmetry enriched topological phases with exactly solvable models. *Phys. Rev. B*, 87:155115, Apr 2013. doi: 10.1103/PhysRevB.87.155115. URL <https://link.aps.org/doi/10.1103/PhysRevB.87.155115>.
- [7] Yuan-Ming Lu and Ashvin Vishwanath. Classification and properties of symmetry-enriched topological phases: Chern-simons approach with applications to  $Z_2$  spin liquids. *Phys. Rev. B*, 93:155121, Apr 2016. doi: 10.1103/PhysRevB.93.155121. URL <https://link.aps.org/doi/10.1103/PhysRevB.93.155121>.
- [8] Maissam Barkeshli, Parsa Bonderson, Meng Cheng, and Zhenghan Wang. Symmetry, Defects, and Gauging of Topological Phases. *arXiv e-prints*, art. arXiv:1410.4540, Oct 2014.
- [9] Lukasz Fidkowski, Xie Chen, and Ashvin Vishwanath. Non-abelian topological order on the surface of a 3d topological superconductor from an exactly solved model. *Phys. Rev. X*, 3:041016, Nov 2013. doi: 10.

- 1103/PhysRevX.3.041016. URL <https://link.aps.org/doi/10.1103/PhysRevX.3.041016>.
- [10] Zheng-Cheng Gu and Xiao-Gang Wen. Tensor-entanglement-filtering renormalization approach and symmetry-protected topological order. *Phys. Rev. B*, 80:155131, Oct 2009. doi: 10.1103/PhysRevB.80.155131. URL <https://link.aps.org/doi/10.1103/PhysRevB.80.155131>.
- [11] Ashvin Vishwanath and T. Senthil. Physics of three-dimensional bosonic topological insulators: Surface-deconfined criticality and quantized magnetoelectric effect. *Phys. Rev. X*, 3:011016, Feb 2013. doi: 10.1103/PhysRevX.3.011016. URL <https://link.aps.org/doi/10.1103/PhysRevX.3.011016>.
- [12] Chong Wang and T. Senthil. Boson topological insulators: A window into highly entangled quantum phases. *Phys. Rev. B*, 87:235122, Jun 2013. doi: 10.1103/PhysRevB.87.235122. URL <https://link.aps.org/doi/10.1103/PhysRevB.87.235122>.
- [13] Max A. Metlitski, C. L. Kane, and Matthew P. A. Fisher. Bosonic topological insulator in three dimensions and the statistical witten effect. *Phys. Rev. B*, 88:035131, Jul 2013. doi: 10.1103/PhysRevB.88.035131. URL <https://link.aps.org/doi/10.1103/PhysRevB.88.035131>.
- [14] F. J. Burnell, Xie Chen, Lukasz Fidkowski, and Ashvin Vishwanath. Exactly soluble model of a three-dimensional symmetry-protected topological phase of bosons with surface topological order. *Phys. Rev. B*, 90:245122, Dec 2014. doi: 10.1103/PhysRevB.90.245122. URL <https://link.aps.org/doi/10.1103/PhysRevB.90.245122>.
- [15] Chong Wang, Andrew C. Potter, and T. Senthil. Gapped symmetry preserving surface state for the electron topological insulator. *Phys. Rev. B*, 88:115137, Sep 2013. doi: 10.1103/PhysRevB.88.115137. URL <https://link.aps.org/doi/10.1103/PhysRevB.88.115137>.
- [16] Chong Wang, Andrew C. Potter, and T. Senthil. Classification of interacting electronic topological insulators in three dimensions. *Science*, 343(6171): 629–631, 2014. ISSN 0036-8075. doi: 10.1126/science.1243326. URL <http://science.sciencemag.org/content/343/6171/629>.
- [17] Xie Chen, Lukasz Fidkowski, and Ashvin Vishwanath. Symmetry enforced non-abelian topological order at the surface of a topological insulator. *Phys. Rev. B*, 89:165132, Apr 2014. doi: 10.1103/PhysRevB.89.165132. URL <https://link.aps.org/doi/10.1103/PhysRevB.89.165132>.
- [18] Max A. Metlitski, C. L. Kane, and Matthew P. A. Fisher. Symmetry-respecting topologically ordered surface phase of three-dimensional electron topological insulators. *Phys. Rev. B*, 92:125111, Sep 2015. doi: 10.1103/PhysRevB.

- 92.125111. URL <https://link.aps.org/doi/10.1103/PhysRevB.92.125111>.
- [19] Anton Kapustin and Ryan Thorngren. Anomalous discrete symmetries in three dimensions and group cohomology. *Phys. Rev. Lett.*, 112:231602, Jun 2014. doi: 10.1103/PhysRevLett.112.231602. URL <https://link.aps.org/doi/10.1103/PhysRevLett.112.231602>.
- [20] Anton Kapustin and Ryan Thorngren. Anomalies of discrete symmetries in various dimensions and group cohomology. *arXiv e-prints*, art. arXiv:1404.3230, Apr 2014.
- [21] Gil Young Cho, Jeffrey C. Y. Teo, and Shinsei Ryu. Conflicting symmetries in topologically ordered surface states of three-dimensional bosonic symmetry protected topological phases. *Phys. Rev. B*, 89:235103, Jun 2014. doi: 10.1103/PhysRevB.89.235103. URL <https://link.aps.org/doi/10.1103/PhysRevB.89.235103>.
- [22] Xie Chen, F. J. Burnell, Ashvin Vishwanath, and Lukasz Fidkowski. Anomalous symmetry fractionalization and surface topological order. *Phys. Rev. X*, 5:041013, Oct 2015. doi: 10.1103/PhysRevX.5.041013. URL <https://link.aps.org/doi/10.1103/PhysRevX.5.041013>.
- [23] Juven C. Wang, Luiz H. Santos, and Xiao-Gang Wen. Bosonic anomalies, induced fractional quantum numbers, and degenerate zero modes: The anomalous edge physics of symmetry-protected topological states. *Phys. Rev. B*, 91:195134, May 2015. doi: 10.1103/PhysRevB.91.195134. URL <https://link.aps.org/doi/10.1103/PhysRevB.91.195134>.
- [24] C. L. Kane and E. J. Mele.  $z_2$  topological order and the quantum spin hall effect. *Phys. Rev. Lett.*, 95(14):146802–, September 2005. URL <http://link.aps.org/doi/10.1103/PhysRevLett.95.146802>.
- [25] Liang Fu, C. L. Kane, and E. J. Mele. Topological insulators in three dimensions. *Phys. Rev. Lett.*, 98(10):106803–, March 2007. URL <http://link.aps.org/doi/10.1103/PhysRevLett.98.106803>.
- [26] J. E. Moore and L. Balents. Topological invariants of time-reversal-invariant band structures. *Phys. Rev. B*, 75(12):121306–, March 2007. URL <http://link.aps.org/doi/10.1103/PhysRevB.75.121306>.
- [27] Rahul Roy. Topological phases and the quantum spin hall effect in three dimensions. *Phys. Rev. B*, 79(19):195322–, May 2009. URL <http://link.aps.org/doi/10.1103/PhysRevB.79.195322>.
- [28] M. Z. Hasan and C. L. Kane. Colloquium: Topological insulators. *Rev. Mod. Phys.*, 82:3045–3067, Nov 2010. doi: 10.1103/RevModPhys.82.3045. URL <https://link.aps.org/doi/10.1103/RevModPhys.82.3045>.

- [29] M. Zahid Hasan and Joel E. Moore. Three-dimensional topological insulators. *Annual Review of Condensed Matter Physics*, 2(1):55–78, 2011. doi: 10.1146/annurev-conmatphys-062910-140432. URL <https://doi.org/10.1146/annurev-conmatphys-062910-140432>.
- [30] Rahul Roy. Topological superfluids with time reversal symmetry. *arXiv e-prints*, art. arXiv:0803.2868, Mar 2008.
- [31] Xiao-Liang Qi, Taylor L. Hughes, S. Raghu, and Shou-Cheng Zhang. Time-reversal-invariant topological superconductors and superfluids in two and three dimensions. *Phys. Rev. Lett.*, 102:187001, May 2009. doi: 10.1103/PhysRevLett.102.187001. URL <http://link.aps.org/doi/10.1103/PhysRevLett.102.187001>.
- [32] Xiao-Liang Qi and Shou-Cheng Zhang. Topological insulators and superconductors. *Rev. Mod. Phys.*, 83:1057–1110, Oct 2011. doi: 10.1103/RevModPhys.83.1057. URL <https://link.aps.org/doi/10.1103/RevModPhys.83.1057>.
- [33] Shinsei Ryu, Andreas P Schnyder, Akira Furusaki, and Andreas W W Ludwig. Topological insulators and superconductors: tenfold way and dimensional hierarchy. *New Journal of Physics*, 12(6):065010, jun 2010. doi: 10.1088/1367-2630/12/6/065010. URL <https://doi.org/10.1088/1367-2630/12/6/065010>.
- [34] Alexei Kitaev. Periodic table for topological insulators and superconductors. *AIP Conference Proceedings*, 1134(1):22–30, 2009. doi: 10.1063/1.3149495. URL <http://link.aip.org/link/?APC/1134/22/1>.
- [35] Michael Atiyah. Topological quantum field theories. *Publications Mathématiques de l'Institut des Hautes Études Scientifiques*, 68(1):175–186, Jan 1988. ISSN 1618-1913. doi: 10.1007/BF02698547. URL <https://doi.org/10.1007/BF02698547>.
- [36] Edward Witten. Topological quantum field theory. *Communications in Mathematical Physics*, 117(3):353–386, Sep 1988. ISSN 1432-0916. doi: 10.1007/BF01223371. URL <https://doi.org/10.1007/BF01223371>.
- [37] Edward Witten. Quantum field theory and the jones polynomial. *Communications in Mathematical Physics*, 121(3):351–399, Sep 1989. ISSN 1432-0916. doi: 10.1007/BF01217730. URL <https://doi.org/10.1007/BF01217730>.
- [38] Turaev Vladimir G. Quantum invariants of knots and 3-manifolds. 2019-01-26T22:29:41.544+01:00 2016 PB - De Gruyter CY - Berlin, Boston. doi: 10.1515/9783110435221. URL <https://www.degruyter.com/view/product/461906>.

- [39] Eric Rowell, Richard Stong, and Zhenghan Wang. On classification of modular tensor categories. *Communications in Mathematical Physics*, 292(2):343–389, Dec 2009. ISSN 1432-0916. doi: 10.1007/s00220-009-0908-z. URL <https://doi.org/10.1007/s00220-009-0908-z>.
- [40] Michael A. Levin and Xiao-Gang Wen. String-net condensation: A physical mechanism for topological phases. *Phys. Rev. B*, 71:045110, Jan 2005. doi: 10.1103/PhysRevB.71.045110. URL <https://link.aps.org/doi/10.1103/PhysRevB.71.045110>.
- [41] Xie Chen, Zheng-Cheng Gu, Zheng-Xin Liu, and Xiao-Gang Wen. Symmetry protected topological orders and the group cohomology of their symmetry group. *Phys. Rev. B*, 87:155114, Apr 2013. doi: 10.1103/PhysRevB.87.155114. URL <http://link.aps.org/doi/10.1103/PhysRevB.87.155114>.
- [42] Zheng-Cheng Gu and Xiao-Gang Wen. Symmetry-protected topological orders for interacting fermions: Fermionic topological nonlinear  $\sigma$  models and a special group supercohomology theory. *Phys. Rev. B*, 90:115141, Sep 2014. doi: 10.1103/PhysRevB.90.115141. URL <https://link.aps.org/doi/10.1103/PhysRevB.90.115141>.
- [43] F. Verstraete, V. Murg, and J.I. Cirac. Matrix product states, projected entangled pair states, and variational renormalization group methods for quantum spin systems. *Advances in Physics*, 57(2):143–224, 2008. doi: 10.1080/14789940801912366. URL <https://doi.org/10.1080/14789940801912366>.
- [44] Andrew C. Potter and Ashvin Vishwanath. Protection of topological order by symmetry and many-body localization. *arXiv e-prints*, art. arXiv:1506.00592, Jun 2015.
- [45] Kevin Walker and Zhenghan Wang. (3+1)-tqfts and topological insulators. *Frontiers of Physics*, 7(2):150–159, Apr 2012. ISSN 2095-0470. doi: 10.1007/s11467-011-0194-z. URL <https://doi.org/10.1007/s11467-011-0194-z>.
- [46] Xie Chen, Yuan-Ming Lu, and Ashvin Vishwanath. Symmetry-protected topological phases from decorated domain walls. *Nat Commun*, 5, 03 2014. URL <http://dx.doi.org/10.1038/ncomms4507>.
- [47] C. W. von Keyserlingk, F. J. Burnell, and S. H. Simon. Three-dimensional topological lattice models with surface anyons. *Phys. Rev. B*, 87:045107, Jan 2013. doi: 10.1103/PhysRevB.87.045107. URL <https://link.aps.org/doi/10.1103/PhysRevB.87.045107>.
- [48] Nicolas Tarantino and Lukasz Fidkowski. Discrete spin structures and commuting projector models for two-dimensional fermionic symmetry-protected topological phases. *Phys. Rev. B*, 94:115115, Sep 2016. doi: 10.1103/PhysRevB.

- 94.115115. URL <https://link.aps.org/doi/10.1103/PhysRevB.94.115115>.
- [49] Brayden Ware, Jun Ho Son, Meng Cheng, Ryan V. Mishmash, Jason Alicea, and Bela Bauer. Ising anyons in frustration-free majorana-dimer models. *Phys. Rev. B*, 94:115127, Sep 2016. doi: 10.1103/PhysRevB.94.115127. URL <https://link.aps.org/doi/10.1103/PhysRevB.94.115127>.
- [50] Qing-Rui Wang and Zheng-Cheng Gu. Construction and classification of symmetry protected topological phases in interacting fermion systems. *arXiv e-prints*, art. arXiv:1811.00536, Nov 2018.
- [51] F. D. M. Haldane and E. H. Rezayi. Periodic Laughlin-Jastrow wave functions for the fractional quantized Hall effect. *Phys. Rev. B*, 31:2529–2531, Feb 1985. doi: 10.1103/PhysRevB.31.2529. URL <https://link.aps.org/doi/10.1103/PhysRevB.31.2529>.
- [52] X. G. Wen. Vacuum degeneracy of chiral spin states in compactified space. *Phys. Rev. B*, 40:7387–7390, Oct 1989. doi: 10.1103/PhysRevB.40.7387. URL <https://link.aps.org/doi/10.1103/PhysRevB.40.7387>.
- [53] X. G. Wen and Q. Niu. Ground-state degeneracy of the fractional quantum Hall states in the presence of a random potential and on high-genus Riemann surfaces. *Phys. Rev. B*, 41:9377–9396, May 1990. doi: 10.1103/PhysRevB.41.9377. URL <https://link.aps.org/doi/10.1103/PhysRevB.41.9377>.
- [54] X. G. Wen. Gapless boundary excitations in the quantum Hall states and in the chiral spin states. *Phys. Rev. B*, 43:11025–11036, May 1991. doi: 10.1103/PhysRevB.43.11025. URL <https://link.aps.org/doi/10.1103/PhysRevB.43.11025>.
- [55] XIAO-GANG WEN. Theory of the edge states in fractional quantum Hall effects. *International Journal of Modern Physics B*, 06(10):1711–1762, 1992. doi: 10.1142/S0217979292000840. URL <https://doi.org/10.1142/S0217979292000840>.
- [56] Frank Wilczek. Magnetic flux, angular momentum, and statistics. *Phys. Rev. Lett.*, 48:1144–1146, Apr 1982. doi: 10.1103/PhysRevLett.48.1144. URL <https://link.aps.org/doi/10.1103/PhysRevLett.48.1144>.
- [57] Frank Wilczek. Quantum mechanics of fractional-spin particles. *Phys. Rev. Lett.*, 49:957–959, Oct 1982. doi: 10.1103/PhysRevLett.49.957. URL <https://link.aps.org/doi/10.1103/PhysRevLett.49.957>.
- [58] Daniel Arovas, J. R. Schrieffer, and Frank Wilczek. Fractional statistics and the quantum Hall effect. *Phys. Rev. Lett.*, 53:722–723, Aug 1984. doi: 10.1103/PhysRevLett.53.722. URL <https://link.aps.org/doi/10.1103/PhysRevLett.53.722>.

- [59] Frank Wilczek and A. Zee. Appearance of gauge structure in simple dynamical systems. *Phys. Rev. Lett.*, 52:2111–2114, Jun 1984. doi: 10.1103/PhysRevLett.52.2111. URL <https://link.aps.org/doi/10.1103/PhysRevLett.52.2111>.
- [60] X. G. WEN. Topological orders in rigid states. *International Journal of Modern Physics B*, 04(02):239–271, 1990. doi: 10.1142/S0217979290000139. URL <https://doi.org/10.1142/S0217979290000139>.
- [61] ESKO KESKI-VAKKURI and XIAO-GANG WEN. The ground state structure and modular transformations of fractional quantum hall states on a torus. *International Journal of Modern Physics B*, 07(25):4227–4259, 1993. doi: 10.1142/S0217979293003644. URL <https://doi.org/10.1142/S0217979293003644>.
- [62] F A Bais and J C Romers. The modular S-matrix as order parameter for topological phase transitions. *New Journal of Physics*, 14(3):035024, mar 2012. doi: 10.1088/1367-2630/14/3/035024. URL <https://doi.org/10.1088%2F1367-2630%2F14%2F3%2F035024>.
- [63] Robbert Dijkgraaf and Edward Witten. Topological gauge theories and group cohomology. *Communications in Mathematical Physics*, 129(2):393–429, Apr 1990. ISSN 1432-0916. doi: 10.1007/BF02096988. URL <https://doi.org/10.1007/BF02096988>.
- [64] Yidun Wan, Juven C. Wang, and Huan He. Twisted gauge theory model of topological phases in three dimensions. *Phys. Rev. B*, 92:045101, Jul 2015. doi: 10.1103/PhysRevB.92.045101. URL <https://link.aps.org/doi/10.1103/PhysRevB.92.045101>.
- [65] Shenghan Jiang, Andrej Mesaros, and Ying Ran. Generalized modular transformations in  $(3 + 1)$ D topologically ordered phases and triple linking invariant of loop braiding. *Phys. Rev. X*, 4:031048, Sep 2014. doi: 10.1103/PhysRevX.4.031048. URL <https://link.aps.org/doi/10.1103/PhysRevX.4.031048>.
- [66] Chenjie Wang and Michael Levin. Braiding statistics of loop excitations in three dimensions. *Phys. Rev. Lett.*, 113:080403, Aug 2014. doi: 10.1103/PhysRevLett.113.080403. URL <https://link.aps.org/doi/10.1103/PhysRevLett.113.080403>.
- [67] Sergio Doplicher and John E. Roberts. A new duality theory for compact groups. *Inventiones mathematicae*, 98(1):157–218, Feb 1989. ISSN 1432-1297. doi: 10.1007/BF01388849. URL <https://doi.org/10.1007/BF01388849>.
- [68] Michael Levin and Zheng-Cheng Gu. Braiding statistics approach to symmetry-protected topological phases. *Phys. Rev. B*, 86:115109, Sep 2012.

- doi: 10.1103/PhysRevB.86.115109. URL <https://link.aps.org/doi/10.1103/PhysRevB.86.115109>.
- [69] V. Kalmeyer and R. B. Laughlin. Equivalence of the resonating-valence-bond and fractional quantum hall states. *Phys. Rev. Lett.*, 59:2095–2098, Nov 1987. doi: 10.1103/PhysRevLett.59.2095. URL <https://link.aps.org/doi/10.1103/PhysRevLett.59.2095>.
- [70] G. 't Hooft. *Naturalness, Chiral Symmetry, and Spontaneous Chiral Symmetry Breaking*, pages 135–157. Springer US, Boston, MA, 1980. ISBN 978-1-4684-7571-5. doi: 10.1007/978-1-4684-7571-5\_9. URL [https://doi.org/10.1007/978-1-4684-7571-5\\_9](https://doi.org/10.1007/978-1-4684-7571-5_9).
- [71] Chenjie Wang, Chien-Hung Lin, and Michael Levin. Bulk-boundary correspondence for three-dimensional symmetry-protected topological phases. *Phys. Rev. X*, 6:021015, May 2016. doi: 10.1103/PhysRevX.6.021015. URL <https://link.aps.org/doi/10.1103/PhysRevX.6.021015>.
- [72] Daisuke Tambara and Shigeru Yamagami. Tensor categories with fusion rules of self-duality for finite abelian groups. *Journal of Algebra*, 209(2): 692 – 707, 1998. ISSN 0021-8693. doi: <https://doi.org/10.1006/jabr.1998.7558>. URL <http://www.sciencedirect.com/science/article/pii/S0021869398975585>.
- [73] Yi Zhang, Tarun Grover, Ari Turner, Masaki Oshikawa, and Ashvin Vishwanath. Quasiparticle statistics and braiding from ground-state entanglement. *Phys. Rev. B*, 85:235151, Jun 2012. doi: 10.1103/PhysRevB.85.235151. URL <https://link.aps.org/doi/10.1103/PhysRevB.85.235151>.
- [74] L. Cincio and G. Vidal. Characterizing topological order by studying the ground states on an infinite cylinder. *Phys. Rev. Lett.*, 110:067208, Feb 2013. doi: 10.1103/PhysRevLett.110.067208. URL <https://link.aps.org/doi/10.1103/PhysRevLett.110.067208>.
- [75] Huan He, Heidar Moradi, and Xiao-Gang Wen. Modular matrices as topological order parameter by a gauge-symmetry-preserved tensor renormalization approach. *Phys. Rev. B*, 90:205114, Nov 2014. doi: 10.1103/PhysRevB.90.205114. URL <https://link.aps.org/doi/10.1103/PhysRevB.90.205114>.
- [76] Fangzhou Liu, Zhenghan Wang, Yi-Zhuang You, and Xiao-Gang Wen. Modular transformations and topological orders in two dimensions. *arXiv e-prints*, art. arXiv:1303.0829, March 2013.
- [77] Yuting Hu, Yidun Wan, and Yong-Shi Wu. Twisted quantum double model of topological phases in two dimensions. *Phys. Rev. B*, 87:125114, Mar 2013. doi: 10.1103/PhysRevB.87.125114. URL <https://link.aps.org/doi/10.1103/PhysRevB.87.125114>.

- [78] Heidar Moradi and Xiao-Gang Wen. Universal topological data for gapped quantum liquids in three dimensions and fusion algebra for non-abelian string excitations. *Phys. Rev. B*, 91:075114, Feb 2015. doi: 10.1103/PhysRevB.91.075114. URL <https://link.aps.org/doi/10.1103/PhysRevB.91.075114>.
- [79] Juven C. Wang and Xiao-Gang Wen. Non-abelian string and particle braiding in topological order: Modular  $SL(3, \mathbb{Z})$  representation and  $(3 + 1)$ -dimensional twisted gauge theory. *Phys. Rev. B*, 91:035134, Jan 2015. doi: 10.1103/PhysRevB.91.035134. URL <https://link.aps.org/doi/10.1103/PhysRevB.91.035134>.
- [80] Andreas P. Schnyder, Shinsei Ryu, Akira Furusaki, and Andreas W. W. Ludwig. Classification of topological insulators and superconductors in three spatial dimensions. *Phys. Rev. B*, 78(19):195125–, November 2008. URL <http://link.aps.org/doi/10.1103/PhysRevB.78.195125>.
- [81] Xie Chen, Zheng-Cheng Gu, Zheng-Xin Liu, and Xiao-Gang Wen. Symmetry-protected topological orders in interacting bosonic systems. *Science*, 338(6114):1604–1606, 2012. doi: 10.1126/science.1227224.
- [82] Zheng-Cheng Gu and Xiao-Gang Wen. Symmetry-protected topological orders for interacting fermions: Fermionic topological nonlinear  $\sigma$  models and a special group supercohomology theory. *Phys. Rev. B*, 90:115141, Sep 2014. doi: 10.1103/PhysRevB.90.115141. URL <http://link.aps.org/doi/10.1103/PhysRevB.90.115141>.
- [83] Qing-Rui Wang and Zheng-Cheng Gu. Towards a complete classification of fermionic symmetry protected topological phases in 3D and a general group supercohomology theory. *arXiv e-prints*, art. arXiv:1703.10937, Mar 2017.
- [84] Shinsei Ryu, Andreas P Schnyder, Akira Furusaki, and Andreas W W Ludwig. Topological insulators and superconductors: tenfold way and dimensional hierarchy. *New Journal of Physics*, 12(6):065010, jun 2010. doi: 10.1088/1367-2630/12/6/065010. URL <https://doi.org/10.1088/1367-2630/12/6/065010>.
- [85] Lukasz Fidkowski and Alexei Kitaev. Topological phases of fermions in one dimension. *Phys. Rev. B*, 83:075103, Feb 2011. doi: 10.1103/PhysRevB.83.075103. URL <https://link.aps.org/doi/10.1103/PhysRevB.83.075103>.
- [86] Lukasz Fidkowski, Xie Chen, and Ashvin Vishwanath. Non-abelian topological order on the surface of a 3d topological superconductor from an exactly solved model. *Phys. Rev. X*, 3:041016, Nov 2013. doi: 10.1103/PhysRevX.3.041016. URL <https://link.aps.org/doi/10.1103/PhysRevX.3.041016>.

- [87] Chong Wang and T. Senthil. Interacting fermionic topological insulators/superconductors in three dimensions. *Phys. Rev. B*, 89:195124, May 2014. doi: 10.1103/PhysRevB.89.195124. URL <https://link.aps.org/doi/10.1103/PhysRevB.89.195124>.
- [88] Zheng-Cheng Gu and Michael Levin. Effect of interactions on two-dimensional fermionic symmetry-protected topological phases with  $Z_2$  symmetry. *Phys. Rev. B*, 89:201113, May 2014. doi: 10.1103/PhysRevB.89.201113. URL <https://link.aps.org/doi/10.1103/PhysRevB.89.201113>.
- [89] Anton Kapustin. Symmetry Protected Topological Phases, Anomalies, and Cobordisms: Beyond Group Cohomology. *arXiv e-prints*, art. arXiv:1403.1467, Mar 2014.
- [90] Anton Kapustin. Bosonic Topological Insulators and Paramagnets: a view from cobordisms. *arXiv e-prints*, art. arXiv:1404.6659, Apr 2014.
- [91] David Cimasoni and Nicolai Reshetikhin. Dimers on surface graphs and spin structures. i. *Communications in Mathematical Physics*, 275(1):187–208, Oct 2007. ISSN 1432-0916. doi: 10.1007/s00220-007-0302-7. URL <https://doi.org/10.1007/s00220-007-0302-7>.
- [92] N. Read and Dmitry Green. Paired states of fermions in two dimensions with breaking of parity and time-reversal symmetries and the fractional quantum hall effect. *Phys. Rev. B*, 61:10267–10297, Apr 2000. doi: 10.1103/PhysRevB.61.10267. URL <https://link.aps.org/doi/10.1103/PhysRevB.61.10267>.
- [93] D. W. Anderson, E. H. Brown, and F. P. Peterson. The structure of the spin cobordism ring. *Annals of Mathematics*, 86(2):271–298, 1967. ISSN 0003486X. URL <http://www.jstor.org/stable/1970690>.
- [94] R.C. Kirby and L.R. Taylor. *Pin structures on low-dimensional manifolds*, volume 2 of *London Mathematical Society Lecture Note Series*, pages 177–242. Cambridge University Press, 1991. doi: 10.1017/CBO9780511629341.015.
- [95] R. Blumenhagen, D. Lüst, and S. Theisen. *Basic Concepts of String Theory*. Theoretical and Mathematical Physics. Springer Berlin Heidelberg, 2012. ISBN 9783642294969. URL <https://books.google.com/books?id=-3PNFQn6AzcC>.
- [96] R. C. Kirby and L. R. Taylor. A calculation of pin+ bordism groups. *Commentarii Mathematici Helvetici*, 65(1):434–447, Dec 1990. ISSN 1420-8946. doi: 10.1007/BF02566617. URL <https://doi.org/10.1007/BF02566617>.
- [97] Stephan Stolz. Exotic structures on 4-manifolds detected by spectral invariants. *Inventiones mathematicae*, 94(1):147–162, Feb 1988. ISSN 1432-1297. doi: 10.1007/BF01394348. URL <https://doi.org/10.1007/BF01394348>.

- [98] Egidio Barrera-Yanez. The moduli space  $\mathcal{M}(M)$  of certain non-orientable manifolds of even dimension. *Differential Geometry and Applications. Proceedings of the 7th International Conference on Differential Geometry and Applications, Satellite Conference of ICM in Berlin, Aug. 10 - 14, 1998, Brno, Czech Republic*, pages 23–27, 1999.
- [99] J.W. Milnor and J.D. Stasheff. *Characteristic Classes*. Annals of mathematics studies. Princeton University Press, 1974. ISBN 9780691081229. URL <https://books.google.com/books?id=5zQ9AFk1i4EC>.